Scientific report

Mapping the vulnerability and exposure to extreme heat waves of populations living in housing in Canadian communities

Université Laval
Faculté de foresterie, de géographie et de géomatique
Département de géographie
CMHC SCHL
National Housing Strategy
Canada

Financing:

The Department of Geography at Université Laval, as part of the project to map the vulnerability and exposure to extreme heat waves of populations, received funding under the Data-driven round of the Housing Supply Challenge program; however, the opinions expressed are the opinions of the authors and the CMHC accepts no responsibility for these opinions.

Key words:

Heat waves, vulnerability, exposure, urban heat islands, synthetic index, ecumene, dasymetric mapping, principal component analysis, remote sensing, machine learning, housing.

Reference to cite:

Brousseau, Y., Lalonde, B., Robitaille, M.-J., Vandersmissen, M.-H., Barrette, N., Tessier, K., Gilbert, J.-P., Giguère, M., Juteau, J., Lapointe, J., Piché, S. (2023). Scientific report of the project Mapping the Vulnerability and Exposure to Extreme Heat Waves of Populations. Geography Department at Université Laval. 127 pages.

Abstract

Increasingly frequent around the world, heat waves are affecting Canada, where their frequency and intensity are increasing with climate change. This threat weighs on the health of the population, as oppressive heat is associated with increased mortality and many health problems. The vulnerability and exposure of the population vary over time and space, placing certain groups at greater risk. The effects of heat waves on the health and well-being of communities are mostly modulated by people's ability to access resources, including adequate housing. The main objective of this project is to develop an interactive online mapping application that provides valid information on the geographical distribution of populations' vulnerability and exposure in 156 urban regions of the country, specifying their intensity at the dissemination area scale. The tool is intended for professionals in the field while remaining accessible to the general public. Four indices were calculated (sensitivity, coping capacity, vulnerability, and exposure) based on socio-economic, demographic, proximity to services, and characterization of the built and natural environment data associated with the population's vulnerability and exposure to extreme heat waves. A map of urban heat islands has also been produced.

Résumé

De plus en plus fréquentes à travers le monde, les vagues de chaleur n'épargnent pas le Canada, où leur fréquence et leur intensité augmentent avec les changements climatiques. Cette menace pèse sur la santé de la population alors que la chaleur accablante est associée à une augmentation de la mortalité et de nombreux problèmes de santé. La vulnérabilité et l'exposition de la population varient dans le temps et dans l'espace, faisant en sorte que certains groupes sont plus à risque. Les effets des vagues de chaleur sur la santé et le bien-être des communautés sont majoritairement modulés par la capacité des personnes à accéder à des ressources, notamment à un logement adéquat. L'objectif principal de ce projet est d'élaborer une application cartographique interactive en ligne fournissant des informations valides sur la distribution géographique de la vulnérabilité et de l'exposition des populations de 156 régions urbaines du pays en spécifiant, à l'échelle de l'aire de diffusion, leur intensité. L'outil est destiné aux professionnels du milieu tout en demeurant accessible au grand public. Quatre indices ont été calculés (sensibilité, capacité à faire face, vulnérabilité et exposition) à partir de données socio-économiques, démographiques, de proximité des services et de caractérisation de l'environnement bâti et naturel associé à la vulnérabilité et l'exposition de la population aux vagues de chaleur accablante. Une carte des îlots de chaleur urbains a également été réalisée.

Team members

The research team from the Université Laval's Geography Department that carried out this project is made up of faculty members, professional staff, and students.

Project leaders

Yves Brousseau, *Principal researcher, associate professor*

Marie-Hélène Vandersmissen, *Co-researcher, professor*

Nathalie Barrette, *Co-researcher, professor*

Professionals

Benoit Lalonde, Head of research and practical works

Marie-Janick Robitaille, *Professional researcher*

Karine Tessier, *Research, and teaching technician*

Jean-Philippe Gilbert, *Professional researcher*

Graduate students

Mathilde Giguère, *Master's student in geographical sciences*

Janis Lapointe, *Master's student in geographical sciences*

Stéphanie Piché, *Master's student in geographical sciences*

Jérémi Juteau, *Master's student in geographical sciences*

Table of Contents

List of Figures

List of Tables

List of Equations

List of Abbreviations, Singles and Acronyms

API	Application Programming Interface
AGOL	ArcGIS Online
BCCS	British Columbia Coroners Service
CA	Census Agglomeration
CERFO	Centre d'enseignement et de recherche en foresterie
CMA	Census Metropolitan Area
DA	Dissemination Area
DB	Dissemination Block
DGUL	Department of Geography, Université Laval
ESRI	Environmental Systems Research Institute
ExB	Experience Builder
FNCC	Fully convolutional neural networks
GHS	Global Human Settlement
GHSL	Global Human Settlement Layer
GIS	Geographic Information System
IPCC	Intergovernmental Panel on Climate Change
KMO	Test de Kaiser-Meyer-Olkin
LODE	Linkable Open Data Environment
NAD	North American Datum
NDBI	Normalized Difference Built-up Index
NDVI	Normalized Difference Vegetation Index
NIR	Near-infrared
NRes	Non-residential
OSM	Open Street Map
PCA	Principal Component Analysis

ReLU	Rectified Linear Unit
Res	Residential
RF	Random Forest
RMSE	Root Mean Square Error
SSE	Sum of Squares Error
SST	Sum of Squares Total
SWIR	Short-wave Infrared Band
TIN	Triangulated Irregular Network
UHI	Urban Heat Island
WGS	World Geodetic System

1 INTRODUCTION

1.1 PROBLEM

Climate change is inevitable and can be observed globally (Masson-Delmotte *et al.*, 2021). In Canada, the estimated warming rate for the 1948-2016 period was much higher than the global rate (1.7°C compared to 0.8°C) (Bush & Lemmen, 2019). The impacts of global warming are being strongly felt across the country, particularly with the increase in the frequency of extremely hot days (Zhang *et al*., 2019). Several factors exacerbate the problem of heat waves. Firstly, in urban areas, the heat island phenomenon aggravates the situation, as the temperature difference between certain sectors of the city, such as paved parking areas and rural and natural environments on the outskirts, can reach several degrees Celsius (Oke, 1987; Oke *et al.*, 2017). In 2021, nearly three in four Canadians (73.7%) lived in one of Canada's major urban centers (Statistics Canada, 2022a). Secondly, the country's population is aging. According to the 2021 latest census data, the proportion of the Canadian population aged 65 and over was approximately 18.1%, or about one in five Canadians, and this proportion is expected to continue to increase in the coming years, reaching nearly 25% by 2031 (Statistics Canada, 2022e). Finally, the climate will continue to warm over the next few years, while by 2050, in certain regions of the country, the number of days with temperatures of 30°C or more could double, and by 2051-2080, some regions could observe more than 50 days a year where the mercury reaches 30°C (Climate Atlas of Canada, 2019).

This threat weighs heavily on the population's health, as extreme heat is associated with an increase in mortality (Gasparrini *et al*., 2015; Martin *et al*., 2012). Several studies show that extreme heat is associated with an increase in health problems, including the resurgence of respiratory and cardiovascular diseases and pathologies, as well as an increased number of syncope, periods of exhaustion, sunstroke, or heat stroke (Adam-Poupart *et al.,* 2021; Hajat *et al.*, 2010; Gough, W., Anderson, V., & Herod, K. 2016). In the summer of 2021, British Columbia recorded 619 heat-related deaths. Of those, 93% occurred within the week of June 25 to July 1, during which temperatures in the village of Lytton reached a high of 49.6°C. (British Columbia Coroners Service, 2022).

Exposure and vulnerability to heat waves vary over time and across space, which leaves some groups at greater risk (Hajat *et al.*, 2010, Basu et Samet, 2002). A study of the impact of the heat wave that affected the region of Laval (Quebec) from June 29 to July 5, 2018, showed that people living in high-vulnerability areas were 1.5 times more likely to die than those living in less vulnerable areas (Centre intégré de santé et de services sociaux de Laval, 2019).

The impact of heat waves on the health and well-being of individuals in a community depends predominantly on their access to resources— particularly adequate housing. Governmental and non-governmental organizations, whether local, regional, or provincial, must contend with the social and economic repercussions of climate change (Berry, Schnitter *et al.*, 2022).

Geographic data are particularly useful when it comes to identifying and mapping vulnerability across time and space. They also contribute to a better understanding of the underlying processes of vulnerability, facilitating the development of more effective mitigation strategies. Decision makers and citizens alike benefit when knowledge gained from research is made more broadly available, thus making the decision-making processes, the setting of standards, and the establishment of procedures, at a local and regional level, more concrete.

1.2 Objective

The main objective of this project is to develop an interactive online mapping application that provides accurate information about the geographic distribution of the vulnerability and exposure of major Canadian communities to heat waves while also specifying, for each geographic unit, the intensity of these weather events. In our view, such tools give the public meaningful and context-appropriate information for a geographic analysis of the vulnerability of communities living in Canada's major urban centres. With this information, public authorities will be better equipped to deal with heat waves and the health effects they can cause.

The specific objectives are:

- Produce a dasymetric map of the study area to represent only the different sectors of the ecumene (inhabited areas only).

- Construct several mappable indices to estimate the different dimensions of vulnerability and exposure to heat waves, by considering the appropriate geographic scale so that the designated authorities can adequately develop various prevention and intervention measures.

- Produce an online application to allow the diffusion of the heat wave vulnerability and exposure indices produced for the 156 Canadian urban regions.

To meet the project's specific objectives, this report is divided into three chapters:

- Dasymetric mapping
- Construction and mapping of the indices
- Production of a cartographic tool

1.3 Study Area

The study area covered by our project consists of 156 urban regions: 42 census metropolitan areas (CMAs) and 114 census agglomerations (CAs) in Canada (Tables 1 and 2), representing 83.9% of the Canadian population, or over 31 million people (Statistics Canada, 2022c). The complete list of CMAs can be found in Appendix 1. The indicators were calculated at the dissemination area (DA) level, which is the smallest standard geographic area for which all Canadian census data are disseminated. A dissemination area (DA) is composed of 400 to 700 persons (Statistics Canada, 2022d). The 2021 census year was chosen as it is the most recent census. Moreover, since we were seeking to represent the vulnerability of the population at the finest scale possible, i.e., the environment in which individuals live, a dasymetric mapping of the ecumene was applied to the dissemination areas to determine and only represent the inhabited zones (see Chapter 2).

Table 1: Study Area Description

Country	Type urban area	Number of urban areas	Population in 2021	Percentage of the population out of the total population of Canada
Canada	CA	114	3 753 167	10.1
	CMA	42	27 281 119	73.7
	Total	**156**	**31 034 286**	**83.9**

Table 2: Study Area Description by Province and Territory

Provinces	Type of urban area	Number of urban areas	Population in 2021	Percentage of the population out of the total population per province
Alberta	CA	13	385 351	9.0
	CMA	4	3 124 615	73.3
	Total	**17**	**3 509 966**	**82.3**
British Columbia	CA	21	676 430	13.5
	CMA	7	3 801 318	76.0
	Total	**28**	**4 477 748**	**89.5**
Prince Edward Island	CA	2	97 015	62.9
	CMA	0	0	0.0
	Total	**2**	**97 015**	**62.9**
Manitoba	CA	5	131 034	9.8
	CMA	1	834 678	62.2
	Total	**6**	**965 712**	**72.0**
New Brunswick	CA	4	93 110	12.0
	CMA	3	396 940	51.2
	Total	**7**	**490 050**	**63.2**
Nova Scotia	CA	4	205 801	21.2
	CMA	1	465 703	48.0
	Total	**5**	**671 504**	**69.3**
Ontario	CA	27	1 057 651	7.4
	CMA	16	11 742 189	82.6
	Total	**43**	**12 799 840**	**90.0**
Quebec	CA	25	817 111	9.6
	CMA	7	6 136 400	72.2
	Total	**32**	**6 953 511**	**81.8**
Saskatchewan	CA	8	180 382	15.9
	CMA	2	566 697	50.0
	Total	**10**	**747 079**	**66.0**
Newfoundland and Labrador	CA	3	57 029	11.2
	CMA	1	212 579	41.6
	Total	**4**	**269 608**	**52.8**
Northwest Territories	CA	1	20 340	49.5
	CMA	0	0	0.0
	Total	**1**	**20 340**	**49.5**
Yukon	CA	1	31 913	79.3
	CMA	0	0	0.0
	Total	**1**	**31 913**	**79.3**

2 DASYMETRIC MAPPING

2.1 INTRODUCTION

One of the major initial challenges of this project was to develop an accurate cartographic representation of the geographical distribution of residential environments. To better visualize these environments, our team outlined the dissemination areas using a file representing the settlement ecumene of the inhabited area for the whole country. In other words, we have produced a so-called dasymetric map.

Dasymetric mapping is a type of mapping that allows inhabited areas to be delimited or weighted using additional data. This makes it possible to add precision to the various types of data used for the cartographic representation of population distribution or population density within an urban area, for example. Bhaduri et al. (2007), Linard et al. (2011), and Archila Bustos et al. (2020) describe dasymetric mapping as a method that is based on the assumed relationship between population density and different characteristics of the mapped territory, including the presence of bodies of water, topography (slopes), the presence of a road, etc. In fact, any feature or data providing information on the exact number of people at a specific point or a specific area can be used to refine disaggregated census data at fine scale over a territory.

A number of map files exist to represent the ecumene in Canada, such as the ecumene produced by Natural Resources Canada or Statistics Canada's population ecumene. However, for the majority of these files, the level of precision did not meet the minimum requirements of representativeness of the residential environment for our mapping needs. Therefore, we carried out a wide-ranging review of the literature on dasymetric mapping. This made it possible to identify and acquire a much more precise geospatial data layer (Global Human Settlement Layer – GHSL). It is a benchmark in terms of representing the distribution of the population over an area. Indeed, several authors identify this product as being one of the best built environment and population mapping products to date (Klotz et *al.*, 2016; Florczyck et *al.*, 2020). This layer was also thoroughly validated. Considering the conclusive results of the validation process, a methodology for producing a dasymetric layer from the GHSL layer was developed.

A literature review inspired by systematic review methods was conducted in winter and summer 2022. The main objective of this review was to guide the team in the steps to be taken to obtain geospatial data representing the geographic distribution of residential environments. The state of current knowledge and methods for fine-scale population mapping was highlighted. The literature review focused on two main concepts: the notion of settlement or human population, and the notion of mapping or mapping tools. The results of this review were then sorted in several stages to ensure that only relevant articles were retained to continue the project.

A number of datasets representing the geographic distribution of the population were inventoried at this stage. Various characteristics specific to each dataset (spatial resolution, year of coverage, main feature represented, etc.) were identified. This approach enabled the team to make its choice and continue the process with the validation of the GHSL product.

2.2 GHSL VALIDATION

2.2.1 Methodology

The data layer that was the subject of the validation process is the GHS BUILT C FUN E2018 product. This layer is part of the latest version of the Global Human Settlement Layer project, which was made available online in June 2022. This project includes a set of datasets and tools available online free of charge online to assess human presence on the planet. The project is led by the European Commission's Joint Research Centre. The validated layer identifies three functional classes of land use: unbuilt, built residential, and built non-residential (Schiavina et *al.*, 2022). This characteristic is the main reason why the team chose this layer for the current project.

The validation process began with a sampling of areas in the GHSL layer to check the consistency of land-use classes that are indeed currently occupied. The sampling study area was constructed in two stages. First, the GHS layer was cut to match the boundaries of major Canadian cities. Second, a one-kilometre buffer zone was generated around areas classified as built residential and built non-residential to limit the number of sampling points in uninhabited areas. As a result, areas within the perimeter of major Canadian cities that are more than one kilometre from a pixel identified as a built area were excluded from the sampling area.

Subsequently, following the recommendations of Olofsson et al. (2014), a sampling plan stratified by city and land-use class was then drawn up to distribute 33,010 validation points across the study area. As it was desirable to be able to validate the accuracy of the different land cover classes, this sampling method was the most appropriate (Stehman, 2009). A seed of random points was scattered using a 6.7 km2 grid. One point per grid cell was generated and points not located in the extended residential zone (with a 1 km buffer zone) were then removed. The parameter of 6.7 km2 was chosen through an iterative process to obtain a total number of points (33,010) allowing good coverage of the study area while respecting the time and labour resources available within the team. Of these, 25,142 points were scattered over the entire area described, without class distinction. The additional 7,868 points were added by oversampling only in built residential and non-residential areas (without the buffer zone) to enable better representation and assessment of settlements, considering that a large proportion of the study area is classified as unbuilt.

The validation process was carried out using a web mapping application deployed on ArcGIS Online. The application efficiently compiled the data input of the five team members who were simultaneously mobilized for the validation. The study area was divided into sectors, which were allocated to the various members. For each point sampled, members compared the class indicated by the GHS data layer with observations made using satellite images. Information was entered for each sample point. A drop-down menu was used to select the land cover class observed on the satellite imagery and compare it with the class indicated by the GHS layer. These recordings made it possible to produce and analyze a confusion matrix, which represents the basis of a quantitative analysis in the validation of a geospatial layer (Strahler et *al*., 2006; Stehman, 2009). At the same time, we made a general observation of the GHS layer on the satellite image. The aim of this general observation was to identify errors outside the sample points. Not all errors outside the sample points were recorded, but some have been listed as additional points. For each point added at members' discretion, they had to enter the GHS layer category, the satellite imagery observation category, and a brief explanation of the error observed. This additional step made it possible to produce a quality qualitative analysis of the GHS layer complementary to the confusion matrix. This approach is suggested by Strahler et *al*. (2006).

At a technical level, it is important to bear in mind that certain aspects beyond the control of the research team may have led to biases in the results of the validation process. We identified two main sources of uncertainty. The first concerns the correspondence between the year of production of the satellite imagery and the year of production of the GHS data layer. In the cartographic application used for validation, the production date of the satellite imagery displayed varies based on the geographical sector and spatial resolution. The GHS layer includes data produced in 2018 only. Therefore, some of the identified errors may be caused by this chronological inconsistency. The second concerns a cartographic projection problem. Inaccuracy was introduced into the data owing to the different coordinate systems of the GHS layer (Mollweide [world] with WGS 1984 datum) and the point layer for validation (NAD 1983). When the spatial intersection between the two layers was initially performed, the correct projection transformations were not applied. This led to errors in the intersection result, causing some points to be associated with the wrong category in the GHS layer. The problem is as follows: on the map, a point superimposes a GHSL class (built residential, built non-residential or unbuilt) which is not the same as the GHSL class indicated in the layer's descriptive data. To solve this problem, a few steps had to be taken. First, the GHS layer was correctly converted to NAD 1983. We then performed a new spatial intersection between the GHS layer converted to NAD 1983 and the points layer (also in NAD 1983). Lastly, the results of the initial intersection and the new intersection were compared in order to identify and correct points containing erroneous information. Four hundred and sixty-eight points out of a total of 33,010 had to be corrected. Errors generated by the map projections also led to some shifts in the position of water bodies in some parts of the area. However, this error was marginal. No specific corrections were made, as the team felt that this error had no significant effect on the results of the validation process.

Certain aspects linked to the human nature of the judgment made by those carrying out the validation also need to be taken into consideration. Olofsson et *al*. (2014) also explains this source of variability and bias in the results of any validation process. The main source of heterogeneity in the raters' interpretations concerns the boundaries between the different classes identified by the GHS layer. Despite the use of decision criteria, zone boundaries generally remain more ambiguous than the interior of the various land-use class zones. At first glance, the identification of the GHSL non-residential building class is less consistent than for the other class types. This necessarily leads to more uncertainty for the raters at the validation level when it comes to this land use class. To control for these possible biases and ensure the validity of the process, two interrater agreement tests were carried out (see 2.2.2 Statistical Analysis (Interrater Reliability and Agreement Test)). Also, as the sample was based on the occupancy classes of the GHS layer, some internal errors may have been induced. This approach may have made some errors more difficult for the raters to spot, since the GHS layer provides reference points even though it is what is being validated.

The criteria for deciding how to classify were established during the group discussions, before returning to the initial interrater agreement test. Generally, any building of a residential nature (house, apartment building, campsite, hotel, etc.) was considered a residential building. This category also includes mixed-use buildings, such as those with one commercial floor and one residential floor. When it comes to roads, borders, and urban vegetation, there are a few well defined principles that inform decisions of which category to choose. Roads within residential areas, for example, are considered to be residential surfaces, since they form part of the same built and inhabited environment. In general, a surface is considered residential if it is surrounded by a residential environment but is not large enough (plus or minus one pixel) to contain another type of environment. However, in the context of a more isolated residential building, the distance criterion of 10 m from the building was established. In other words, if the point sampled is located more than 10 m from the building, the category chosen will correspond to unbuilt land. This same criterion is also applied to the margins of residential environments. The critical distance was set at 10 m, so as not to dwell on inaccuracies smaller than the layer resolution.

In the case of borders, e.g., between residential areas, industrial zones, forests, vacant lots, etc., the 10 m distance criterion applies in the same way as for roads. In the case of vegetation, if an urban park is larger than 10 m by 10 m, it is considered an unbuilt space. If the dimensions of the green space are less than 10 m by 10 m, the green space is considered to be integrated into the surrounding built environment (often residential).

For built non-residential areas, the general 10 m distance criterion also applies. Any non-residential building or structure and its immediate surroundings (less than 10 m away) is considered to be a built non-residential area.

As far as the unbuilt category is concerned, any element of the area corresponding to something other than buildings, such as vegetation, roads, mineral surfaces, crops, etc., is considered as such. There may be some ambiguity if we think of certain human structures that are not buildings in themselves, such as quarries, mines, port structures, and so on. In these cases, built structures have generally been considered as built non-residential areas to which the 10-m distance rule has been applied.

2.2.2 Statistical Analysis (Interrater Reliability and Agreement Test)

The validation process continued with a preliminary test to better define the parameters relating to the sampling plan and decision criteria and to assess interrater agreement between the five team members engaged for the validation. Two types of sampling (single-point and multi-point) were verified by separating the points to be validated in two separate geographical areas: Kingston, Ontario and Sherbrooke, Quebec. For the Kingston area, 20 multi-points (five points per location with an offset of 10 m and 20 m) were generated, while for the Sherbrooke area, 20 single points were generated. In both cases, 10 points were also added in the built areas identified by the GHS layer to ensure better representation of these sectors. Thus, a total of 140 points were validated. Five team members took part in the validation for this test and the whole process. Therefore, the aim of this interrater agreement test was to ensure consistency between the decisions of the individuals carrying out the validation. This is a statistical quantitative measure of the degree of consensus for a qualitative measure. Once the validation process had been completed, a second interrater agreement test was carried out to check for bias due to interpretation in the validation of the sampled points. For this second test, a sample of 500 points located in the Saguenay CMA in Quebec was validated, once again, by the five team members.

2.2.3 Results

Overall, there was a high degree of agreement between the raters' decisions (Fleiss' and Light's kappa = 0.85). However, agreement between various pairs of raters varies (kappas between 0.73 and 0.96), indicating some variability in decision agreement between some team members. This exercise made it possible to clarify the decision criteria before beginning the validation of the GHSL layer, and consequently to achieve greater consistency between team members in carrying out the process. The test also enabled us to more precisely determine the time and human resources required to complete the entire process. Overall, consistency between the different raters' decisions was still high and even slightly higher than in the first test (Fleiss' and Light's kappa = 0.87). Consistency was also more constant across all team members (kappas ranging from 0.83 to 0.93) for the various pairs of raters.

Once the sampled points had been assessed one by one by the team, the information gathered during the process was processed statistically. A confusion matrix (Table 3) was generated to read and analyze the results of the validation process, i.e., the accuracy of the GHS layer by functional land use class type.

The confusion matrix reveals that of the 6,110 observations in the residential building class, 5,956 (97.5%) points were correctly classified by GHSL. However, GHSL identified a total of 8,803 points in this category. Of this total, 1,293 (14.7%) points were actually located in built non-residential areas and 1,554 (17.7%) in unbuilt areas. This suggests that GHSL detects and maps the vast majority of built residential areas and, to some extent, overestimates their presence. A number of elements are frequently identified incorrectly as built residential areas (these errors are described in greater detail in section 3.5.2 Additional Points).

Of the 1,926 observations in the non-residential building class, 593 points (30.8%) were correctly recorded by GHSL. In addition, GHSL identifies a total of 695 points in this functional occupancy class, of which 10 (1.4%) are actually located in a built residential area and 92 (13.2%) in unbuilt spaces. It seems that GHSL is unable to recognize a relatively large proportion of built non-residential areas. In other words, the GHSL layer neglects to index some of these environments and underestimates their presence. There also seems to be some confusion between built non-residential areas and unbuilt areas within the GHS layer. These various remarks about the class of built non-residential environments were raised by team members even before the validation results were analyzed, as indicated in the sources of uncertainty. The major problem observed in identifying this class is that the borders of this type of environment are mostly identified as a built residential environment, doubtless owing to the characteristics of the ground surface. This error contributes to both the phenomenon of overestimation of the built residential environment and the underestimation of the built non-residential environment.

In the unbuilt functional class, of the 24,974 points classified as such by observations, GHSL lists 23,328 (93.4%) correctly. At the GHSL level, a total of 23,512 points are identified in the unbuilt class. Of these, 144 points (0.6%) are classified as built residential and 40 (0.2%) as built non residential. GHSL performs better than the other two classes when it comes to identifying this occupancy class, which is to be expected given that the ground characteristics of this class differ more from the two built classes than the two built classes do from each other.

Validation analyses revealed substantial agreement between what is represented cartographically by the GHSL layer and field observations (kappa = 0.769). Generally, GHSL and field observations are the same for 90.5% of validated points. Interpretation of the confusion matrix reveals that the errors in GHSL mainly concern the distinction between built residential (overestimated) and built non-residential (underestimated).

Table 3: Confusion matrix for the GHSL data validation analysis

		GHSL			
		Built residential	Built non residential	Non built	**Total**
Observations	Built residential	5956	10	144	**6110**
	Built non residential	1293	593	40	**1926**
	Non built	1554	92	23 328	**24 974**
	Total	8803	695	23 512	**33 010**

Additional points added manually by the raters during the validation process identify errors noted while browsing the GHS layer. Therefore, these are errors outside the sampled points. However, the analysis of these additional points may provide an insightful perspective to explain and characterize GHS layer errors also in the sample of points, considering that the majority of errors have a repetitive nature. A qualitative analysis was carried out to read and analyze the additional points. Based on the comment field and the satellite imagery category field, a classification by theme or type of error was drawn up (Table 4). Each additional point was then associated with a theme based on its descriptive data.

Seventeen themes characterize the 4,210 additional points. The source of each type (theme) of error is a source of confusion in GHSL, either between built and unbuilt environments, or between built residential and built non-residential environments (Res-NRes). In this respect, 61.7% of the errors recorded were due to confusion between the Res-NRes built classes, while the remaining 38.3% of the errors recorded were due to confusion between the unbuilt and general built classes. The higher proportion of errors attributable to GHSL differentiation of the built residential environment from the built non-residential environment is consistent with the results of the sample point validation.

The various themes can sometimes be used to identify specific and problematic elements in the identification of the correct functional land use class, and sometimes only to indicate an error.

For errors originating in the distinction between built residential and built non-residential, more than half of the points recorded (2,160) indicate a non-residential building incorrectly identified as residential. The presence of certain specific structures (port, rail and energy structures, warehouses, and storage yards) and visible patterns (built non-residential area) in the GHS layer may explain this. The reverse of this situation (residential building identified as non residential) also occurs, albeit to a lesser extent (88).

For errors originating in the distinction between unbuilt and built, the elements identified as causing confusion are rock outcrops (11), a certain type of vegetation (58), open environments and exposed mineral soil (176), quarries, mines, and agricultural fields (298), and asphalt surfaces (398). These types of ground elements can cover large areas. As a result, their misidentification affects the quality of GHSL data to some extent. Corrections were made in order of priority, especially as the difference between the built and unbuilt environment is greater than between the built residential and non-residential environment.

Table 4: Thematic analysis of errors listed in the validation of the GHSL data.

Theme	Error Source	Frequency	Relative frequency (%)
Rock outcrops/rocks	Non built	11	0.3
Non residential built perimeter	Res-NRes	11	0.3
Residential buildings identified as a non built surface	Non built	14	0.3
Non built surface identified as a non-residential building	Non built	31	0.7
Non residential buildings identified as a non built surface	Non built	38	0.9
Port structures	Res-NRes	58	1.4
Vegetation	Non built	58	1.4
Warehouses and storage yards	Res-NRes	78	1.9
Railway structures	Res-NRes	78	1.9
Residential buildings identified as non residential	Res-NRes	88	2.1
Energy structures	Res-NRes	123	2.9
Open areas and mineral soil	Non built	176	4.2
New residential developments	Non built	253	6.0
Quarries, mines, and agricultural fields	Non built	298	7.1
Non built surface identified as a residential building	Non built	337	8.0
Asphalt surfaces	Non built	398	9.5
Non residential buildings identified as residential	Res-NRes	2160	51.3
TOTAL	**-**	**4210**	**100**

2.3 Dasymetric Mapping

2.3.1 Methodology

After a conclusive validation process, the team decided to go ahead with the use of GHSL data. However, these were not used in their raw form. A chain of geoprocessing operations transformed the GHSL data to produce a layer that met specific mapping needs, while avoiding highlighting certain gaps in the GHS layer.

The two GHSL built classes (residential and non-residential) were selected as the basis for our residential environment mapping approach. Even though retaining built non-residential areas can be a source of inaccuracy in the mapping of residential areas, certain factors justify this choice. One factor is that the validation highlighted certain shortcomings in the distinction between the built residential and the built non-residential environment within the GHSL layer. Using both functional classes, the area covered by our mapping will necessarily be larger than the actual area covered by residential environments. Nonetheless, this overestimation bias will be due to this choice and not to a recurring error in the base data. This procedure was deemed preferable in order to limit the omission of certain settlements. However, as the accuracy of our population layer is important, dissemination block areas with no residents were removed to avoid unnecessarily overestimating the presence of residential areas. Therefore, built non-residential areas located in inhabited dissemination blocks have been preserved. A second factor justifying our methodological choice concerns the aesthetics of the final layer. The more extensive the base data, the more continuous the final layer, which is visually desirable for cartographic representation.

The geoprocessing chain to be applied to the GHSL data was established through an iterative process. Using the methodological information on dasymetric mapping data and methods gathered in the literature review, a number of geoprocessing and sequencing operations were tested in succession. Lastly, a processing chain inspired by the cartographic methodology of the Vulnerability Atlas produced the most satisfactory map layers according to the team's visual assessment (Figure 1) (Barette et *al.*, 2018).

This chain is divided into four main geoprocessing groups. The first group (iteration of tessellation files) takes the tessellation files one by one, i.e., a hexagonal grid of 10,000 m2 in our case, previously produced and sorted by a Python script for each of the 156 major Canadian cities making up our study area. These files correspond to a basic grid covering the entire extent of the CMAs, with no consideration, at this stage, for the location of the built areas identified by GHSL. The iteration subsequently allows us to take each of the files associated with the various CMAs and pass them individually, but automatically, into the set of processing groups. Owing to processing time issues, the 156 files were not all processed at once, but rather in sub-groups corresponding to the Canadian provinces.

The second group (tessellation processing) refines the general framework of our dasymetric layer by integrating GHSL data. At this stage, only tessellation cells touching (intersecting) a built residential or non-residential area are retained for vertex extraction. To simplify geoprocessing and reduce processing times, the GHS layer, initially retrieved in raster format, was converted to a polygon vector layer. Extracting the vertices has enabled us to produce a simplified overall grid with more natural boundaries (elimination of hexagonal shapes). This simplification (reducing the number of vertices in mapped polygons) is an aesthetic choice, but also, and above all, a technical one. As the layers are used and integrated into web mapping, one of the major challenges is display speed. Therefore, reducing the complexity of the layer is critical to increasing display speed.

The third group (TIN processing) contains all the steps required to simplify the adjusted framework of the hexagonal grid. To do so, a triangulated irregular network (TIN) was produced from the vertices extracted by the processing of the second group. Once the TINs and TIN triangles have been produced, the perimeter of each triangle is calculated. A number of trials were carried out to determine a threshold for the perimeter of the triangles to be preserved. The logic of this step is that smaller triangles are generated in the inhabited built raster that is the subject of our mapping, since the points are closer together. The triangles between the zones of interest zones are necessarily larger or longer, since the spacing between the points used to create the TIN is greater. Triangles with a perimeter greater than 350 m have been removed from the layer so that only the sectors under study are represented using triangles.

The fourth and final group of processes (addition of census data and finalization of the layer) allowed us to integrate some final details and modifications into the layer. It was at this stage that the uninhabited dissemination blocks were removed from the layer produced. Smoothing treatments were applied to improve the visual appearance of the final dasymetric mapping product. The final production stage involves integrating the dissemination area boundaries to join the various indices produced by the team to the dasymetric cartographic layer in the project's perceived cartographic applications.

Figure 1: Geoprocessing Model to Produce the Dasymetric Layer.

2.3.2 Results

Dasymetric mapping was first produced by the CMA. As the processing model is the same for all of Canada, the final visual product may vary according to the context and configuration of the CMA, or even the mapped area of a CMA. The Figure 2 shows the asymmetrical layer produced in four sectors in different CMAs. The files for the 156 CMAs were then merged to create a layer covering all of Canada (within the study area).

Figure 2:Results of the cartographic representation of the residential areas (dasymetric layer). (A) Calgary, Alberta sector. (B) Toronto, Ontario sector. (C) Québec city, Québec sector. (D) Halifax, Nova Scotia sector.

2.4 DISCUSSION

The dasymetric maps produced will have a scope that will be able to go far beyond the current project. As mentioned, no geospatial data is currently available for Canada representing residential living spaces at such a fine scale. These maps will be made publicly available via geospatial data portals for reuse in other projects and research where an accurate representation of population distribution is relevant or even essential.

Dasymetric maps could also be improved in the future. The map production method could be reproduced with new, more accurate data. For example, if a new generation of GHSL products is released with certain corrections, the dasymetric maps produced with this update would potentially be more representative of the geographic distribution of the population in major Canadian cities.

2.5 CONCLUSION

In short, after discovering the GHS layer in the scientific literature, a comprehensive validation process was implemented by the team to ensure its quality. The conclusive results from the validation allowed the team to move forward with the use of this layer to better represent the geographical distribution of the population of the area under study. Nonetheless, to improve the visual representation and correct certain shortcomings of the GHS layer, the team developed a cartographic processing chain to produce a dasymetric map better suited to the project's needs.

3 BUILDING AND MAPPING INDICES

3.1 INTRODUCTION

The geographical analysis of the vulnerability and exposure of populations fosters a better understanding of territorial issues and makes it possible to design better impact mitigation strategies. In recent years, the assessment of heat wave vulnerability has progressed considerably, inspiring various adaptation and development strategies at the local, regional, and national levels. Studies on the subject have identified population density, ethnicity, socio-economic status, characteristics of the built environment, gender, and age as characteristics of social vulnerability. It goes without saying that the location of the dwelling where people live can be a predominant factor in tempering the protective capacity it provides to cope with the onset of an extreme heat wave. This section will list its specific objectives and then present an overview of the literature review on heat wave mapping and exposure. It will also describe the methodology used by our team to map the vulnerability and exposure of Canadian households in large cities to the extreme heat wave phenomenon. Following the example of a prior project (Barrette *et al.*, 2018) our team adopted an indicator-based mapping approach to spatially represent the phenomenon being studied. Four indices have been calculated for the current project.

3.2 OBJECTIVES

The main objective is to map the vulnerability and exposure to extreme heat waves of populations living in housing located in 156 urban regions across Canada. The specific objectives include:

- Defining the concept of vulnerability and the theory behind it;
- Developing a methodology for selecting and creating indicators of sensitivity, coping capacity, vulnerability, and exposure to extreme heat waves;
- Mapping and categorizing sensitivity, coping capacity, vulnerability, and exposure to extreme heat waves in 156 Canadian urban regions.

3.3 CONCEPTUAL FRAMEWORK AND LITERATURE REVIEW

The starting point for the project was the conceptual framework and literature review of the Atlas of the Vulnerability of the Quebec Population to Climate Hazards by Barrette *et al.* (2018). Some impressive research work was carried out between 2010 and 2018. The information gathered provided a solid basis for the start of this project. Nevertheless, we needed to update our knowledge to be able to incorporate the most recent studies. The following four databases were queried using keywords: GeoBase, Elsevier, PubMed, and Web of Science. Around a hundred scientific articles published between 2017 and 2022 were selected, based on relevance and similarity to the context being studied. Interestingly, only a few of the selected articles focus on Canada (Krstic *et al*., 2017; Ho *et al.*, 2018; Yu *et al*., 2021). We also consulted publications from the grey literature to complete the portrait of the phenomenon. Most of these originate from public or government bodies. The following sections summarize the information consulted.

3.3.1 Relevance of the Vulnerability Index

A vulnerability index can be used to identify vulnerable populations and areas exposed to heat (Niu *et al*., 2021). The level of vulnerability varies across time and space and according to the populations who live there (Wolf *et al.*, 2015). A vulnerability index can be used as a decision-making tool. Identifying the populations and areas most vulnerable to heat enables resources to be allocated where prevention and intervention needs are greatest (Bao *et al*., 2015). In recent years, epidemiological studies have demonstrated the effects of heat on human health (Santamouris, 2021) and identified the population and environmental characteristics associated with them (Ellena *et al*., 2020). The results of epidemiological studies also affect the choice of indicators for the vulnerability index (Liu *et al.*, 2020).

3.3.2 Conceptual Framework

The choice of conceptual framework plays a fundamental role in the creation of the vulnerability index and the selection of indicators (Cheng *et al.*, 2021). There is no consensus on the choice of conceptual framework (Li *et al.*, 2022), but two of them appear more frequently in the scientific literature. Population vulnerability is a conceptual framework described by Cutter *et al*. (2003) and the Intergovernmental Panel on Climate Change (IPCC) (Parry *et al.*, 2007), according to which vulnerability is the sum of sensitivity, exposure, and adaptive capacity. The risk triangle as described by Crichton (1999) is another conceptual framework which explains that risk equals hazard, exposure, and vulnerability. That same conceptual framework can be interpreted in different ways, especially in terms of the choice of indicators (Li *et al*., 2022). For example, economic status and level of education are considered indicators of sensitivity by Zhang *et al.* (2018), but as indicators of adaptive capacity by Mallen *et al*. (2019).

3.3.3 Choice of Indicators

The local situation is the most decisive factor in the selection of indicators. The characteristics of the population and the environment that contribute to vulnerability can vary from one area to another. For example, the vulnerability index calculated by Nayak *et al.* (2018) in the state of New York places particular emphasis on racial inequalities. Indicator selection is also affected by data availability and the subjective judgment of the research team (Li *et al.*, 2022). In the majority of scientific articles, indicators are used to represent the demographic and socio-economic characteristics of the population (age, economic status, social isolation, level of education, ethnicity, unemployment, housing conditions, air conditioning, language skills, gender, etc.), the health of the population (pre-existing medical conditions, mental disorders, disability, access to healthcare facilities, etc.), and the characteristics of the natural and built environment (land surface temperature, air temperature, vegetation cover, humidity, air quality, topography, land use, land-use density, surface imperviousness, etc.). Very few studies include qualitative variables among their indicators. However, the article by Cheng *et al*. (2021) highlights the answers to a questionnaire on residents' habits during extreme heat episodes in the construction of their vulnerability index.

3.3.4 Index Composition

The research team needed to select the conceptual framework and indicators and then determine the weighting of each vulnerability indicator. The higher an indicator's weighting in the equation, the greater its impact on vulnerability. In the scientific literature, vulnerability is calculated using various weighting methods. Sometimes, a number of these methods are combined for a single index (Li *et al.*, 2022). The most popular method is principal component analysis (PCA) (Azhar *et al.*, 2017; Chen *et al.*, 2018; Mendez-Lazaro *et al.*, 2018; Nayak *et al.*, 2018; Guo *et al.*, 2019; Hulley *et al*., 2019; Janicke *et al*, 2019; Mallen *et al.*, 2019; Zuhra *et al.*, 2019; Alonso and Renard, 2020; Conlon *et al.*, 2020; Dong *et al.*, 2020; Houghton and Castillo-Salgado, 2020; Jagarnath *et al.*, 2020; Song *et al*., 2020; Zheng *et al.*, 2020). This statistical technique is particularly useful when there is a large number of indicators, since PCA allows for them to be grouped together and reduces the analysis dimensions. The equal weights method is another method in which each indicator is assigned the same weight, since their contribution to vulnerability is assumed to be the same (Christenson *et al.*, 2017; Liu *et al*., 2020). Several studies include arithmetic (adding, subtracting, dividing, and/or multiplying the value of each indicator) (Ho *et al.*, 2017; Koman *et al.*, 2019; Estoque *et al.*, 2020; Maragno *et al*., 2020; Turek-Hankins *et al.*, 2020). The analytic hierarchy process, which is less frequently used, allows weights to be assigned based on the experience and judgment of a panel of experts (Apreda *et al.*, 2019; Tran *et al.*, 2020).

3.4 METHODOLOGY

Four indices were created for this project: sensitivity, coping capacity, vulnerability, and exposure.

3.4.1 Sensitivity Index

3.4.1.1 Choice of variables

The literature review presented in section 3.3 identified the most relevant variables for the sensitivity index. Remember that sensitivity is defined as "an intrinsic condition of an element (community, organization, etc.) that makes it particularly vulnerable" [translation] (ADEME, 2013, p. 7). Various conditions can make a population more susceptible to consequences during a heat wave, but above all, it is the combination of these conditions that will cause the most impact. We need to integrate information on the socio-economic status and the quality of the built environment to gain a more complete picture of sensitivity. This information must have the same impact on the index, i.e., measure only the negative aspect of vulnerability. A total of 12 variables were included in the selection (Table 5). This choice was also influenced by data availability. All variables are taken from Statistics Canada's 2021 Census of Population. It is the only database that provides reliable information at various geographic scales for all of Canada. The statistical unit used is the dissemination area (DA). This is the smallest geographic area for which all census data is distributed, with a population of between 400 and 700.

Table 5: Sensitivity Index Variables

Dimensions	Sub-dimensions	Variables
Sensitivity (socio-economic)	Demography	Proportion of elderly (≥ 65 years old) and children (≤ 4 years old) (%)
	Instruction	Proportion of people with no certificate, diploma, or degree (%)
	Immigration et citizenship	Proportion of recent immigrants (%)
		Proportion of people who don't know either official languages (%)
	Household composition and characteristics	Proportion of people living alone (%)
		Proportion of single-parent families (%)
		Proportion of rented dwellings (%)
	Income and economic activities	Prevalence of low income based on the Low-Income Measure after tax (%)
		Proportion of renter households spending 30% or more of income on shelter costs (%)
Sensitivity (geographic)	Built environment	Proportion of dwellings in need of major repairs (%)
		Proportion of apartments in a building that has five or more storeys (%)
		Proportion of dwellings built before 1980 (%)

3.4.1.2 Variable Description

a) Proportion of Elderly (≥ 65 years old) and Children (≤ 4 years old) (%)

Young children and the elderly are part of the population with low autonomy. Additional resources are needed to take care of them during a heat wave, since they are not always able to do so themselves. The 0–4 age group and those aged 65 and over are generally more sensitive to prolonged exposure to heat, as they are less effectively able to thermoregulate. Elderly people are even more fragile as a result of chronic illness, medication, and loss of independence. The two age groups are calculated in the same variable so as not to cancel out their presence, which often varies in opposite directions.

b) Proportion of People with No Certificate, Diploma, or Degree (%)

Education plays a multidimensional role in vulnerability. Highly educated people have a better economic status, particularly due to higher-paying jobs. This stability provides them with more resources to prepare for and respond to a heat wave. Conversely, a low level of education impedes the ability to understand risk information. This lack of understanding will negatively impact the level of preparation.

c) Proportion of Recent Immigrants (%)

Adapting to a new country takes time. New immigrants face many challenges, such as learning about a new culture and getting their bearings. Consequently, they may not be aware of local hazards or available information and resources. Cultural differences and language barriers affect the way people prepare for and respond to risks. Immigrants may also have other vulnerability factors, such as income level, size of social circle, or tendency to reside in high-exposure areas.

d) Proportion of People Who Do Not Know Either Official Language (%)

Not speaking an official language can be a true danger during a heat wave. Language barriers hinder access to information and understanding of awareness or warning messages. As a result, people may not take on the correct protective behaviors and may further expose themselves to the heat.

e) Proportion of People Living Alone (%)

Living alone means less contact with the outside world, both in terms of information and of family and friends. Social isolation and lack of communication increase the risks during a heat wave, as the person is alone to look after themselves.

f) Proportion of Single-Parent Families (%)

Single-parent families are often limited financially, as the child's needs are met by one income. As a result, they have limited resources to prepare for and respond to a heat wave. The parent must assume all the responsibilities alone and take care of the other members of the family.

g) Proportion of Rented Dwellings (%)

The presence of rented units is generally an indicator of low income. Being a tenant suggests that these individuals have fewer financial resources than homeowners. Tenants often have little control over their homes, which limits their ability to install appropriate heat protection.

h) Prevalence of Low Income Based on the Low-Income Measure, after Tax (%)

Individuals with low income have limited resources to prepare for and respond to a heat wave. For example, they are less likely to have air conditioning, stay informed, and be in touch with a broad social network. This segment of the population often lives in the most at-risk areas, where housing is older and in poor condition.

i) Proportion of Renter Households Spending 30% or More of Income on Shelter Costs (%)

Similar to the explanations for the previous variable, renter households that spend 30% or more of their income on housing do not have much flexibility to absorb the economic impact of a crisis. This statistic is a useful benchmark for housing affordability, though it should be noted that a household could have a very high income or choose to put more money down on its home than on other assets.

j) Proportion of Dwellings in Need of Major Repairs (%)

According to Statistics Canada (2022b), “The ‘major repairs needed’ category includes dwellings needing major repairs such as dwellings with defective plumbing or electrical wiring, and dwellings needing structural repairs to walls, floors or ceilings.” Infrastructure in need of repair is more vulnerable to heat. This variable gives an overview of the condition of housing stock. Note that this is a subjective figure, since it is assessed by each respondent based on their knowledge of the subject. The assessment may be over- or underestimated, as it was not carried out by a professional. However, this variable is still interesting because it is also tied to the economic factor. As a general rule, a high income means a home of adequate quality. For tenants, there may be a lack of control or motivation in relation to repair issues in a unit.

k) Proportion of Apartments in a Building That has Five or More Storeys (%)

Larger buildings are exposed to more solar radiation and accumulate more heat. Indoor temperatures are higher, especially on the upper floors. People living in this type of dwelling face a greater risk of extreme heat.

l) Proportion of Dwellings Built Before 1980 (%)

In general, newer infrastructure is less vulnerable. Knowing the building’s year of construction makes it possible to determine the construction standards in effect at that time. Therefore, it is a proxy variable that makes it possible to estimate the physical and structural aspects of buildings’ vulnerability to heat. The year 1980 is relevant, as it corresponds to the introduction of the first energy-saving measures in the National Building Code of Canada.

3.4.1.3 Creating the Sensitivity Index

3.4.1.3.1 Data Downloading and Preparation

Given that the sensitivity index variables come solely from the 2021 Census of Population, it was simpler to use the cancensus package to download the data directly into the R software. A total of

24 variables were downloaded for all of Canada at the dissemination area (DA) level (Table 7). These data were used to calculate percentages for 10 of the 12 index variables. However, the incidence of low income based on the Low-income measure, after tax (%) and the proportion of renters spending 30% or more of household income on housing (%) are only available as percentages. Statistics Canada does the calculation, and we cannot access the raw data, unlike the other variables in the index. A selection was then made from data for all of Canada, retaining only census metropolitan areas (CMAs) and census agglomerations (CAs). The number of DAs dropped from 57,932 to 45,089. Since raw census data are rounded to preserve the confidentiality of respondents, some DAs may have values higher than 100% when calculating percentages. DAs whose values were greater than 100% were simply replaced by the value 100. Since our project concerns Canadian communities, DAs with a population equal to 0 were removed from the sample. This caused the removal of 255 DAs. One hundred and eighty-seven DAs also had missing values for a number of our variables, which were also removed. The sample now comprises 44,647 DAs. Information was missing for almost 10,000 DAs at the time of data upload. Rather than remove them from our sample, we used an imputation process to assign replacement values to missing values. We chose the missMDA package in R for the operation. After imputation, some 30 DAs showed a value below 0, which was manually replaced by 0.

3.4.1.3.2 Principal Component Analysis

Once data preparation was complete, we could proceed with the principal component analysis (PCA). Remember that PCA is a factor analysis used to study the relationships between different variables, to group the variables into components and to create a hierarchy between the components with the aim of explaining a phenomenon (Stafford and Bodson, 2006). In other words, PCA produces a kind of synthesis between correlated variables. PCA reduces the number of variables thanks to the correlation patterns between them (Durand, 2003; Fernandez *et al.*, 2016). Because the number of variables is decreased with PCA, it reduces redundancy while minimizing the loss of information contained in the initial variables. Each component explains part of the total variance of the variables (Stafford and Bodson, 2006). In preparation for the analysis, it was decided that our sample of 44,647 DAs would be split by province and territory (Table 6). Preliminary tests showed that PCA on DAs across Canada mitigated local variability. Eleven new samples were created using the sensitivity index data to better represent the situation in each province. Because PCA requires a minimum of five observations per variable (Osborne and Costello, 2004), the Northwest Territories and Yukon were included in the same sample. With 12 variables for the sensitivity index, the sample size must be at least 60 DAs. Combining the Northwest Territories and Yukon makes a total of 69 DAs. In addition, these are the two northernmost territories, which face similar climatic challenges.

Table 6: Number of Dissemination Areas Per Province or Territory

Province or territory	**Number of dissemination areas**
Alberta	4613
British Columbia	6396
Prince Edward Island	169
Manitoba	1430
New Brunswick	829
Nova Scotia	1044
Ontario	17 678
Quebec	10 784
Saskatchewan	1194
Newfoundland and Labrador	441
Northwest Territories	35
Yukon	34

PCA hypotheses include correlation matrix testing, Bartlett's test of sphericity, and the Kaiser-Meyer-Olkin (KMO) test (Pett *et al.*, 2003). The PCA calculation highlights the components that explain 100% of the variance. In order for the analysis to be of interest, we needed to keep only the components that were significant. There are various ways of selecting the number of components to retain. The most widely used criterion is based on the eigenvalue. The higher the eigenvalue of a component, the more it explains a significant proportion of the total variance. By convention, all components with an eigenvalue greater than 1 are considered significant (Bourque *et al.*, 2006).

3.4.1.3.3 Calculation of the Sensitivity Index

Running the PCA enabled us to create new synthetic components from our data. Once we had decided on the number of relevant components to be retained, a score was assigned to each DA. For each component, scores were weighted by the proportion of variance associated with them to provide a more representative result. Lastly, the weighted scores were added together to produce the sensitivity index.

Table 7: Calculation of the Sensitivity Index Variables

Variable name	Abbreviation	Calculation
Proportion of elderly (≥ 65 years old) and children (≤ 4 years old) (%)	AgeSens	$\frac{\text{Population aged between 0 et 4 years + Population aged 65 years and over}}{\text{Total population by age groups}} \times 100$
Proportion of people with no certificate, diploma, or degree (%)	SansDpl	$\frac{\text{Population with no certificate, diploma, or degree}}{\text{Total population aged 15 years and over by highest certificate, diploma, or degree}} \times 100$
Proportion of recent immigrants (%)	ImmiRcn	$\frac{\text{Population having immigrated between 2016 and 2021}}{\text{Total population by immigrant status and period of immigration}} \times 100$
Proportion of people who don't know either official languages (%)	LangOff	$\frac{\text{Population speaking neither French nor English}}{\text{Total population by knowledge of official languages}} \times 100$
Proportion of people living alone (%)	PrSeul	$\frac{\text{Households composed of one person}}{\text{Total private households by household size}} \times 100$
Proportion of single-parent families (%)	FamMono	$\frac{\text{Singe-parent families}}{\text{Total census families in private households}} \times 100$
Proportion of rented dwellings (%)	LogLoue	$\frac{\text{Tenants}}{\text{Total private households by tenure}} \times 100$
Prevalence of low income based on the Low-Income Measure after tax (%)	FaiblRv	Calculation by Statistics Canada
Proportion of renter households spending 30% or more of income on shelter costs (%)	Loyer30	Calculation by Statistics Canada
Proportion of dwellings in need of major repairs (%)	RepaMaj	$\frac{\text{Dwellings in need of major repairs}}{\text{Total occupied private dwellings by dwelling condition}} \times 100$
Proportion of apartments in a building that has five or more storeys (%)	Res5etg	$\frac{\text{Apartments in a building that has five or more storeys}}{\text{Total occupied private dwellings by type of residential construction}} \times 100$
Proportion of dwellings built before 1980 (%)	Log1980	$\frac{\text{Dwellings built before 1960 + Dwellings built between 1961 and 1980}}{\text{Total occupied private dwellings by period of construction}} \times 100$

3.4.2 Coping Capacity Index

Coping capacity is an essential element in the analysis of vulnerability to heat waves since it helps reduce negative effects by strengthening the population's resilience to this climatic hazard (Matthies *et al.*, 2008, Bélanger *et al.*, 2008). While sensitivity represents the intrinsic socio-economic characteristics of a population in the face of a climatic hazard, coping capacity represents "[t]he ability of people, institutions, organisations and systems, using available skills, values, beliefs, resources and opportunities, to address, manage and overcome adverse conditions in the short to medium term" (Masson-Delmotte *et al.*, 2018). For our study, coping capacity refers to the population's ability to prepare for, respond to, and recover during and after a heat wave.

As in the Atlas of the Vulnerability of the Quebec Population to Climate Hazards (Barrette *et al.,* 2018), the creation of proximity indicators was chosen in order to avoid the trap of having one variable for sensitivity and its opposite as a variable for coping capacity. For example, data representing a person with a high income in coping capacity is the opposite of data representing a person with a low income in the sensitivity index. As a result, many studies that include coping capacity in vulnerability calculations use socio-economic variables (Jagarnath *et al.*, 2020; Zemstov *et al.*, 2020). For the current study, local places, facilities, or services offering a cool shelter during an oppressive heatwave, and hospitals for access to care, were selected to construct the coping capacity index.

3.4.2.1 Variable Selection

The variables for the coping capacity index were selected in two stages. The first stage in the process was to identify the appropriate variables through a literature review. This step enabled us to identify variables that have been used in similar studies and have proven relevant for assessing coping capacity. The second stage involved a search and selection of available variables for the entire study area.

3.4.2.1.1 Literature Review

In constructing their heat wave coping capacity index, a number of studies incorporate the proximity or accessibility of populations to hospitals or healthcare (Kim *et al.*, 2017; Alonso and Renard, 2020; Dong *et al.*, 2020; Ellena *et al.*, 2020; Grigorescu *et al* , 2021), while other studies include the proximity or absence of green spaces (Hulley *et al.*, 2019; Mallen *et al.*, 2019; Liu *et al.*, 2020; Zheng *et al.*, 2020; Grigorescu *et al.*, 2021) or public swimming pools and splash pads (Harlan *et al.,* 2006; Alberini, Grand and Alhassan, 2011; Nayak *et al.,* 2017; Fraser *et al.,* 2017).

Lastly, many studies incorporate accessibility to a cooling centre (Alberini *et al.*, 2011; Fraser *et al.*, 2017; Fraser *et al.*, 2018; Voelkel *et al.,* 2018; Hulley *et al.*, 2019; Liu *et al.*, 2020; Maragano et *al.*, 2020). A cooling centre is an air-conditioned building, or a cooler site designated as a safe place in the event of a heat wave. Examples include community centres, movie theatres, schools, museums, and air-conditioned shops. Public accessibility to cooling centres is a common strategy employed by various levels of government to reduce the vulnerability of populations to heat waves (Widerynski *et al.*, 2017). Although there are official cooling centres, people often take refuge in informal cooling centres such as shopping malls and movie theatres near their homes during a heat wave (Fraser *et al.,* 2018).

3.4.2.1.2 Variable Selections Available for the Entire Study Area

After selecting the variables for the coping capacity index, the data available for the entire study area were identified to ensure comparability between the different areas. Despite data availability limitations, we selected a set of 10 proximity indicators to build the index. The data selected and the reasons given are presented in Table 8.

Table 8: Datasets Used to Estimate the Coping Capacity Dimensions of Vulnerability

Variables names	Raisons
Pools and splash pads	Allows people to cool down
Parks	Allows people to go to cooler places
Community centers	Allows people to go to a cool zone and where community workers can act to protect vulnerable populations
Hospitals	Allows people experiencing heat discomfort to obtain care
Art galleries	Allows people to go to a cool zone
Libraries	Allows people to go to a cool zone
Museums	Allows people to go to a cool zone
Shopping centers	Allows people to go to a cool zone
Beaches	Allows people to go to a cool zone
Cinema	Allows people to go to a cool zone

3.4.2.2 Construction of the Coping Capacity Index

3.4.2.2.1 Data Acquisition

The open databases (The Linkable Open Data Environment (LODE)) released by Statistics Canada were used to acquire most of the data required to create the coping capacity index. These databases, under the Linkable Open Data initiative, aim "at enhancing the use and harmonization of open micro data primarily from municipal, provincial and federal sources" (Statistics Canada, 2022f). They include specific data on the locations of buildings and schools, and on healthcare, cultural and artistic, and recreational and sports facilities.

In-depth research also uncovered a website containing a list of all shopping centres in Canada, including their street addresses. The website data was acquired using a method called web scraping, enabling all the web page data to be acquired with just a few lines of code. As the data used for geocoding was not consistent in its nomenclature, geolocation was carried out by Google Maps using an R program. This program uses the shopping centre data file, then sends this information to the Google Maps servers via an application programming interface (API). The inconsistency problem is thereby sent back to Google, which is in a much better position to deal with it. The servers return latitude and longitude coordinates. These coordinates were then added to the shopping centre database. Lastly, the data were transformed into geospatial data in a geographic information system. On rare occasions, when some shopping centres could not be located, geocoding was carried out manually. A member of the team performed a validation of the layer along with staff from the Centre GéoStat at Université Laval, who found no apparent errors in the shopping centre file.

For movie theatres, the database used comes from the International Showtimes website, which is a business that offers an API for accessing various data related to movie theatres around the world. After we requested it, this company sent us a list of movie theatres across Canada with addresses and geolocation coordinates.

3.4.2.2.1.1 Missing Data from Open Databases Released by Statistics Canada

Certain variables used for the coping capacity index could not be located in the standard database for all CMAs and CAs. In these cases, the data were found and geolocated manually. Data for missing variables were located on several websites, including government, regional, municipal, tourism, and commercial sites and blogs. The variables that were missing for each province and territory are included in Table 9. There were no missing data for British Columbia, New Brunswick, Ontario, and Quebec. Data geolocation was carried out manually in Google Maps, using longitude and latitude coordinates. These coordinates were then changed into geospatial data in a geographic information system (ArcGIS Pro).

Table 9: Missing Data for Each Province and Territory

Province or territory	Missing variables
Alberta	Beaches
Prince Edward Island	Libraries, shopping centers, community centers, art galleries, parks, pools and splash pads, beaches
Manitoba	Beaches
Nova Scotia	Pools and splash pads, beaches
Newfoundland and Labrador	Community centers, parks, pools and splash pads, beaches
Northwest Territories	Community centers, pools and splash pads, beaches
Saskatchewan	Shopping centers, pools and splash pads, beaches
Yukon	Community centers, pools and splash pads, beaches

3.4.2.2.2 Data Processing

3.4.2.2.2.1 Relocation of Batch Barycentres and Creation of a New Centre for Dissemination Areas

The approach applied to calculate proximity indices is similar to that used by Barrette *et al.* (2018) in the Atlas of the Vulnerability project. The method estimates the distance by car between the weighted centre of a DA and one of the locations shown in Table 9. More specifically, the centre of the DA was weighted using the number of people residing in the dissemination block (DB). According to Statistics Canada (2017), a DB is "an area bounded on all sides by roads and/or boundaries of standard geographic areas. The dissemination block is the smallest geographic area for which population and dwelling counts are disseminated." The new, "corrected" centre better represents the distribution of the population within the DA.

3.4.2.2.2.2 Proximity Measurement

The corrected centre was then moved to the nearest road section so that the network analysis could be carried out. This eliminates excessive distortion when calculating the proximity index for distant corrected centres. To achieve this, a 5-m buffer zone was calculated around each of the roads. The corrected centre of the DAs was then moved to the 5-m line of the buffer zone.

With a view to data sharing and method reproducibility for tool users, we developed Network Analysis in R using the OSMR library. The driving distance between the corrected centre and each of the variables was calculated by CMA. A table containing all the distances between each point entity of each variable was designed and a centre was specified. The smallest distance was then used to calculate the coping capacity index.

The decision to use distance by car rather than distance on foot was justified by the fact that there may be no destination (e.g., swimming pool, hospital) within a CMA. To avoid having zero values when calculating the PCA, we chose to include all the points of a variable. We felt it was unreasonable to choose a walking distance. It also eliminates the border issue. For example, for two neighbouring CMAs, the closest destination may be in the neighbouring CMA. However, this choice poses a major technical challenge. R's basic library does not allow users to have a matrix with more than 10,000 entries. Considering that there are over 40,000 DAs, we quickly reached the library maximum.

To understand the nature of the problem, it is important to indicate that R's OSMR library makes an API request to the OpenStreetMap servers. The coordinates of the various points were sent to the servers in the request. These servers calculate the distance between points using the road network and relay the distance. The point limit for a request is a matrix of 10,000 trips. However, the source codes and this data are available since OpenStreetMap is open source. This makes it possible to have your own OpenStreetMap server. Canadian road data were downloaded from Geofabrik. Then, the network file was built inside Docker. For the road network file, we specified that the method of transportation for the purposes of distance calculation is by car. Lastly, the server was launched in local mode, making sure to increase the size of the matrix to make it as large as possible. The only thing left to do was to indicate the address of the local server in the distance calculation function in R, so that calculations were performed on the local server rather than on the OpenStreetMap servers.

3.4.2.2.3 Principal Component Analysis

As with the sensitivity index (see section 3.4.1.3.2), we decided that the sample of 44,647 DAs would be split by province and territory for the PCA calculation. The results of the preliminary tests showed that the PCA on DAs for the whole country mitigated local variabilities in the coping capacity index. To this end, 11 new samples were created with the data to better represent provincial realities. As with the sensitivity index, the Northwest Territories and Yukon were included in the same sample.

Before proceeding with the PCA, the following assumptions were checked to ensure that the results of the analysis were reliable and interpretable: verification of the correlation matrix, Bartlett's Test of Sphericity, and the Kaiser-Meyer-Olkin (KMO) test (Pett *et al.*, 2003). Although the PCA calculation identifies the components that explain 100% of the variance, only significant components should be retained for relevant analysis. There are several methods for selecting the number of components. The most common method uses the eigenvalue. The higher the eigenvalue of a component, the greater the proportion of total variance it explains. By convention, all components with an eigenvalue greater than 1 are considered significant (Bourque *et al.*, 2006).

3.4.2.2.4 Calculation of the Coping Capacity Index

As with the sensitivity index, running the PCA created new synthetic components from the data. Once we had decided on the number of relevant components to be retained, a score was assigned to each DA. For each component, scores were weighted by the proportion of variance associated with them to provide a more representative result. Lastly, the weighted scores were added together to produce the coping capacity index.

3.4.3 Vulnerability Index

The vulnerability index is the total of the sensitivity index and the coping capacity index for each DA. There is no consensus on how to calculate the vulnerability index in the scientific literature. The choice of adding or subtracting vulnerability components depends on the conceptual framework. According to the variables and methodology chosen for this project, the indices had to be added. For example, the higher the sensitivity index score, the greater the vulnerability. And for the coping capacity index, the higher the score, the greater the vulnerability. We could say that it is an index of the "inability" to cope. As the two indices measure the negative aspect of vulnerability in the same way, their cumulative effects can be better represented by adding them together. Before calculation, the results of each index were normalized between 0 and 1, so that they could be compared over a common range of values. For this step, we used the normalize feature from the BBmisc package in R. The vulnerability index is calculated using data from one province at a time, i.e., the same samples as for the PCA.

3.4.4 Exposure Index

According to the IPCC (Field et *al.,* 2014), exposure is linked to the presence of people, livelihoods, species or ecosystems, environmental resources and services, infrastructure, or economic, social, or cultural assets in a place likely to suffer damage (due to climate change and its impacts).

3.4.4.1 Model Selection

Although there are several different types of modeling available to study urban heat islands (Ketterer and Matzarakis, 2015, Khatami, Mountrakis and Stehman, 2016, Oukawa, Krecl and Targino, 2022, Almeida, Teodoro and Gonçalves, 2021), the team chose the Random Forests (RF) model (Breiman, 2001) to predict the temperature difference of a pixel with respect to the mean temperature value of a reference group of pixels located in a non-urban environment. RF is a supervised machine learning algorithm commonly used to study the phenomenon of urban heat islands (Bernard et al., 2017, Chen et al., 2022, Gage and Cooper 2017, Marchal et al., 2022, Straub et al., 2019). RF models allow complex non-linear relationships to be modeled, enabling a more accurate prediction to be formulated in the case of urban heat island mapping. They are generally flexible and easily interpreted, since they consider multiple variables simultaneously when making a decision, whether it is on the physical characteristics of the city, meteorological characteristics, or environmental characteristics. RF also enables the prdocution of prediction maps with a high degree of spatial accuracy, an important parameter when mapping the intensity of urban heat islands at fine spatial resolution.

3.4.4.2 Data Used

The aim of this section is to describe the data used to map a heat wave exposure index.

3.4.4.2.1 Landsat Image Processing

Landsat 8 is a satellite launched in 2013 that revisits the same point every 16 days. Notably, it has an infrared thermal sensor on board that operates on two thermal bands (i.e., band 10 [B10] with a wavelength of 10 μm and band 11 [B11] with a wavelength of 12 μm) at a spatial resolution of 30 m (García-Santos et al., 2018). In recent years, satellite-based measuring instruments have been widely used for heat island mapping and monitoring (Kaplan, 2019). The combined use of various satellite instruments allows for surface temperature to be evaluated. Surface temperature is used in the scientific literature both as an element of heat exposure and for mapping surface heat islands (Ho *et al.*, 2015; Zhang et al., 2018; Cheng *et al.*, 2019; Räsänen *et al.*, 2019; Conlon *et al.*, 2020; Zhang *et al.*, 2021). An atmospheric correction must be applied to the B10 and B11 measurements to get an accurate estimate of ground surface temperature. There are four main methods for providing this atmospheric correction, namely Radiative-Transfer Equation, Mono-Window, Single-Channel, and Split-Window (García-Santos *et al.*, 2018).

As of 2017, the Landsat team no longer recommends the use of band 11 (B11) for Split-Window, since calibration problems have been detected (Sagris et Sepp, 2017; García-Santos *et al.*, 2018). The methodological framework used to calculate soil temperatures is that of Wang *et al.* (2020), which implements a generalized version of Single-Channel in the Google Earth Engine interface. The use of this framework is justified by the validation of the results obtained by Wang *et al.* (2020). These authors also publicly provide the code for the implementation, and the calculations are performed on Google's servers rather than locally, which greatly reduces computation time. This avoids errors by users during calculation and ensures the quality of surface temperatures.

In concrete terms, the generalized Single-Channel is calculated as follows:

Equation 1 Ground temperature calculation using the Single-Channel Method

$$T_S = \frac{c_2/\lambda}{\ln\left(\frac{c_1}{\lambda^5 \cdot B(T_s)} + 1\right)}$$

with

$$B(T_s) = a_0 + a_1 w + (a_2 + a_3 w + a_4 w^2)\frac{1}{\varepsilon} + (a_5 + a_6 w + a_7 w^2)\frac{L_{sen}}{\varepsilon}$$

Where $Lsen$ represents radiance at the instrument, ε represents ground surface emissivity, w represents atmospheric water vapor, $c1$ = 1.19104 × 108$W\mu m$−2 sr−1 , $c2$ = 1.43877 × 104μmK, $B(Ts)$ represents the Planck radiance of temperature Ts and λ represents effective wavelength (in this case, 10.904 μm).

For the temperature, only images from a so-called hot day (i.e., a maximum temperature of 30 °C or more) were used. To do this, Environment Canada meteorological data for each of the active stations in Canada from 2015 to 2020 were used to identify hot days temporally and spatially. Landsat images from 2020, taken between May and September inclusively, coinciding with a warm day and with less than 10% cloud cover, were downloaded. The Single-Channel method was applied to these images.

3.4.4.2.2 Built Environment and Vegetation Density Indices

The Normalized Difference Vegetation Index (NDVI) and the Normalized Difference Built-Up Index (NDBI) are two variables frequently used to identify urban heat islands. NDVI and NDBI variables are not directly accessible on Google Earth Engine for Landsat satellite images. For Landsat 8 images, NDVI is calculated as follows:

Equation 2 Normalized Different Vegetation Index (NDVI)

$$NDVI = \frac{(NIR - Red)}{(NIR + Red)}$$

Where NIR corresponds to the near-infrared band and Red to the red band. The NDBI is calculated as follows:

Equation 3 Normalized Difference Built-up Index (NDBI)

$$NDBI = \frac{(SWIR - NIR)}{(SWIR + NIR)}$$

Where, again, NIR corresponds to the near-infrared band and SWIR to the short-wave infrared band.

The median value of these three bands between the first day of May and the last day of September for each pixel was used in the 2020 calculations. These calculations were carried out using Google Earth Engine.

3.4.4.2.3 Surface Imperviousness

In order to estimate the percentage of imperviousness at fine resolution, we created a file for southern Quebec. To this end, we adopted the following methodological framework (Li *et al.*, 2020). Simply put, the method is based on training an artificial intelligence algorithm (a fully convolutional neural network [FCNN]) on the U.S. Geological Survey's National Land Cover Database surface imperviousness percentage data, all of which was implemented on a Google platform called Colab, allowing us to use Google's cloud services. Since the training images are all found in the United States, it is expected that the algorithm will perform well for the Quebec region, which shares a similar summer climate and built and natural environment, particularly with the northeastern United States. The use of an FCNN is preferred for its ability to extract information from multi-spectral band imagery (such as colour and thermal imagery) in addition to being able to take into account the value of neighbouring pixels (by incorporating them into one or more convolutional layers) (Li *et al.*, 2020). The model used is the pre-trained one, with the optimization parameter Rectified Linear Unit (ReLU), with 50 epochs. In data analysis, an epoch refers to a complete iteration of the training process of a machine learning model (Li *et al.*, 2020). Epochs are therefore used to measure a model's training progress over time. The model required 25 h of processing and produced an RMSE of ~0.08, indicating a very low margin of error.

3.4.4.2.4 Relative Temperature

The methodology used to calculate heat island intensity is based on Li *et al*. (2018). This method was chosen for several reasons. First, it allows for reproducibility, as there is no longer any subjectivity on the part of researchers as to the location of urban and rural pixels. Deployment of the method is also fairly straightforward, yet scientifically sound, making heat island mapping possible for all Canadian CMAs and CAs.

In order to roughly determine the difference observed between urban environments and the surrounding rural areas, a difference was estimated between the pixel temperature and the average temperature of pixels in a control zone. This control zone was identified by selecting the pixels in the image with the lowest level of surface imperviousness. The different images were then integrated into a mosaic, with overlapping pixel values aggregated by the mean temperature.

3.4.4.2.5 Elevation, Longitude, Latitude, and Proximity to a Body of Water

The elevation of each pixel in the study area was estimated using the GTOPO30 Global Digital Elevation Model file developed and distributed by Esri. Geographical coordinates were calculated using ArcGIS software in the Web Mercator projection (Nad 83), the same projection that will be used to display the web maps. Lastly, the Euclidean distance between the pixel and the nearest body of water was calculated to construct three separate indicators: distance to the nearest large body of water (1,000 km^2 or more), distance to the nearest small body of water (less than 1,000 km^2), and distance to the nearest body of water.

3.4.4.3 Study Area and Sampling

The modelling area covers the inhabited portion of 156 Canadian CMAs and CAs. To delimit this territory, a 500-m buffer zone was defined around the residential areas delimited by dasymetric mapping (see section 2). Observations were divided into groups of provinces (Table X). A small number of pixels used in the multivariate model were selected using a simple random sampling design. To determine whether the samples were representative of the population from which they were drawn, we used two parametric statistical tests (analysis of variance [ANOVA] and Student's t-test) and two non-parametric tests (Kruskal-Wallis test and Mann-Whitney U test) (Hair *et al.*, 2014).

3.4.4.4 Modelling

Random forest modelling was used to predict the temperature difference of a pixel compared with the mean temperature of a reference group of pixels located in a non-urban environment. Of the sample of pixels initially selected, 75% were used to train an algorithm, while the remaining pixels (25%) were used to validate the model. In addition to listing the number of pixels sampled per territory, Table 10 shows the various optimal parameters used to create random forests.

Table 10: Number of Pixels and Parameters Used For the Modelling by Major Canadian Region

Region	Number of sampled pixels	Number of trees	Minimum number of nodes	Randomly sampled variables
Maritimes	100 000	2000	2	4
Quebec	100 000			
Ontario	200 000			
Centre	200 000			
West Coast	150 000			

Figure 3 illustrates the approach used to select optimal model parameters. Three parameters were used:

- The number of decision trees to be constructed by the forest algorithm.
- The minimum number of samples required to form a leaf on the decision tree.
- The number of variables to consider when searching for the best division at each node.

These parameters were adjusted using a grid search to obtain the best results for a regression model using the tidymodels library, based on maximizing the value of the coefficient of determination (R^2) and minimizing the root mean square error (RMSE).

RMSE is a commonly used measure for assessing the performance of regression models (Gareth *et al.*, 2013). It allows the prediction error to be expressed in the same unit as the target variable, making it easy to interpret. A lower RMSE indicates better model performance in terms of predicting the target variable. This is calculated as follows:

Equation 4 Root-mean-square error (RMSE)

$$RMSE = \sqrt{\frac{\sum_{i=1}^{N}(y_i - \hat{y}_i)^2}{N}}$$

where N is the number of observations, y is the actual value of the target variable, and ŷ is the value predicted by the model for that observation.

For its part, the coefficient of determination (R^2) is a measure of the quality of the fit of a regression model (Gareth *et al.*, 2013). It specifies the proportion of the total variance of the dependent variable (y) that is "explained" by the model. The R^2 is calculated by comparing the total variance of the dependent variable (y) with the residual variance (prediction error) after model adjustment. The R^2 is calculated as follows:

Equation 5 Coefficient of determination (R2)

$$R^2 = \frac{SSE}{SST} = 1 - \frac{\sum(\hat{y}_i - \bar{y})^2}{\sum(y - \bar{y})^2}$$

where SSE is the sum of squared differences between the observed values of the dependent variable (y) and the values predicted by the model, and SST is the sum of squared differences between the observed values of y and the mean of y. Note that the closer the R^2 is to 1, the more the model "explains" or accounts for a significant proportion of the variance in the dependent variable, and the better the model's fit.

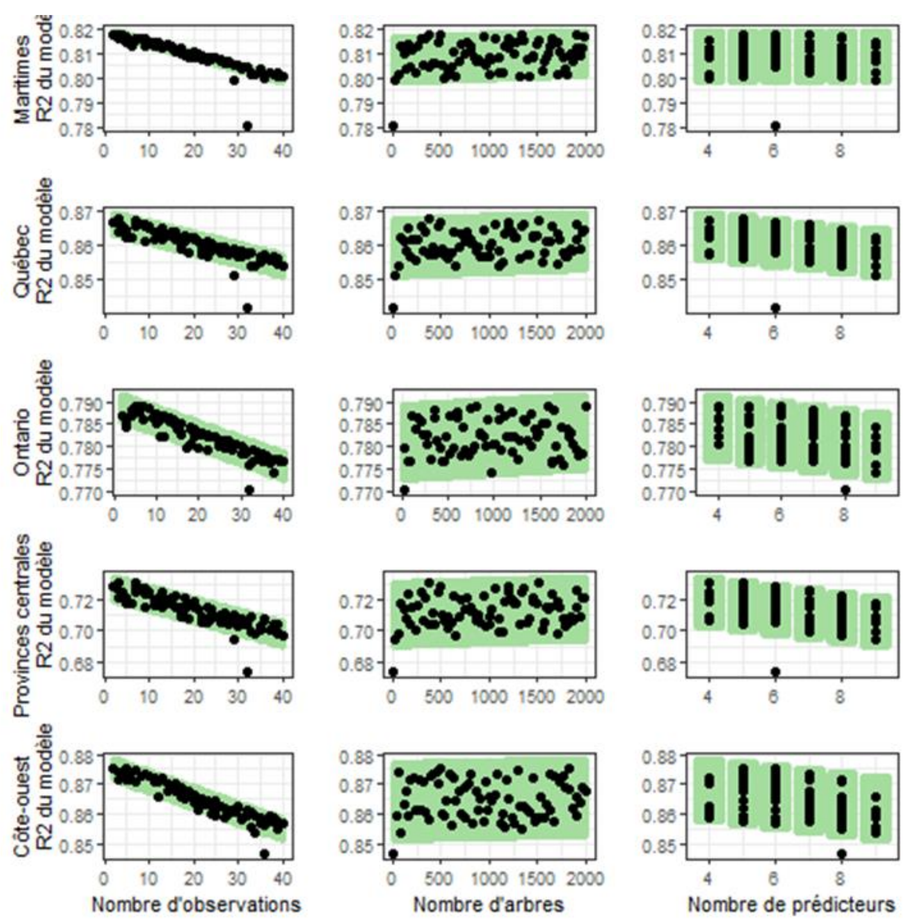

Figure 3: Scatter plot matrix representing the effect of changing the parameters on the model optimization.

3.5 RESULTS

3.5.1 Creating Synthetic Indices

3.5.1.1 Sensitivity Index

Adherence to the Assumptions

Before proceeding with the PCA for the sensitivity index, it is essential to check that the data for each province and territory adhere to the assumptions.

1) Correlation Matrix

By observing the correlation matrices, we were able to validate the existence of correlations between the 12 sensitivity index variables for each province and territory.

2) Bartlett's Test of Sphericity

Bartlett's Test of Sphericity is used to test the hypothesis that the correlation matrix is an identity matrix, i.e., that the variables are independent overall. The results indicate that the test is significant ($p < 0.001$). The variables are therefore related and there are inter-item correlations (Table 11).

Table 11: Results of Barlett's Test of Sphericity for the Sensitivity Index

Province or territory	Chi-squared (χ^2)	Degrees of freedom	Probability value (*p-value*)
Alberta	22 106.73	66	< 0.001
British Columbia	24 655.74	66	< 0.001
Prince Edward Island	796.53	66	< 0.001
Manitoba	8 353.23	66	< 0.001
New Brunswick	4 443.93	66	< 0.001
Nova Scotia	5 94.,2	66	< 0.001
Ontario	86 125.33	66	< 0.001
Quebec	57 901.61	66	< 0.001
Saskatchewan	6 509.37	66	< 0.001
Newfoundland and Labrador	2 179.67	66	< 0.001
Northwest Territories + Yukon	362.9	66	< 0.001

3) Kaiser-Meyer-Olkin (KMO) Index

The KMO index is used to check the quality of inter-item correlations. Most provinces and territories score between 0.7 and 0.8 (Table 12). This means that the data show an average fit. British Columbia is the only province to achieve a mediocre value, with a KMO index between 0.6 and 0.7. This is probably not due to sample size, since this is the province with the third most DAs in its territory. Based on the results, we could now perform a PCA for each province and territory.

Table 12: Results of the Kaiser-Meyer-Olkin Index for the Sensitivity Index

Province or territory	**KMO index**
Alberta	0.766
British Columbia	0.664
Prince Edward Island	0.738
Manitoba	0.785
New Brunswick	0.757
Nova Scotia	0.745
Ontario	0.776
Quebec	0.769
Saskatchewan	0.772
Newfoundland and Labrador	0.784
Northwest Territories + Yukon	0.710

Results of the Principal Component Analysis

a) Alberta

The results for Alberta show that the first four components have an eigenvalue greater than 1 (Table 13). These components explain 68.5% of the variance. When looking at the graph of contributions of variables, we note that the proportion of renters spending 30% or more of household income on housing (Rent30), the proportion of dwellings in need of major repairs (MajRepa), and the proportion of residences with five or more storeys (Res5sty) contribute more to the fifth component than to the first four. The final decision was to retain the first five components of the PCA instead of four (Dim. 1 to 5 in the Figure 4), in order to retain their representativeness in the calculation of the sensitivity index. The five components account for 75.9% of the variance explained.

Table 13: PCA of the Sensitivity Index for Alberta

Component	Eigenvalue	Explained variance (%)	Cumulative explained variance (%)
1	3.911	32.595	32.595
2	1.663	13.859	46.454
3	1.615	13.462	59.916
4	1.025	8.538	68.454
5	0.897	7.472	75.926
6	0.702	5.854	81.779
7	0.624	5.197	86.977
8	0.497	4.141	91.118
9	0.378	3.152	94.270
10	0.321	2.676	96.946
11	0.219	1.826	98.772
12	0.147	1.228	100.000

Figure 4: Variable Contribution for Each Component of the Sensitivity Index for Alberta

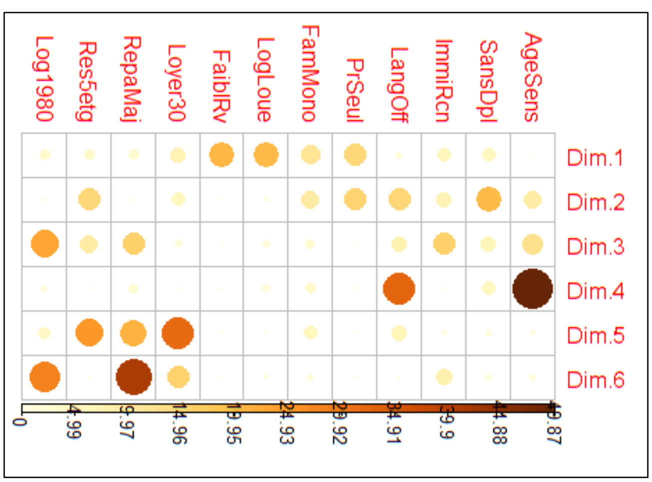

b) British Columbia

For British Columbia, the PCA results show that the first four components have an eigenvalue greater than 1 (Table 14). These components explain 66.8% of the variance. Figure 5 shows that the proportion of renters spending 30% or more of household income on housing (Rent30), the proportion of dwellings in need of major repairs (MajRepa), and the proportion of homes with five or more storeys (Res5sty) contribute more to the fifth component than to the first four. The contribution of the proportion of dwellings built before 1980 (Dwe1980) is higher for the sixth component. It also already contributes to components two and four. To ensure that all variables are represented in the sensitivity index calculation, the first five components of the PCA were retained rather than four. The five components account for 73.5% of the variance explained.

Table 14: PCA of the Sensitivity Index for British Columbia

Component	Eigenvalue	Explained variance (%)	Cumulative explained variance (%)
1	3.167	26.390	26.390
2	1.859	15.488	41.877
3	1.771	14.755	56.632
4	1.215	10.126	66.758
5	0.807	6.723	73.481
6	0.730	6.080	79.561
7	0.665	5.541	85.102
8	0.493	4.111	89.213
9	0.452	3.769	92.982
10	0.378	3.149	96.131
11	0.290	2.419	98.550
12	0.174	1.450	100.000

Figure 5: Variable Contribution for Each Component of the Sensitivity Index for British Columbia

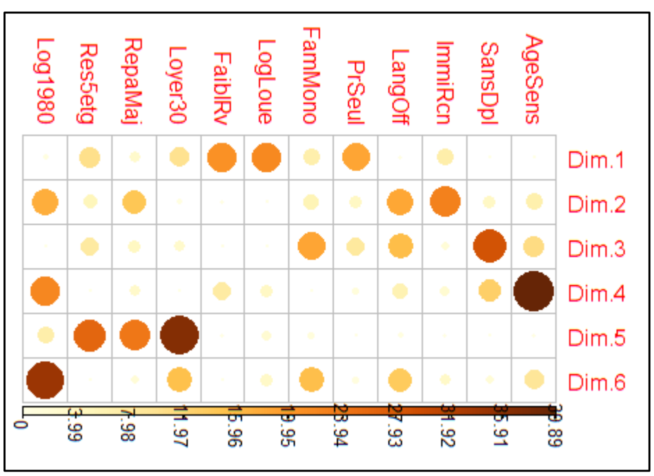

c) Prince Edward Island

The results for the province of Prince Edward Island show that the first four components have an eigenvalue greater than 1 (Table 15). These components explain 67.5% of the variance. Looking at Figure 6, we see that the proportion of people with no certificate, diploma, or degree (NoDpl) and the proportion of dwellings built before 1980 (Dwe1980) contribute more to the fifth component than to the first four. Therefore, it is worth retaining the fifth component, since its eigenvalue (0.955) is very close to 1. Its inclusion in the calculation of the sensitivity index explains 75.5% of the variance.

Table 15: PCA of the Sensitivity Index for Prince Edward Island

Component	Eigenvalue	Explained variance (%)	Cumulative explained variance (%)
1	3.735	31.127	31.127
2	2.038	16.979	48.107
3	1.214	10.117	58.224
4	1.117	9.308	67.532
5	0.955	7.955	75.488
6	0.751	6.262	81.750
7	0.670	5.583	87.333
8	0.487	4.055	91.388
9	0.402	3.350	94.738
10	0.314	2.613	97.351
11	0.177	1.478	98.829
12	0.141	1.171	100.000

Figure 6: Variable Contribution for Each Component of the Sensitivity Index Prince Edward Island

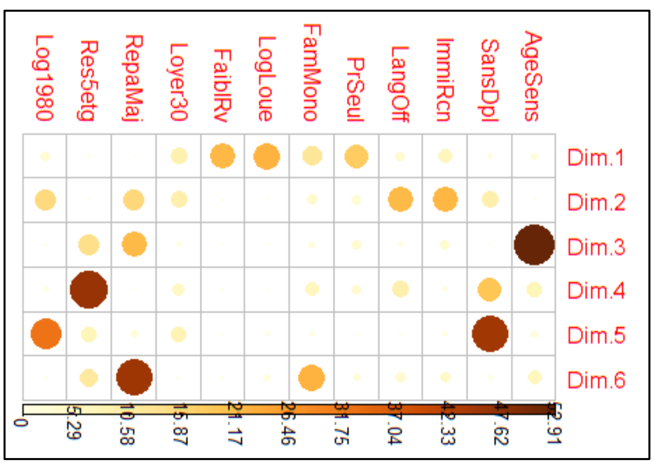

d) Manitoba

For Manitoba, the PCA results indicate that the first three components have an eigenvalue greater than 1 (Table 16). These components explain 64.4% of the variance. The proportion of people with no certificate, diploma, or degree (NoDpl) and the proportion of recent immigrants (RcnImm) contribute more to the fourth component than to the first three (Figure 7). It has an eigenvalue (0.993) that approaches our criterion of 1. The contribution of variables for components five and six is less significant than for the others, with the exception of the proportion of renters spending 30% or more of household income on housing (Rent30), which contributes the most. Thus, the first four components of the PCA were used to calculate the sensitivity index. The four components account for 72.6% of the variance explained.

Table 16: PCA of the Sensitivity Index for Manitoba

Component	Eigenvalue	Explained variance (%)	Cumulative explained variance (%)
1	4.259	35.493	35.493
2	1.890	15.748	51.240
3	1.574	13.114	64.355
4	0.993	8.272	72.627
5	0.803	6.693	79.320
6	0.614	5.115	84.435
7	0.535	4.459	88.894
8	0.417	3.472	92.366
9	0.336	2.797	95.162
10	0.289	2.406	97.568
11	0.156	1.301	98.870
12	0.136	1.130	100.000

Figure 7: Variable Contribution for Each Component of the Sensitivity Index for Manitoba

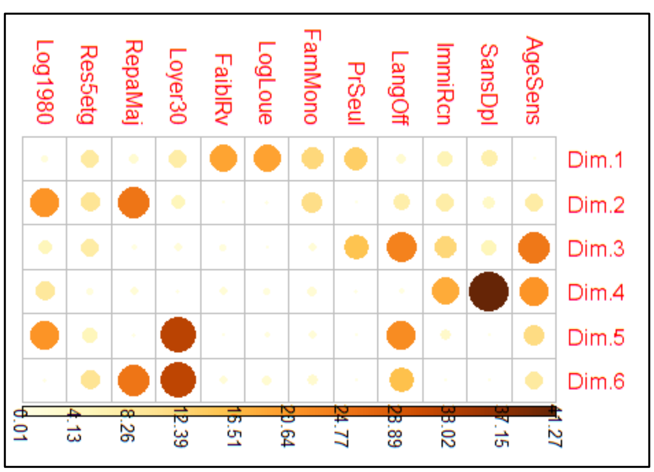

e) New Brunswick

The results for New Brunswick show that the first four components have an eigenvalue greater than 1 (Table 17). These components explain 69.9% of the variance. The proportion of homes with five or more storeys (Res5sty) and the proportion of dwellings built before 1980 (Dwe1980) contribute more to the fifth and sixth components, respectively (Figure 8). However, the eigenvalues of these components deviate greatly from our criterion of 1, and the variables concerned already contribute to the other components. The sensitivity index was calculated using only the first four components of the PCA.

Table 17: PCA of the Sensitivity Index for New Brunswick

Component	Eigenvalue	Explained variance (%)	Cumulative explained variance (%)
1	4.052	33.766	33.766
2	1.750	14.581	48.347
3	1.562	13.019	61.366
4	1.026	8.552	69.918
5	0.787	6.557	76.475
6	0.748	6.231	82.706
7	0.636	5.297	88.003
8	0.473	3.943	91.947
9	0.371	3.096	95.042
10	0.319	2.661	97.703
11	0.144	1.200	98.902
12	0.132	1.098	100.000

Figure 8: Variable Contribution for Each Component of the Sensitivity Index for New Brunswick

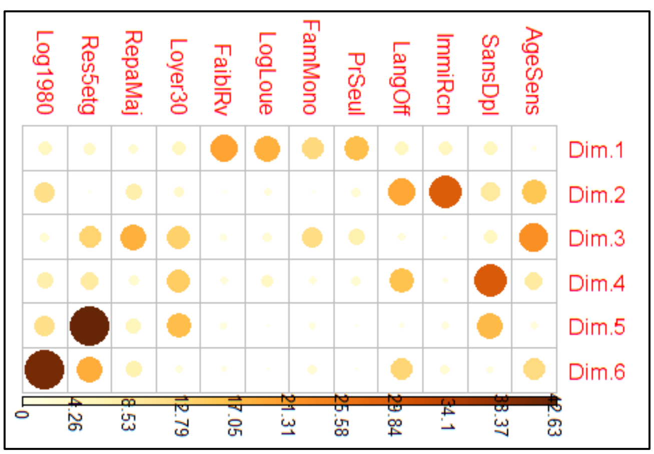

f) Nova Scotia

For Nova Scotia, the PCA results indicate that the first four components have an eigenvalue greater than 1 (Table 18). These components explain 72.7% of the variance. Only the proportion of dwellings built before 1980 (Dwe1980) significantly contributes to the fifth component (Figure 9). As for the sixth component, its eigenvalue (0.664) is too low compared to our criterion of 1. The proportion of dwellings in need of major repairs (MajRepa) and the proportion of residences with five or more storeys (Res5sty) also contribute to dimension two. As a result, only the first four components of the PCA were used to calculate the sensitivity index.

Table 18: PCA of the sensitivity index for Nova Scotia

Component	Eigenvalue	Explained variance (%)	Cumulative explained variance (%)
1	3.791	31.592	31.592
2	2.427	20.227	51.819
3	1.497	12.479	64.298
4	1.003	8.358	72.656
5	0.795	6.622	79.278
6	0.664	5.531	84.809
7	0.525	4.373	89.182
8	0.372	3.100	92.282
9	0.319	2.656	94.938
10	0.291	2.424	97.362
11	0.176	1.465	98.827
12	0.141	1.173	100.000

Figure 9: Variable Contribution for Each Component of the Sensitivity Index for Nova Scotia

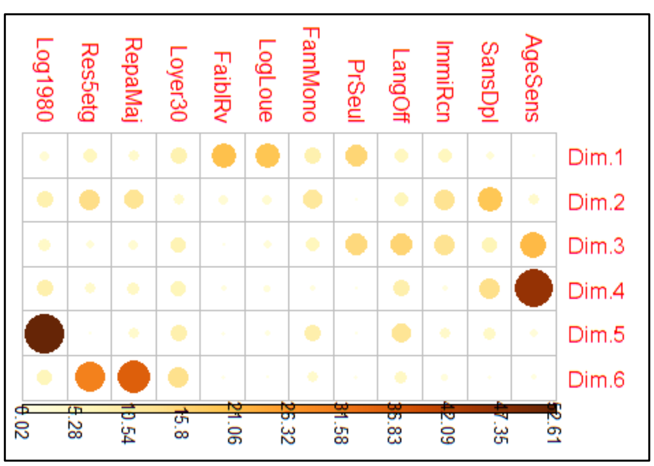

g) Ontario

The results for Ontario show that the first four components have an eigenvalue greater than 1 (Table 19). These components explain 70.1% of the variance. The proportion of renters spending 30% or more of household income on housing (Rent30) contributes more to components five and six (Figure 10). The eigenvalues of these components are much lower than our criterion of 1. As a result, only the first four components of the PCA were used to calculate the sensitivity index.

Table 19: PCA of the sensitivity index for Ontario

Component	Eigenvalue	Explained variance (%)	Cumulative explained variance (%)
1	4.027	33.556	33.556
2	1.763	14.688	48.245
3	1.484	12.365	60.610
4	1.138	9.486	70.095
5	0.739	6.159	76.255
6	0.694	5.786	82.041
7	0.574	4.787	86.828
8	0.469	3.906	90.735
9	0.400	3.332	94.067
10	0.345	2.879	96.946
11	0.196	1.635	98.581
12	0.170	1.419	100.000

Figure 10: Variable Contribution for Each Component of the Sensitivity index for Ontario

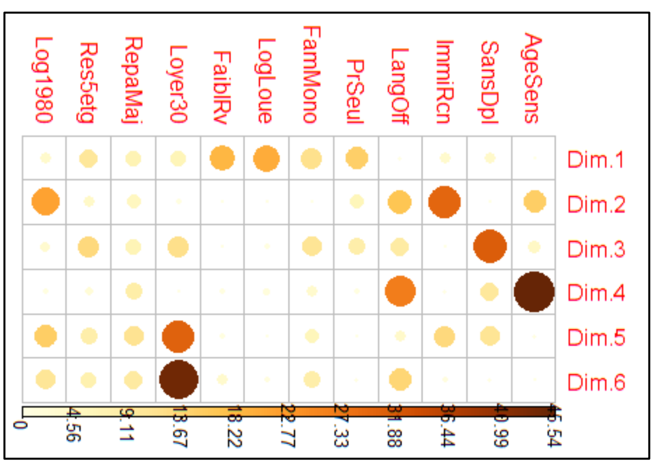

h) Quebec

For Quebec, the PCA results show that the first four components have an eigenvalue greater than 1 (Table 20). These components explain 69.8% of the variance. The proportion of people of sensitive ages (SensAge) and the proportion of people who do not know either official language (OffLang) contribute more to the fifth component than to the first four (Figure 11). It makes sense to keep the fifth component, since its eigenvalue (0.947) is very close to 1. Its inclusion in the calculation of the sensitivity index explains 77.7% of the variance.

Table 20: PCA of the Sensitivity Index for Quebec

Component	Eigenvalue	Explained variance (%)	Cumulative explained variance (%)
1	4.190	34.916	34.916
2	1.588	13.231	48.147
3	1.470	12.247	60.394
4	1.132	9.436	69.831
5	0.947	7.888	77.719
6	0.618	5.148	82.867
7	0.565	4.709	87.576
8	0.421	3.508	91.084
9	0.411	3.421	94.506
10	0.372	3.099	97.604
11	0.174	1.449	99.053
12	0.114	0.947	100.000

Figure 11: Variable Contribution for Each Component of the Sensitivity Index for Quebec

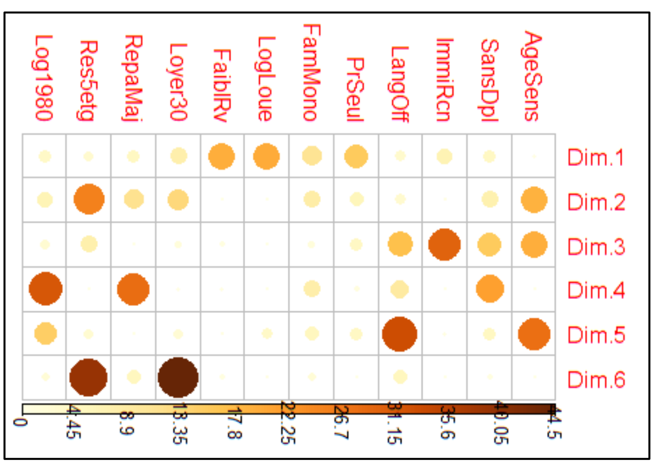

i) Saskatchewan

The results for Saskatchewan show that the first three components have an eigenvalue greater than 1 (Table 21). These components explain 63. 8% of the variance. A number of variables contribute significantly to components four, five, and six. This includes the proportion of people with no certificate, diploma, or degree (NoDpl), the proportion of people who do not know either official language (OffLang), the proportion of renters spending 30% or more of household income on housing (Rent30), and the proportion of dwellings in need of major repairs (MajRepa) (Figure 12). The first five components of the PCA were retained rather than three to ensure that all variables are represented in the sensitivity index calculation. The five components account for 77.4% of the variance explained.

Table 21: PCA of the sensitivity index for Saskatchewan

Component	Eigenvalue	Explained variance (%)	Cumulative explained variance (%)
1	4.043	33.693	33.693
2	1.923	16.028	49.722
3	1.686	14.050	63.771
4	0.837	6.976	70.747
5	0.800	6.665	77.412
6	0.641	5.339	82.750
7	0.603	5.025	87.776
8	0.498	4.147	91.923
9	0.379	3.157	95.080
10	0.278	2.314	97.394
11	0.187	1.558	98.951
12	0.126	1.049	100.000

Figure 12: Variable Contribution for Each Component of the Sensitivity Index for Saskatchewan

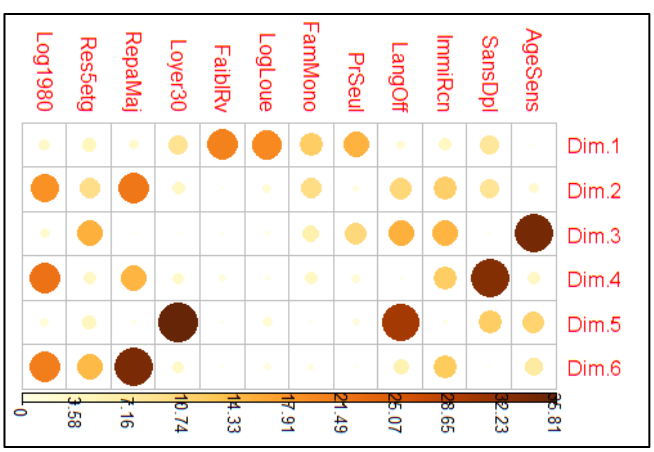

j) Newfoundland and Labrador

For Newfoundland and Labrador, the PCA results indicate that the first three components have an eigenvalue greater than 1 (Table 22). These components explain 59.3% of the variance. The proportion of renters spending 30% or more of household income on housing (Rent30) contributes more to the fourth than to the first three (Figure 13). To ensure its representativeness in the calculation of the sensitivity index, the first four components of the PCA were retained. The explained variance now represents 67.1%.

Table 22: PCA of the Sensitivity Index for Newfoundland and Labrador

Component	Eigenvalue	Explained variance (%)	Cumulative explained variance (%)
1	4.163	34.692	34.692
2	1.578	13.152	47.844
3	1.379	11.489	59.333
4	0.928	7.731	67.065
5	0.810	6.754	73.819
6	0.787	6.558	80.377
7	0.678	5.647	86.024
8	0.617	5.145	91.169
9	0.465	3.871	95.040
10	0.299	2.494	97.535
11	0.169	1.412	98.947
12	0,126	1.053	100.000

Figure 13: Variable Contribution for Each Component of the Sensitivity Index for Newfoundland and Labrador

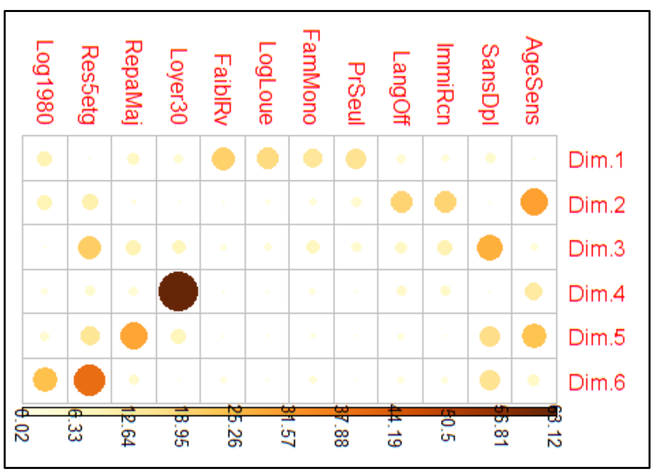

k) Northwest Territories + Yukon

Results for the Northwest Territories and Yukon show that the first three components have an eigenvalue greater than 1 (Table 23). These components explain 63.3% of the variance. The proportion of renters spending 30% or more of household income on housing (Rent30), the proportion of dwellings in need of major repairs (MajRepa), and the proportion of dwellings built before 1980 (Dwe1980) contribute more to the fourth component than to the first three (Figure 14). Additionally, the eigenvalue of the fourth is 0.961, which is near our criterion of 1. The sensitivity index calculation includes the first four components of the PCA instead of three, making it possible to explain 71.3% of the variance.

Table 23: PCA of the sensitivity index for the Northwest Territories and the Yukon

Component	Eigenvalue	Explained variance (%)	Cumulative explained variance (%)
1	4.011	33.425	33.425
2	2.026	16.880	50.306
3	1.563	13.027	63.333
4	0.961	8.009	71.342
5	0.829	6.908	78.250
6	0.716	5.966	84.216
7	0.536	4.464	88.680
8	0.484	4.033	92.714
9	0.323	2.695	95.409
10	0.273	2.272	97.681
11	0.146	1.218	98.899
12	0.132	1.101	100.000

Figure 14: Variable Contribution for Each Component of the Sensitivity Index for the Northwest Territories and the Yukon.

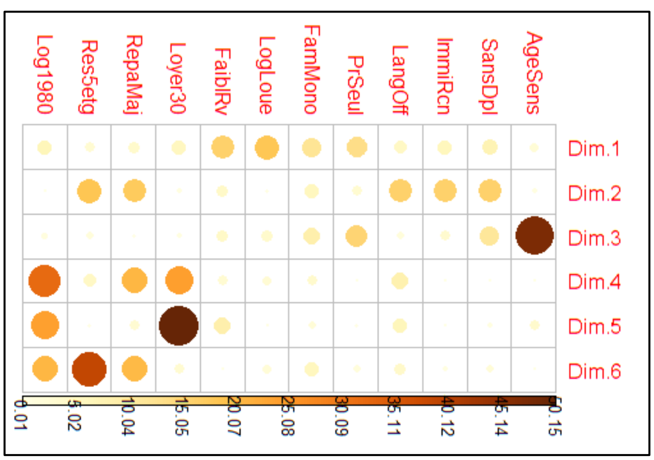

3.5.1.2 Coping Capacity Index

Adherence to the Assumptions

Before proceeding with the PCA for the coping capacity index, it was critical to check that the data for each province and territory adhered to the assumptions.

1) Correlation Matrix

Observation of the correlation matrices validated the existence of correlations between the 10 variables of the coping capacity index for each province and territory.

2) Bartlett's Test of Sphericity

Bartlett's Test of Sphericity was used to test the hypothesis that the correlation matrix is an identity matrix, i.e., that the variables are independent overall. The results indicate that the test is significant ($p < 0.001$). The variables are therefore related and there are inter-item correlations (Table 24).

Table 24: Results of Bartlett's Test of Sphericity for the Coping Capacity Index

Province or territory	**Chi-squared (χ^2)**	**Degrees of freedom**	**Probability (*p-value*)**
Alberta	60 191.14	45	< 0.001
British Columbia	58 609.51	45	< 0.001
Prince Edward Island	2 828.24	45	< 0.001
Manitoba	30 889.73	45	< 0.001
New Brunswick	12 421.85	45	< 0.001
Nova Scotia	15 144.56	45	< 0.001
Ontario	223 344	45	< 0.001
Quebec	97 669.7	45	< 0.001
Saskatchewan	11 375.89	45	< 0.001
Newfoundland and Labrador	3 903.67	45	< 0.001
Northwest Territories + Yukon	2 438.87	45	< 0.001

3) Kaiser-Meyer-Olkin (KMO) Index

The KMO index is used to check the quality of inter-item correlations. Prince Edward Island, Ontario, Northwest Territories, and Yukon have a KMO index between 0.8 and 0.9, which is considered meritorious. The majority of provinces and territories score between 0.7 and 0.8. This means that the data are middling. Saskatchewan is the only province to get a mediocre value, with a KMO index between 0.6 and 0.7. Based on the results, we applied the PCA for each province and territory (Table 25).

Table 25: Results of the Kaiser-Meyer-Olkin Index for the Coping Capacity Index

Province or territory	**KMO index**
Alberta	0.708
British Columbia	0.745
Prince Edward Island	0.883
Manitoba	0.743
New Brunswick	0.701
Nova Scotia	0.789
Ontario	0.805
Quebec	0.779
Saskatchewan	0.676
Newfoundland and Labrador	0.715
Northwest Territories + Yukon	0.869

Results of the Principal Component Analysis

a) Alberta

For Alberta, the PCA results indicate that the first two components have an eigenvalue greater than 1 (Table 26). These components explain 75.4% of the variance. Distance to the nearest museum (Museum) and distance to the nearest library (Lib) contribute more to components three and four, respectively (Figure 15). These components were not retained, since their eigenvalues (0.823 and 0.564) fall far short of our criterion of 1. The coping capacity index is calculated using only the first two components of the PCA.

Table 26: PCA of the Coping Capacity Index for Alberta

Component	Eigenvalue	Explained variance (%)	Cumulative explained variance (%)
1	5.256	52.564	52.564
2	2.281	22.813	75.377
3	0.823	8.234	83.611
4	0.564	5.637	89.248
5	0.405	4.051	93.299
6	0.333	3.325	96.625
7	0.184	1.839	98.464
8	0.094	0.942	99.406
9	0.056	0.565	99.971
10	0.003	0.029	100.000

Figure 15: Variable Contribution for Each Component of the Coping Capacity Index for Alberta

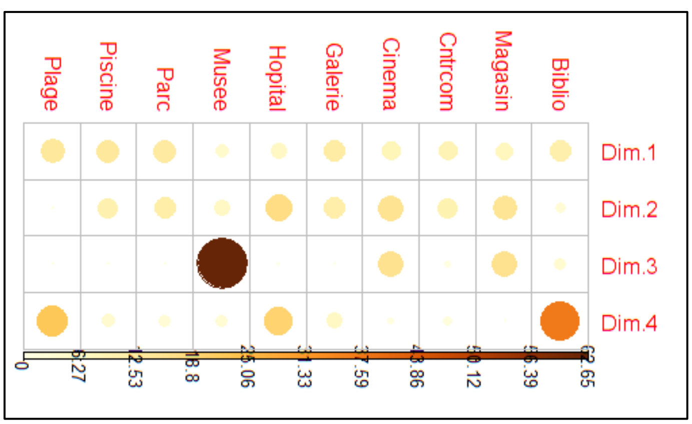

b) British Columbia

The PCA results for British Columbia show that the first two components have an eigenvalue greater than 1 (Table 27). These components explain 73.7% of the variance. Only the first two components of the PCA were used to calculate the coping capacity index (Figure 16).

Table 27: PCA of the Coping Capacity Index for British Columbia

Component	Eigenvalue	Explained variance (%)	Cumulative explained variance (%)
1	4.793	47.934	47.934
2	2.572	25.721	73.656
3	0.647	6.470	80.126
4	0.588	5.879	86.005
5	0.425	4.246	90.251
6	0.330	3.297	93.547
7	0.292	2.918	96.466
8	0.216	2.163	98.628
9	0.115	1.154	99.782
10	0.022	0.218	100.000

Figure 16: Variable Contribution for Each Component of the Coping Capacity Index for British Columbia

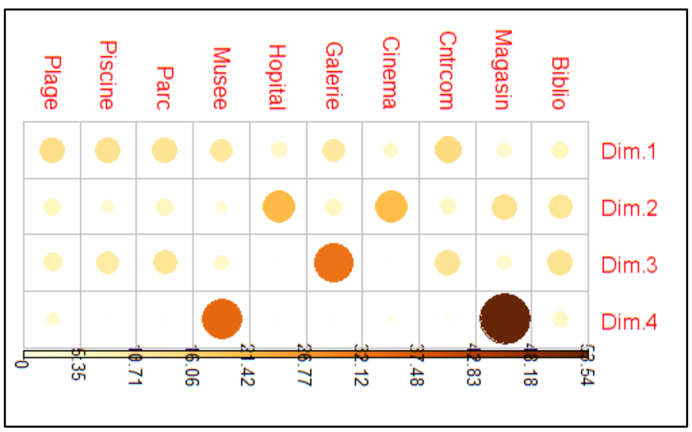

c) Prince Edward Island

For Prince Edward Island, the PCA results indicate that only the first component has an eigenvalue greater than 1 (Table 28). This component explains 78.1% of the variance. Distance to the nearest community centre (Commctr), distance to the nearest library (Lib), and distance to the nearest beach (Beach) contribute more to the other components than to the first (Figure 17). However, their eigenvalues deviate too far from our criterion of 1. Therefore, they were not included in the calculation of the coping capacity index.

Table 28: PCA of the Coping Capacity Index for Prince Edward Island

Component	Eigenvalue	Explained variance (%)	Cumulative explained variance (%)
1	7.810	78.103	78.103
2	0.685	6.847	84.949
3	0.494	4.937	89.887
4	0.381	3.810	93.697
5	0.269	2.693	96.389
6	0.206	2.062	98.452
7	0.094	0.944	99.395
8	0.030	0.298	99.693
9	0.021	0.211	99.904
10	0.010	0.096	100.000

Figure 17: Variable Contribution for Each Component of the Coping Capacity Index for Prince Edward Island

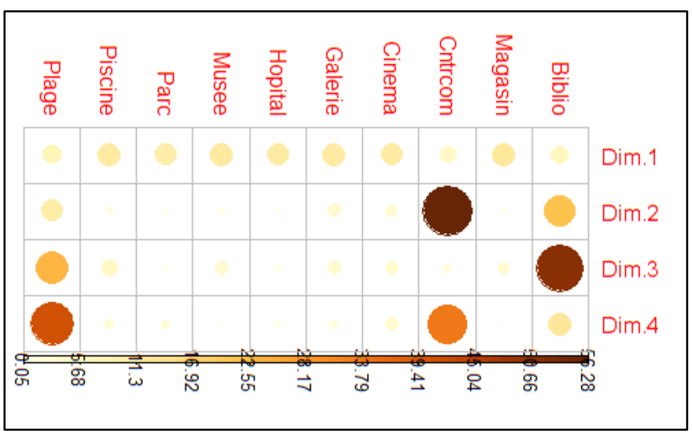

d) Manitoba

The PCA results for Manitoba show that the first three components have an eigenvalue greater than 1 (Table 29). These components explain 89.6% of the variance. Distance to the nearest hospital (Hospital) is a major contributor to component four (Figure 18). Since the eigenvalue (0.377) of the fourth component is too low compared to our criterion of 1, it was not included in the calculation of the coping capacity index.

Table 29: PCA of the Coping Capacity Index for Manitoba

Component	Eigenvalue	Explained variance (%)	Cumulative explained variance (%)
1	4.206	42.057	42.057
2	3.665	36.648	78.705
3	1.086	10.860	89.565
4	0.377	3.775	93.340
5	0.318	3.179	96.519
6	0.206	2.058	98.577
7	0.082	0.823	99.401
8	0.052	0.525	99.925
9	0.007	0.074	99.9997
10	0.00003	0.0003	100.000

Figure 18: Variable Contribution for Each Component of the Coping Capacity Index for Manitoba

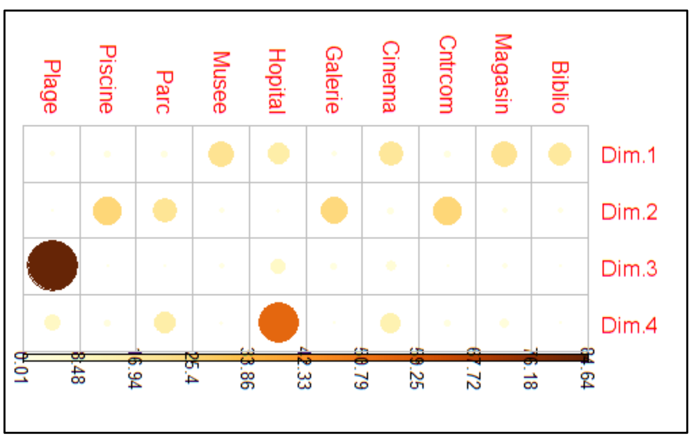

e) New Brunswick

For New Brunswick, the PCA results indicate that the first two components have an eigenvalue greater than 1 (Table 30). These components explain 80.0% of the variance. Distance to the nearest library (Lib) and distance to the nearest beach (Beach) contribute more to component three (Figure 19). Therefore, it was worth retaining the third component since its eigenvalue (0.964) is very close to 1. Its inclusion in the calculation of the coping capacity index explains 89.7% of the variance.

Table 30:PCA of the Coping Capacity Index for New Brunswick

Component	Eigenvalue	Explained variance (%)	Cumulative explained variance (%)
1	4.742	47.417	47.417
2	3.260	32.603	80.020
3	0.964	9.638	89.658
4	0.425	4.248	93.906
5	0.287	2.872	96.779
6	0.138	1.379	98.157
7	0.088	0.881	99.038
8	0.065	0.652	99.691
9	0.022	0.220	99.911
10	0.009	0.089	100.000

Figure 19: Variable Contribution for Each Component of the Coping Capacity Index for New Brunswick

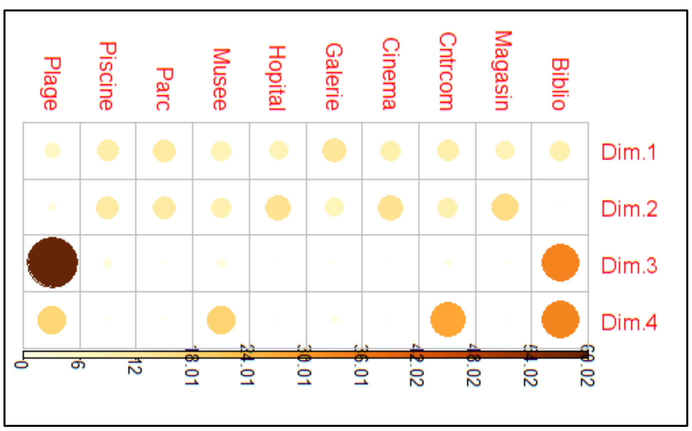

f) Nova Scotia

The PCA results for Nova Scotia show that the first three components have an eigenvalue greater than 1 (Table 31). These components explain 82.7% of the variance. Distance to the nearest hospital (Hospital) contributes more to component four (Figure 20). The fourth component has an eigenvalue (0.631), which is too far from 1, and was not included in the calculation of the coping capacity index.

Table 31: PCA of the Coping Capacity Index for Nova Scotia

Component	Eigenvalue	Explained variance (%)	Cumulative explained variance (%)
1	4.983	49.833	49.833
2	2.205	22.053	71.886
3	1.081	10.807	82.693
4	0.631	6.308	89.001
5	0.340	3.397	92.398
6	0.313	3.134	95.532
7	0.229	2.295	97.827
8	0.142	1.424	99.251
9	0.075	0.746	99.998
10	0.0002	0.002	100.000

Figure 20: Variable Contribution for Each Component of the Coping Capacity Index for Nova Scotia

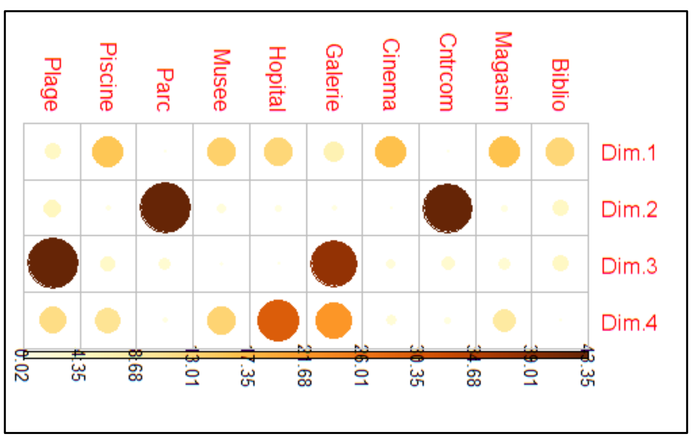

g) Ontario

For Ontario, the PCA results indicate that the first two components have an eigenvalue greater than 1 (Table 32). These components explain 74.1% of the variance. Distance to the nearest art gallery (Gallery) and distance to the nearest hospital (Hospital) contribute more to components three and four (Figure 21). As these variables already contribute to the other components, only the first two components of the PCA were used to calculate the coping capacity index.

Table 32: PCA of the Coping Capacity Index for Ontario

Component	Eigenvalue	Explained variance (%)	Cumulative explained variance (%)
1	4.369	43.691	43.691
2	3.042	30.418	74.109
3	0.874	8.736	82.846
4	0.622	6.216	89.062
5	0.470	4.695	93.757
6	0.369	3.690	97.447
7	0.115	1.147	98.593
8	0.093	0.932	99.525
9	0.042	0.417	99.942
10	0.006	0.058	100.000

Figure 21: Variable Contribution for Each Component of the Coping Capacity Index for Ontario

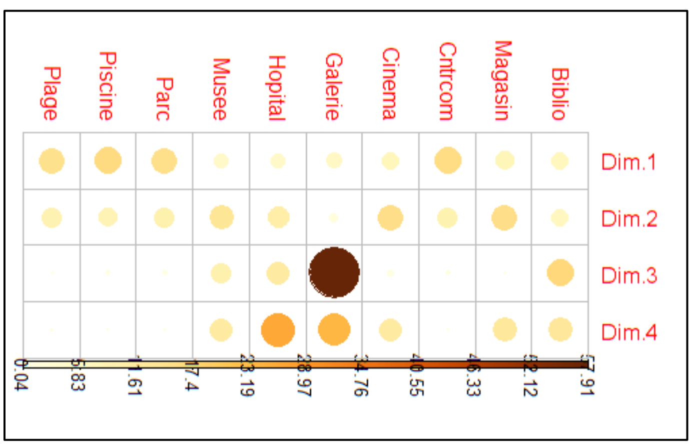

h) Quebec

The PCA results for Quebec show that the first two components have an eigenvalue greater than 1 (Table 33). These components explain 72.7% of the variance. Distance to the nearest beach (Beach) and distance to the nearest library (Lib) contribute more to components three and four, respectively (Figure 22). However, their eigenvalues deviate too far from our criterion of 1. They were not included in the calculation of the coping capacity index.

Table 33:PCA of the Coping Capacity Index for Quebec

Component	Eigenvalue	Explained variance (%)	Cumulative explained variance (%)
1	4.566	45.660	45.660
2	2.707	27.065	72.726
3	0.711	7.113	79.838
4	0.614	6.137	85.975
5	0.428	4.285	90.260
6	0.355	3.555	93.815
7	0.304	3.045	96.860
8	0.159	1.591	98.450
9	0.133	1.330	99.781
10	0.022	0.219	100.000

Figure 22: Variable Contribution for Each Component of the Coping Capacity Index for Quebec

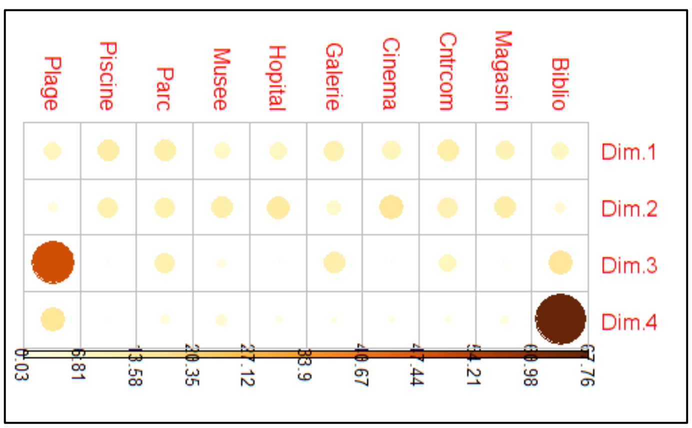

i) Saskatchewan

For Saskatchewan, the PCA results show that the first three components have an eigenvalue greater than 1 (Table 34). These components explain 78.1% of the variance. Distance to the nearest community centre (Commctr) is a major contributor to component four (Figure 23). As this variable already contributes to the other components, the fourth component was not included in the calculation of the coping capacity index.

Table 34:PCA of the Coping Capacity Index for Saskatchewan

Component	Eigenvalue	Explained variance (%)	Cumulative explained variance (%)
1	4.431	44.314	44.314
2	2.065	20.647	64.961
3	1.310	13.102	78.064
4	0.886	8.863	86.926
5	0.642	6.421	93.348
6	0.320	3.204	96.552
7	0.151	1.506	98.058
8	0.095	0.946	99.003
9	0.065	0.653	99.656
10	0.034	0.344	100.000

Figure 23: Variable Contribution for Each Component of the Coping Capacity Index for Saskatchewan

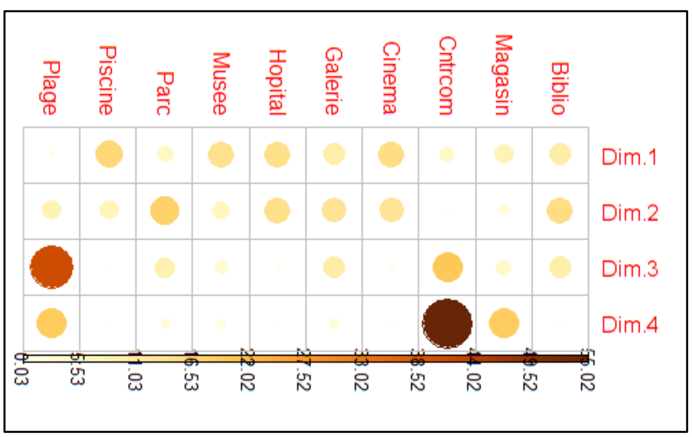

j) Newfoundland and Labrador

The PCA results for Newfoundland and Labrador show that the first three components have an eigenvalue greater than 1 (Table 35). These components explain 78.9% of the variance. Distance to the nearest library (Lib) and distance to the nearest community centre (Commctr) contribute more to dimension four (Figure 24). The fourth component has an eigenvalue (0.787) that is too far from 1, and was therefore not included in the calculation of the coping capacity index.

Table 35: PCA of the Coping Capacity Index for Newfoundland and Labrador

Component	Eigenvalue	Explained variance (%)	Cumulative explained variance (%)
1	4.725	47.250	47.250
2	1.848	18.481	65.731
3	1.316	13.159	78.891
4	0.787	7.869	86.759
5	0.472	4.718	91.477
6	0.364	3.639	95.116
7	0.237	2.367	97.483
8	0.157	1.568	99.051
9	0.051	0.511	99.562
10	0.044	0.438	100.000

Figure 24:Variable Contribution for Each Component of the Coping Capacity Index for Newfoundland and Labrador

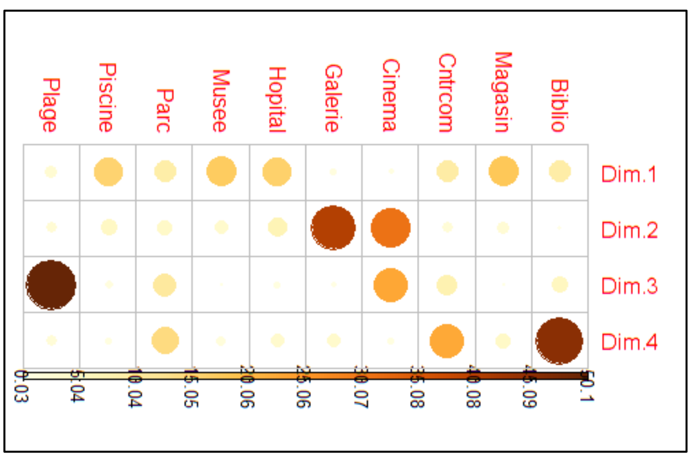

k) Northwest Territories + Yukon

For the Northwest Territories and Yukon, PCA results indicate that only the first component has an eigenvalue greater than 1 (Table 36). This component explains 88.5% of the variance. All variables contribute minimally to the first component (Figure 25). Although some variables contribute more to the subsequent components, their eigenvalues are below our criterion of 1. The coping capacity index was calculated using the first component only.

Table 36: PCA of the Coping Capacity Index for the Northwest Territories and the Yukon

Component	Eigenvalue	Explained variance (%)	Cumulative explained variance (%)
1	8.851	88.515	88.515
2	0.806	8.062	96.577
3	0.195	1.951	98.528
4	0.082	0.816	99.344
5	0.038	0.378	99.722
6	0.021	0.215	99.937
7	0.005	0.049	99.986
8	0.001	0.009	99.995
9	0.0003	0.003	99.998
10	0.0002	0.002	100.000

Figure 25: Variable Contribution for Each Component of the Coping Capacity Index for the Northwest Territories and the Yukon

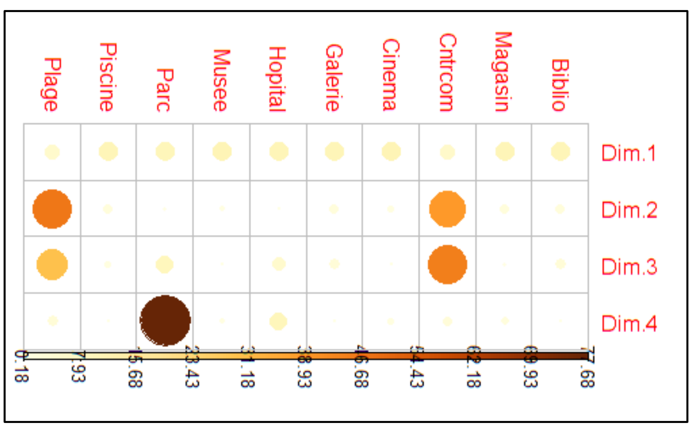

3.5.1.3 Exposure Index and Urban Heat Islands

The final modelling was carried out using ArcGIS Pro software because its use greatly facilitated the visualization of mapping results in rapid processing times. Table 37 lists the coefficients of determination (R^2) and root mean square error (RMSE) produced for each model used in the production of the data layers mapping urban heat islands. Generally, the models produced fit the data fairly well and account for a significant proportion of the variance of the variable of interest while producing, on average, a low quantity of errors. The results obtained are comparable to those of a similar Quebec study (Marchal *et al.*, 2022).

Table 37:Coefficients of determination and root mean square error of the models.

	Validation dataset		**Complete dataset**	
Region	**R^2**	**RMSE**	**R^2**	**RMSE**
Maritimes	0.818	1.096	0.814	1.090
Quebec	0.867	1.589	0.868	1.579
Ontario	0.786	1.619	0.790	1.606
Centre	0.776	1.782	0.778	1.764
West-Coast	0.871	1.584	0.874	1.565

As the example in Figure 26 shows, there does not seem to be any dependence between the errors produced by the models and the value predicted by them. In fact, the error appears to be randomly distributed and only weakly correlated with the predicted temperature.

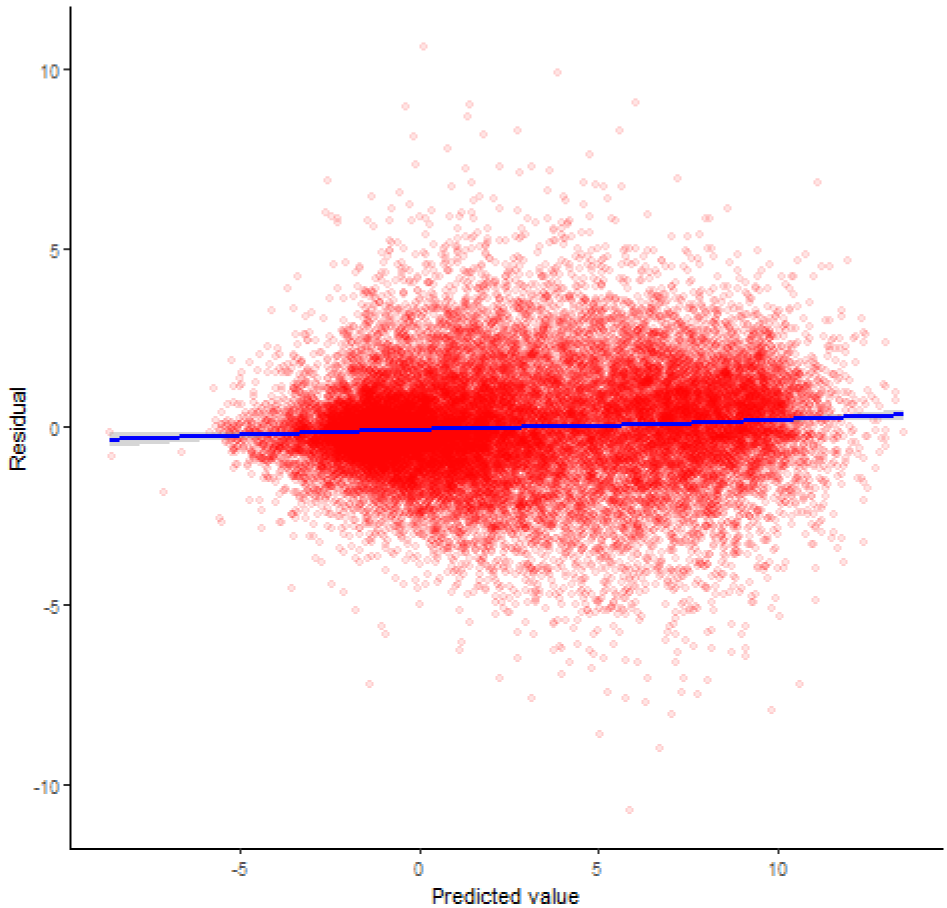

Figure 26: Predicted Values and Errors Produced by the Model, Test Dataset, Province of Quebec.

To validate the results of the analyses described above using external data, we compared the mapped results with two sources of information:

A layer produced by the Centre d'enseignement et de recherche en foresterie (CERFO) for urbanized Quebec using 2012–2013 data mainly derived from satellite imagery. This is a nine-class ordinal variable describing the heat/cold island phenomenon.

Digital data were recorded in the field using 75 temperature sensors distributed throughout Quebec City. These are three average temperature values (24h, diurnal, nocturnal) estimated for the period of July 1 to September 1, 2022.

Table 38 shows the correlation coefficients on the estimated ranks between the temperature predicted by the model and the external validation data. These correlations, of medium intensity, are all statistically significant at the 0.01 threshold.

Table 38: Correlation between the temperature predicted by the model and the external data.

Indicator	Spearman's RHO and p value
CERFO	0.644; $p < 0.01$
Average sensor temperature	0.460; $p < 0.01$
Average daytime sensor temperature	0.346; $p < 0.01$
Average nocturnal sensor temperature	0.448; $p < 0.01$

3.5.2 Cartographic Representation

This section includes the details associated with the representation of the four mapped indices. Table 39 lists the geospatial data layers mapped, the discretization method, the number of classes, and the colour palette used.

Table 39: Discretization and Colour Palettes Used in the Graphic Representation of Different Layers

Layer	Discretization method	Number of classes	Colour palette
Sensitivity	Quantiles per province	5	
Coping capacity	Quantiles per province	5	
Vulnerability	Quantiles per province	5	
Exposure	Quantiles per province	5	
Relation between vulnerability and exposure	Quantiles per variable and per province	4 by 4	
Urban heat islands	Equal amplitude	22	

3.5.2.1 Sensitivity, Coping Capacity and Vulnerability Indices

For the sensitivity and coping capacity indices, the numerical value of the indices obtained was classified into quintiles, by province. The resulting classes were subsequently labeled as follows: very low, low, moderate, high, very high (Figures 27 and 28).

For the vulnerability index, a normalization between 0 and 1 of the sensitivity and coping capacity indices was applied, then an arithmetic operation was performed to create the new index (Section 3.4.3) so that the range of values of the index extends from 0 to 2. This new result was classified into quintiles for each province and then labeled (Figure 29).

Figure 27: Sensitivity Index to Heat Waves – Ottawa Region

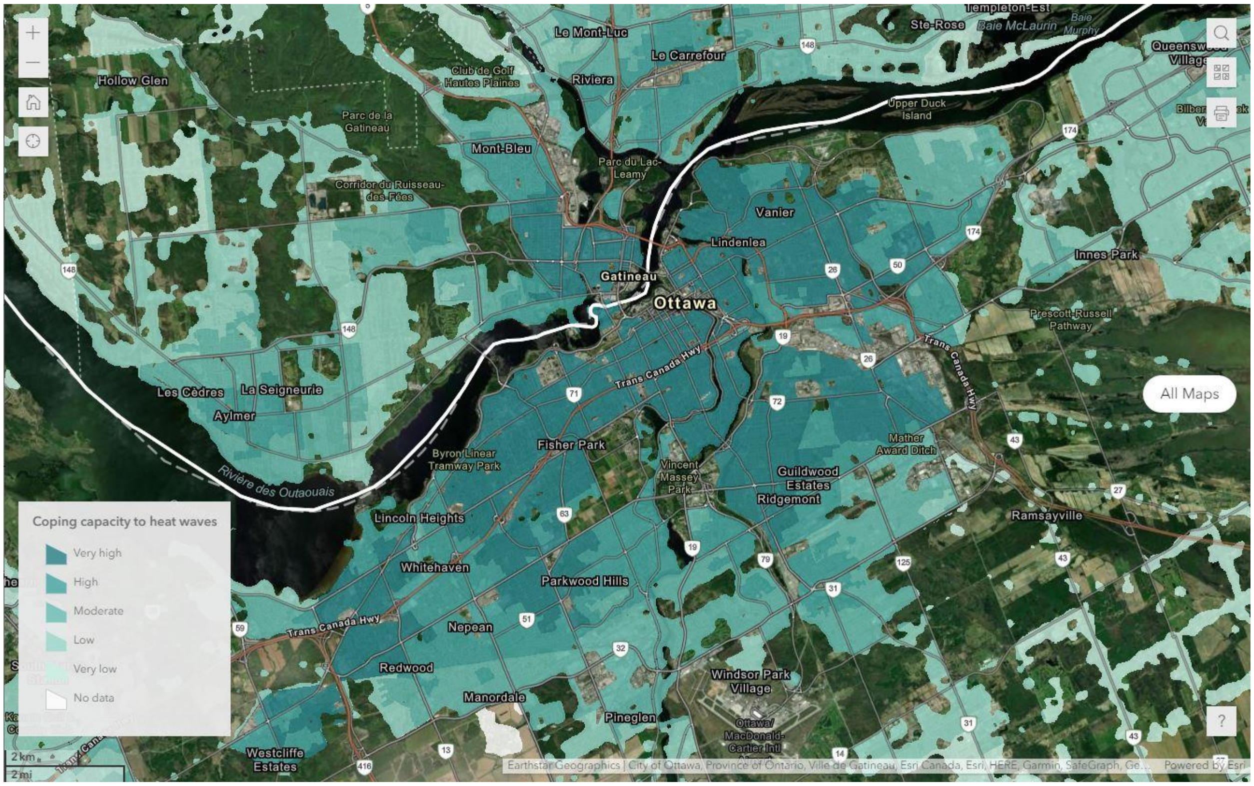

Figure 28: Coping Capacity Index to Heat Waves – Ottawa Region

Figure 29: Vulnerability Index to Heat Waves - Ottawa Region

3.5.2.2 Exposure Index

The map results were processed in two stages in order to display the phenomenon cartographically. First, classification (n=22) at equal intervals of the predicted values of relative temperature was carried out on the pixels overlapping the area covered by the model. Pixel values were smoothed using a cubic resampling method to improve map rendering by reducing image pixelation. Raster tiling was applied to the raster data layer before it was exported to a web service (Figure 30).

Figure 30: Urban Heat Islands or Difference in Temperature Between Urban Areas and Vegetated Areas with High Surface Permeability – Ottawa Region

For the exposure index, the mapping approach consisted in averaging the predicted temperature values relative to the inhabited areas of the Statistics Canada dissemination areas. The vector data were then classified into quintiles before being exported to a web service (Figure 31).

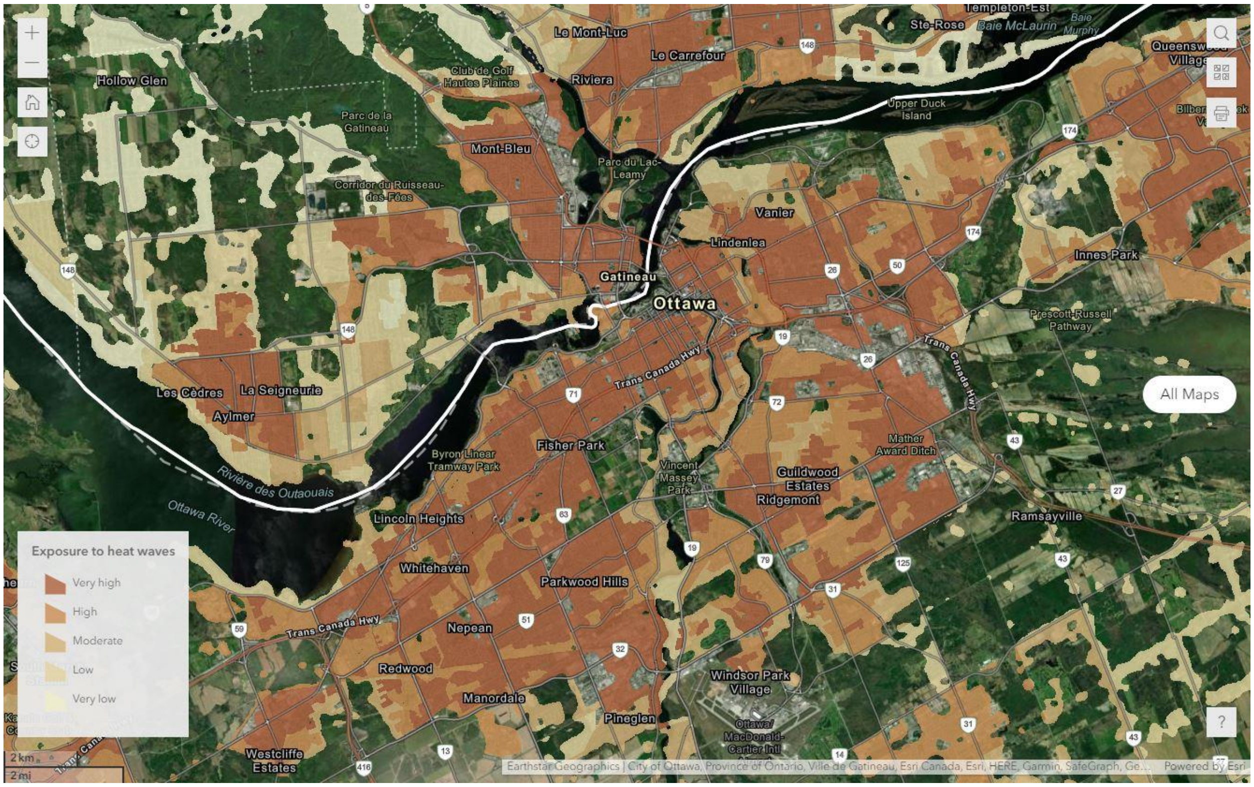

Figure 31: Exposure index to heat waves – Ottawa Region

3.5.2.3 Vulnerability and Exposure (Bivariate Map)

Lastly, the research team used a bivariate choropleth map to display the vulnerability and exposure indices on the same screen. A bivariate choropleth map is a thematic map that allows two variables to be represented simultaneously using different colours or patterns (Figure 32). This mapping method facilitates the visualization of two variables at the same time, allowing relationships between the two to be quickly grasped. This graphical representation can help identify areas where the two variables are correlated or uncorrelated and can aid decision-making by identifying areas with different profiles for the two variables. The data classification method used is a cross-tabulation of quartiles estimated at the provincial level for the vulnerability and exposure indices.

Figure 32: Vulnerability and Exposure (Bivariate Map) – Ottawa Region

3.6 CONCLUSION

One of the aims of this research project was to map the vulnerability and exposure to extreme heat waves of people living in housing in 156 urban regions across Canada. To achieve this, we carried out a literature review and defined the main concepts involved. This enabled us to identify the dimensions of vulnerability and exposure that needed to be estimated and to identify the data that needed to be used to calculate statistical and geographical indicators. The team also documented the methods generally used to synthesize information to create indices.

As part of this project, our team developed a methodology for selecting and constructing indicators of sensitivity, coping capacity, vulnerability, and exposure to extreme heat waves. Socio-economic and demographic indicators were calculated using 2021 Canadian census data aggregated at Statistics Canada's DA level. Indicators of proximity to various services were estimated. Our team used PCA to synthesize this information in the form of indices. A predictive model was used to map the urban heat island phenomenon on a fine scale, using a machine learning algorithm and indicators estimating vegetation density, surface imperviousness, density of built areas, proximity to water, geographical coordinates, and elevation.

Lastly, our team mapped the sensitivity, coping capacity, vulnerability, and exposure to extreme heat waves of 156 urban regions in Canada using univariate and bivariate choropleth mapping methods. A map of relative temperature differences at high spatial resolution was also produced (urban heat islands).

4 PRODUCTION OF A MAPPING TOOL

4.1 INTRODUCTION

The phenomenon of heat waves and urban heat islands is an increasingly significant issue for Canadian cities. To better understand and adapt to these phenomena, an interactive online mapping tool has been developed to meet the needs of two separate audiences. First, local stakeholders such as land-use planning, public health, and climate change adaptation professionals, who work on planning, implementing prevention measures, and managing heat waves and other related issues. Second, the general public, who is interested in understanding heat waves and urban heat islands in their community. This chapter will explore the features of the interactive mapping tool and how it can be used to better understand and adapt to the phenomena of heat waves and urban heat islands.

4.2 OBJECTIFS

The main objective of this component of the project is to produce an online mapping tool to disseminate the sensitivity, coping capacity, vulnerability, and exposure indices, and the location of urban heat islands for 156 urban regions in Canada, intended for the general public and local stakeholders. It also includes the following four sub-objectives:

- To design and produce a prototype of the interactive mapping tool that will be evaluated by local stakeholders to check the accuracy of the maps and gather their comments and assessments to improve the final product.
- To propose a final solution that will allow the maintenance of the mapping tool to ensure the long-term dissemination of results at low cost and without having to resort to costly professionals, who are difficult for the DGUL to mobilize, given the limited duration of the project's funding.
- To develop a website containing an accessible map in a user-friendly application offering some analysis functions.
- To make the information layers and methodology available to enable local stakeholders to extend the geographic scope of the project or customize the tool using local data that are not available at the analysis scale that we used.

4.3 Choice of Web Mapping Technology Solution

Esri (Environmental Systems Research Institute) products were used in the design of the mapping application. ArcGIS Pro software was initially used to design the maps, which were then uploaded to Université Laval's ArcGIS Online (AGOL) portal. AGOL offers a wide range of tools to create interactive web-based maps. Once the web-based maps were designed using the Map Viewer interface, they were integrated into the ArcGIS Experience Builder (ExB) module. ExB is used to develop, customize, and launch web-based applications. One of the reasons the team chose ExB was that the mapping interface adapts well to mobile platforms. ExB supports the switch from conventional web browsers to mobile devices browsers, allowing the interface to be customized according to screen size. In addition, ExB makes it possible to implement several maps in the same application and to synchronize them. To ensure the long-term viability of the work, the team will use the customization offered by ExB, enabling the layers and the application to be stored on the servers used by AGOL. Lastly, ExB enables extensive customization of the map window, including the integration of widgets into multiple applications.

4.4 Prototype Development and Evaluation

4.4.1 Development

To develop the prototype mapping tool, the team drew heavily on the work done for the Atlas of the Vulnerability of the Quebec Population to Climate Hazards (Barrette *et al.*, 2018). The aim was to develop a prototype where stakeholders could navigate and measure the quality of the maps produced, assessing the accuracy and relevance to their specific needs based on their in-depth knowledge of their territory, and leave us comments. It is also an opportunity to identify the improvements needed to guarantee an optimal experience for future users.

In the spring of 2022, an initial cartographic representation of the indices with 2016 Canadian census data was completed (2021 data was not yet available) and two prototype versions were created. For the first version, the sensitivity and exposure indices were integrated into the prototype for the Victoria, Windsor, Toronto, and Ottawa Census Metropolitan Areas (CMAs), along with a bivariate map of these two indices. For the second version, in the summer of 2022 (Victoria CMA only), in addition to the layers mentioned above, a layer representing the proportion of children (≤ 4 years) and elderly (≥ 65 years) was integrated, since 2021 census data was available for these variables.

The following widgets have been integrated: zoom, select, default map view, search, find my location, layer list, legend, basemap library, scale, attribute table and pop-up window. A special feature of the prototype is the integration of the editor widget, which allows users to create polygons in a sector of their city or region on the map and add a comment to identify an area that seems problematic, or simply to write a comment or a question.

4.4.2 Evaluation of the Tool by Local Stakeholders

When the tool was evaluated by local stakeholders, two components were implemented. The first component involved a series of interviews with representatives from the cities of Ottawa, Windsor, Toronto, and Victoria. The second component of the assessment was carried out in collaboration with the City of Victoria and the Capital Regional District. In the spring, a presentation of the prototype was made to a larger group, followed by the availability of the tool for the summer season, and a survey was carried out in the fall to assess its relevance.

4.4.2.1 Interviews with Stakeholders from the Cities of Windson, Toronto, Ottawa and Victoria

From April 8 to May 2, 2022, we met with stakeholders from four major Canadian cities in the study area covered by the project (Ottawa: three stakeholders, Windsor: one stakeholder, Victoria: five stakeholders, and Toronto: one stakeholder). At least one stakeholder per city had been previously contacted in the summer of 2021. The stakeholders were chosen for their in-depth knowledge of their city and the realities related to heat island and heat wave management.

4.4.2.1.1 Objectives

The general objective of the interviews was to discuss with the community stakeholders who the potential users of the cartographic tool would be. The objectives of the meetings were:

- Evaluate whether our indices (sensitivity and exposure) represent the reality experienced in their city.
- Evaluate the user-friendliness of our cartographic tool (use of the different layers of information, use of pop-up windows to see the values of the variables included in our indices).
- Understand how the cartographic tool will assist stakeholders in their field interventions, their projects, and their heat wave management, and whether it meets their needs.

4.4.2.1.2 Interview Methodology

The interviews with the stakeholders were conducted in the form of open discussions, as the team wished to foster an inductive approach to data collection and analysis. The inductive approach is a bottom-up approach prioritizing data and lived experience, while the analysis framework is built as the project progresses. The same questions were asked at each meeting. The interviews were recorded with the Teams (3) or Zoom (1: Windsor) software. They were transcribed using the Word dictation tool and were checked, ordered, and manually corrected in their entirety. The City of Toronto also sent comments through our cartographic tool (editor widget) and the City of Ottawa sent a list of comments after the meeting. In total, six documents make up the corpus of information covered by the current thematic analysis (four interview transcripts and two comment files). The qualitative thematic analysis of the text was performed using the NVivo software version 1.6.1 (QSR International). The entire text was coded, and a hierarchical node structure was used to encode the material (14 parent nodes (themes) and 49 child nodes (sub-themes)).

Apart from our questions, the interventions of both the participants from the four cities and our team from Université Laval were coded. Since these were open discussions, much of the information would have been lost if the text from our team had not been coded. However, the text was coded in two separate files and the results were divided into several categories: suggestions from the stakeholders, assessment of the representation of reality in the field, and general comments from the city stakeholders only.

A thematic analysis of the information drawn from the interviews was conducted. The results were divided into two categories: the assessment of the format and content of the cartographic tool, and the main themes addressed during the interviews.

4.4.2.1.3 Results

Assessment of the format and content of the cartographic tool

All of the main themes relating to the format and content of the cartographic tool (access to project materials, indices and methodology, model and limits, cartographic representation of the ecumene, feedback and evaluation of the cartographic tool, stakeholders' suggestions, interface users, use of the cartographic interface, and general comments) were addressed by stakeholders of the four participating cities, while 25 out of 34 subthemes were addressed by at least three of the four major cities (Table 40).

Access to Project Materials

The question regarding the access to project materials was mentioned several times (47). Several questions were of a general nature (13), others were more specific such as the access to the cartographic tool (13), to the raw data, and to our methodology (21). The stakeholders would like to have access to the raw data and the methodology to integrate one or more of our indices into their own cartographic software, into their regional or local study of heat waves, or to add more specific data to our indices that we were unable to incorporate on a national scale.

Indices and Methodology

A significant portion of the interviews was used to discuss the project's indices and methodology, which were mentioned 122 times. The stakeholders had many questions about the variables included in the sensitivity (45 mentions) and exposure (45 mentions) indices, and the multivariate data analyses that were performed to create them. The coping capacity index that was being developed was also mentioned 10 times. There were also 22 mentions concerning the indices and the methodology in general.

Model and Limits

The theme of the model and its limits was discussed 77 times. The following sub-themes were often mentioned: the absence of data on the air conditioning of housing units in the vulnerability index (7), the absence of data on the effects of bodies of water in the exposure index (6), the delays related to the release dates of the 2021 census data by Statistics Canada (14), the representation of the heterogeneity of the study area in the model (1), the language used for the tool and the methodological documents (12), the use of Statistics Canada dissemination areas as unit boundaries for the indices (14), the variables included in the model (7), and the areas not covered by the indices (16).

Cartographic Representation of the Ecumene

The cartographic representation of the ecumene was mentioned 16 times. This is an important theme since we use Statistics Canada's dissemination areas as unit boundaries, which can lead to inconsistencies when a large part of the unit is in an industrial zone, for example. The subject was addressed in all four interviews and the ecumene map layer will be added to the tool this year.

Feedback and Evaluation of the Cartographic Tool

Feedback and evaluation of the cartographic tool was one of the main objectives for this interview phase and was addressed 85 times. The stakeholders in the four cities assured us that our indices covered their entire region and more. There were 11 mentions of this subject. The usefulness of the tool (6 mentions) and its sustainability (2 mentions) were also discussed. The representation of the reality in the field was mentioned 61 times. Of these, 46 mentioned an accurate representation of reality. On 11 occasions, the stakeholders questioned the representation of the reality in the field in relation to the index, but this was rather due to a lack of knowledge of field data on their part at this precise analysis scale and not a misrepresentation of reality. On only four occasions, the stakeholder did not believe that it was a good representation of reality, and only for a very specific sector of the city. However, at the scale of the city or even neighbourhoods, all the stakeholders found that our indices seemed to be in line with their vulnerability and exposure knowledge of the city.

Stakeholder Suggestions

The stakeholders suggested several ideas during this interview phase (27 mentions). Twelve technical suggestions were counted. These included the addition of a variable to our model, such as the use of air conditioning. The stakeholders also mentioned ideas for alternative uses of the tool on 15 occasions, such as identifying the best place to install a water fountain in a public area, where to prioritize tree planting, or using the vulnerability index to improve socio-environmental equity in their city.

Interface Users

The stakeholders with whom we spoke to come from a variety of backgrounds, although most of them had public health connections. During the interviews, the specialization of several potential interface users was mentioned: land use planning (7), environment and climate change (8), equity, diversity and inclusion (5), heat wave response planning (3), public health (17), and others (4). It was also mentioned on several occasions that the public would benefit from access to this cartographic tool.

Use of the Cartographic Interface

We counted 66 mentions of the use of the cartographic interface, 10 general mentions, 21 concerning the use of the comment tool, 14 concerning the use of the various layers representing the indices, and 21 concerning the use of the pop-up windows. The stakeholders greatly appreciated the presence of pop-up windows presenting the index calculation results and the variables included in them. Although the comment tool was mentioned several times, only the stakeholder from the City of Toronto used it to send us comments.

General Comments

Finally, although an "emotion analysis" (the assessment of emotions, attitudes, and opinions) was not carried out in *NVivo*, a sub-category of encoding was created (positive general comments from stakeholders) and it contains 54 mentions. Overall, general comments from the stakeholders were from very positive for the four cities interviewed, and no negative comments were made.

Table 40: Results of the Qualitative Analysis of the Texts (Evaluation of the Form and the Content of the Mapping Tool)

Themes covered	Number of mentions during the interviews	Number of cities that addressed the theme
Access to project materials	**47**	**4**
General (access to project materials)	13	4
Use of the map interface	13	4
Use of the raw data and methodology	21	4
Indices and methodology	**122**	**4**
General (indices and methodology)	22	4
Sensitivity index	45	4
Exposure index	45	4
Coping capacity index	10	2
Model et limits	**77**	**4**
Lack of data on air conditioning	7	2
Lack of data on water bodies	6	2
Publication date of the census data	14	3
Heterogeneity of the area	1	1
Tool and document language	12	3
Use of the Das of Statistic Canada as unit limits	14	4
Variables included in the model	7	4
Areas not covered by the indices	16	4
Cartographic representation of the ecumene	**16**	**4**
Mapping tool feedback and evaluation	**85**	**4**
Coverage of the stakeholders' area	11	4
Utility of the tool	6	3
Tool durability	2	1
Representation of the reality on the field	**(61)**	**4**
Good representation	46	4
Questions about the representation	11	3
Misrepresentation	4	2
Stakeholder suggestions	**27**	**4**
Technical suggestions	12	3
Alternative uses of the tool and project data	15	4
Tool users	**44**	**4**
Land use planning	7	4
Environment and climate change	8	4
Equity, diversity, and inclusion	5	2
Heat wave response planning	3	2
Public health	17	4
Other	4	3
Use of the map interface	**66**	**4**
General (use of the map interface)	10	4
Use of the comment tool	21	3
Use of the different layers	14	4
Use of the pop-up windows	21	4
General positive comments	**54**	**4**

4.4.2.1.3.1 Main Themes Addressed in the Interviews

Just like in the previous section, the five main themes (environmental equity, affected populations, heatwaves and heat islands, building vulnerability, and land vulnerability) were addressed by the various stakeholders. Thirteen of the sub-themes were addressed by at least two cities (Table 41).

With regards to environmental equity, although addressed by all cities (13 mentions) it was particularly important to the stakeholders from the City of Victoria, who seemed to attribute a more social perspective to their new heat wave action plan. In terms of the populations concerned (53 mentions), underprivileged populations were mentioned most often during the interviews (15 mentions), followed by the general populations (13), newcomers (12), the elderly (6), affluent individuals (6), and children (1). Heat waves and heat islands were mentioned on 34 occasions, and for the majority of these (25), the stakeholders talked about them in general terms; however, on 4 occasions they referred more specifically to adaptation and mitigation strategies, on 3 occasions to future heat waves, and on 2 occasions to past heat waves. Building vulnerability was discussed on 30 occasions. Densely populated neighbourhoods (11 mentions), apartments and high-rise buildings (9 mentions), building age (6 mentions), building air conditioning (3 mentions), and roof albedo (1 mention) were the sub-themes in this category. Finally, the theme of land vulnerability was discussed 31 times during the interviews or through stakeholder comments. For example, the lack of green spaces or the high proportion of impervious surfaces were coded in this category.

Table 41: Results of the Qualitative Analysis of the Texts (Major Themes Covered)

Themes covered	Number of mentions during the interviews	Number of cities that addressed the theme
Socio-environmental equity	**13**	**4**
Concerned populations	**53**	**4**
Disadvantaged people	15	2
General population	13	4
Newcomers	12	3
Elderly people	6	3
Affluent people	6	2
Children	1	1
Heat waves and heat islands	**34**	**4**
General (heat waves and heat islands)	25	4
Adaptation and mitigation strategies	4	2
Heat waves (future)	3	2
Heat waves (past)	2	2
Building vulnerability	**30**	**4**
Densely populated neighbourhoods	11	3
Apartment buildings and towers	9	4
Building age	6	3
Building air conditioning	3	2
Roofing and albedo	1	1
Area vulnerability	**31**	**4**

4.4.2.1.3.2 Feedback and Suitability of the Solution for the Needs Expressed by Users

The feedback from the stakeholder interviews from the cities of Ottawa, Windsor, Victoria, and Toronto was very positive. The feedback was also very encouraging regarding our vulnerability and exposure indices. According to the stakeholders, the indices appear to represent the reality in the four major cities. When it came to assessing the user-friendliness of the cartographic tool (use of different information layers and pop-up windows to view the variable values included in our indices), the stakeholders seemed satisfied with the web interface created. In terms of whether the cartographic tool will be able to help stakeholders in their field interventions, heat wave management, and whether the prototype of the tool did indeed meet their needs, the feedback was also very positive. The stakeholders mentioned several times the tool's usefulness and the different uses they could make if it in the future. The free access to the data and to the team's work was a very positive point. It also seemed very important not only to make the cartographic tool accessible to the public and local stakeholders, to easily visualize the vulnerability of the study area using the maps, but also to make the data and methodology available. As mentioned above, the stakeholders want to have access to the raw data to integrate one or more of their own indices into their own cartographic software or regional or local heat wave study, or to add more precise data to our indices. This way, they will be able to better target the interventions they need to make in their city to mitigate the heat wave effects for the concerned populations: white roofs, park development, addition of municipal swimming pools, etc.

Finally, several of the steps taken later in the project succeeded in responding to certain requests or questions from the stakeholders. For example, the addition of a dasymetric map layer to represent the ecumene and the addition of the coping capacity index in the model to increase the available information on the city's socio-environmental inequalities. Moreover, the 2021 census data was used, which was not available at the time of the prototype, and the methodological documents were translated into English to help stakeholders understand our project methodology.

4.4.2.2 Use of a Prototype in the Summer 2022 by the City of Victoria and Capital Regional District

During the spring 2022 interviews, the City of Victoria showed great interest in our project and cartographic tool following the major heat wave that hit British Columbia in the summer of 2021 that resulted in 619 deaths. Given their needs and interest, it was agreed that the City of Victoria and the Capital Regional District could test the tool prototype in the summer of 2022. To this end, an ArcGIS Online interface was created (see section 4.4.1).

To introduce the prototype and the project, a meeting was held with around 25 stakeholders from the City of Victoria, the Capital Regional District, and the University of British Columbia. The stakeholders came from a variety of backgrounds: land use planning, public health, regional emergency management partnership, municipal emergency management program, climate action program and climate adaptation planning, housing planning program, department of transportation and sustainable transportation planning, office of equity, diversity and inclusion, stormwater management and green infrastructure, community planning, urban forestry services, and UBC's Institute for Resources, Environment and Sustainability.

4.4.2.2.1 Objectives

The meeting objective was not only to present the cartographic tool prototype, but also to answer questions about the tool, the methodology, and the project, and to collect information on the reliability and user-friendliness of the interface from stakeholders who will use the final version in 2023. The prototype of the cartographic tool with explanatory documents was sent to stakeholders a few days before the meeting so that they could go through them.

In exchange, they agreed to complete a survey in the fall of 2022 to give us their opinions and comments, in order to evaluate and improve the prototype before the final version is released in the spring of 2023.

4.4.2.2.2 Results

The survey was published in English using the ESRI tool, Survey 123. The stakeholders had 10 days to complete it. It consisted of 16 questions and 13 people responded, about half of the stakeholders present at the June 13 meeting. Eleven respondents work for the City of Victoria and 2 work for the Capital Regional District. The respondents work in various sectors : climate action program and climate adaptation planning (3 respondents, 31%), housing planning program (1 respondent, 8%), community planning (3 respondents, 23%), office of equity, diversity and inclusion (3 respondents, 23%), land use planning (2 respondents, (15%), stormwater management and green infrastructure (1 respondent, 8%), and geographic information system (GIS) (1 respondent, 8%). This question was a multiple-choice question, where respondents could indicate that they worked in more than one sector. As a result, there are 15 entries.

Five people replied that they had used the cartographic tool during the summer period as part of their work. Three people had used it once, one person 2-3 times, and one person more than 10 times. Moreover, 80% of those who used the tool said it was useful or very useful in their work. The cartographic tool was used in anticipation of a heat wave or during a heat wave on one occasion, and for another reason on three occasions. The alternative reasons listed for the use of the tool by the stakeholders are:

- General interest in shelter mapping
- Urban planning as a teaching tool
- To enrich personal knowledge
- Climate adaptation planning
- As a basis for localized work on local temperatures

Eight stakeholders consulted the summary report as part of their work. According to 75% of them, it answered most or all of their questions. The stakeholders left comments to help us refine the summary report in preparation for the final version in the spring of 2023. Among other things, they wanted more information on data sources and the limitations of the methodology, and the addition of simple graphics to illustrate key points. Only 1 of 13 respondents had downloaded the geospatial files, and none had integrated them with other maps.

One of the main points of the stakeholder consultation process was to find out whether our indices are representative of the reality. With regards to this question, 77% of the respondents said that the information represented on the maps was moderately to very representative of the reality in their neighbourhood, city, or region. However, in the comments, some mentioned that they did not have enough knowledge of the reality at this scale to be able to answer this question properly. Finally, the stakeholders left many comments, notably on the functionalities and improvements they would like to see.

4.4.2.2.3 Use of the Cartographic Tool Prototype

The online prototype of the mapping of the vulnerability and exposure to extreme heat waves of populations in the Victoria census metropolitan area was consulted 257 times between the beginning of May and the end of September (Appendix 2).

4.5 DEVELOPMENT OF A FINAL VERSION OF THE APPLICATION

4.5.1 Mapped Layers

A total of six geospatial data layers (sensitivity, coping capacity, vulnerability, exposure, vulnerability/exposure, and urban heat islands) have been mapped and implemented in the ExB application, where it is possible to view just one of these maps at a time or, in “2-map” mode, to view the bivariate vulnerability/exposure map with the urban heat island map simultaneously. In the “2-map” mode, the map view is synchronized to facilitate exploration and comparison of the two data layers.

4.5.2 Selected Features

The widgets integrated into the final version of the application have been chosen to enhance the user experience, enabling them to better understand the data represented and helping them get the information they are looking for as quickly and efficiently as possible. We had to keep in mind the two separate audiences for this application and ensure that it was user-friendly for all potential users.

Table 42 describes the use of each widget, while Table 43 shows the widgets available for different types of computing devices (computer, tablet or phone).

Table 42: Description of How to Use the Selected Widgets for the Final Version of the Mapping Application.

Widget	Use
Zoom (buttons and tactile)	Adjust the map scale to display the desired details.
Default map view	Return to the default map view. For the current project, we see our entire study, so most of Canada is visible.
Find my location	Detects the user's location and zooms to their area.
Legend	Explains the meaning of the colours on the map for the different maps produced.
Scale	Gives an idea of the ratio between the distance measured on the map and the real distance on the ground. It is displayed in kilometres and miles.
Search	Allows the user to find a specific city, location, or address by entering one or more words in the text box to find an address faster than by browsing the map.
Basemap	Presents different basemap options that can be selected to accompany the layers produced for the project, for example: imagery or topographic.
Print	Allows you to create a map in a JPG format representing the chosen cartographic extent that can be saved on the user's computer or tablet and later printed.
All maps (map list)	Allows the user to select one of more maps
Navigation help	Brings the users to a help section. This section is available for each type of device (computer, tablet, and telephone) and explains how the various widgets integrated in the map application work.
Pop-up window	Provides additional information on the variables and the indices for each dissemination area for the sensitivity, coping capacity, vulnerability, exposure, and vulnerability/exposure maps.

Table 43: Available Widgets According to Different Types of Computing Devices

		Type of support		
		Computer	Tablet	Telephone
Widgets	Zoom in and Zoom out	X		
	Tactile zoom		X	X
	Default map view	X	X	X
	Find my location	X	X	X
	Legend	X		
	Layers (Layers and Legend)		X	X
	Scale	X	X	
	Search	X		
	Basemap	X	X	X
	Print	X	X	
	All maps	X	X	X
	Navigation help	X	X	X
	Pop-up window	X	X	X

4.6 Website

The thematic content populating the various sections of the website was developed by our team. Considering that users of the solution are not necessarily familiar with the scientific terminology used to describe the various concepts and methods employed in the project, a special effort was made to popularize the content. The main sections of the website are as follows:

Map: This is the home page of the website. It provides direct access to the mapping application and to a video explaining the impact of heat waves on the health of Canadians.

Project: This page contains textual information on the impacts of heat waves on population health, the objectives of the research project, the area covered by the analyses, and information on the project's partners and funding sources. It also includes a video popularizing the problem of heat waves and urban heat islands.

Methodology: This page contains textual information on the main methodological steps involved in mapping vulnerability and exposure. There are also brief descriptions of the methodological approaches used to calculate the coping capacity, exposure, sensitivity, and vulnerability indices. It also includes a video popularizing the mapping process.

Extraction: This page allows users to download geospatial files containing the various indicators and indices for Canada's 156 urban regions and for each of the provinces. The downloadable compressed files contain a geodatabase including a raster file and a vector file, along with a PDF metadata file describing the data in detail. Users can download data using a drop-down menu or a dynamic map.

Navigation Help: This page describes the various widgets and functionalities available in the map applications depending on whether the site is consulted using a computer, tablet, or smartphone.

Team: This page lists all the people involved in developing the solution—professors, professionals, and students. In addition to listing these people, their photos are displayed along with the expertise they brought to the project and how they can be reached (email, LinkedIn, ResearchGate).

Contact: This page provides information on how to contact the research team. Users can also write to the team using a contact form embedded in the page.

Frequently Asked Questions (FAQ): This page contains additional information on the various dimensions of the issues addressed by the team (e.g., What is a heat wave?), project dimensions (e.g., How did you create the heat island map?), how the mapped information should be used (e.g., Why should I find out about vulnerability in my neighbourhood?), or certain concepts raised by the team (e.g., What is vulnerability?). This information takes the form of a question-and-answer text.

Useful Links: This page includes URL links to external resources in English and French. These include information on heat waves, urban heat islands, adaptation measures, health impacts, Canadian alert systems, and climate change.

A menu in a banner at the top of the website provides access to each page. The colour of the website also varies according to the time of day, switching to dark mode at dusk and to light mode at sunrise. Site visitors can switch from one mode to another at any time by pressing an icon at the top of the screen. It is also possible to switch from the French to the English version, and vice versa, by pressing a button at the top of the screen.

4.7 CONCLUSION

The ultimate objective of the project was not only to produce a mapping tool, but also to ensure that it was adapted to the needs of its users (planners, public health professionals and elected representatives, but also the general public). Particular attention was paid to the evaluation of the tool by informed users during its development. The team met with planning and public health professionals. It also evaluated the mapping interface by presenting them with a prototype. In addition, these meetings provided an opportunity to assess whether the indices accurately represented the reality of their territory and to learn more about how the mapping tool will meet the stakeholders' needs.

The team had to make technological choices that would enable them to produce an interactive mapping tool with features that would facilitate website navigation, while at the same time favouring updates and the tool's durability.

5 GENERAL CONCLUSION

The conclusion of our scientific report highlights the results of our project aiming to develop an online interactive map for the analysis of the vulnerability and the exposure to extreme heat waves in major Canadian cities. Our main objective was to create a tool used for prevention and intervention by municipal actors and help them better understand at-risk areas and take appropriate action. To this end, we set three specific objectives.

The first specific objective was to identify the needs of municipal managers, professionals, and planners in terms of extreme heat exposure and vulnerability mapping. We then interviewed potential users to identify their needs and concerns. An analysis of the issues and needs identified by the municipal actors then served as a guide in the development of the mapping application.

Our second specific objective was to construct a set of mappable indices representing the various dimensions of vulnerability and exposure to extreme heat waves. We created a heat wave sensitivity index, a coping capacity index, an exposure index, and a vulnerability index. The indices were only mapped for the inhabited areas of major Canadian cities, which involved dividing the dissemination blocks based on a file representing the ecumene of the country's entire inhabited area and applying a dasymetric mapping procedure.

The third specific objective was to produce an interactive online map incorporating the indices. We then launched a website with an interactive mapping application (heatwaves.ffgg.ulaval.ca/ vaguesdechaleur.ffgg.ulaval.ca) including the different layers of geospatial data produced by the research team. The geospatial data can be downloaded directly on the website. The information on the website will provide users with a clear picture of the issues surrounding urban extreme heat waves and the methodology used by the team.

In conclusion, we hope this project will help municipal actors in their work and that the mapping application will be helpful for everyone living in a major Canadian city. We believe that the methodological approaches used could be applicable to other scientific projects and that the results obtained can be used for other similar contexts.

6 BIBLIOGRAPHY

Adam-Poupart, A., Nicolakakis, N., Anassour Laouan Sidi, E., Berry, P., Campagna, C., Chaumont, D., Hamel, D., Labrèche, F., Sassine, M.-P., Smargiassi, A., & Zayed, J. (2021). *Changements climatiques et vulnérabilités à la chaleur des travailleuses et travailleurs canadiens – regard sur les provinces du centre et de l'ouest du Canada*. Institut national de santé publique du Québec. https://www.inspq.qc.ca/publications/2791

ADEME. (2013). *Indicateurs de vulnérabilité d'un territoire au changement climatique*. https://librairie.ademe.fr/changement-climatique-et-energie/3479-indicateurs-de-vulnerabilite-d-un-territoire-au-changement-climatique-recueil-de-litterature-internationale-9782358382663.html

Alberini, A., Gans, W., & Alhassan, M. (2011). Individual and public-program adaptation: coping with heat waves in five cities in Canada. *International Journal of Environmental Research and Public Health*, *8*(12), 4679–4701. https://doi.org/10.3390/ijerph8124679

Almeida, C. R. D., Teodoro, A. C., & Gonçalves, A. (2021). Study of the urban heat island (UHI) using remote sensing data/techniques: A systematic review. *Environments*, *8*(10), 105. https://doi.org/10.3390/environments8100105

Alonso, L., & Renard, F. (2020). A Comparative Study of the Physiological and Socio-Economic Vulnerabilities to Heat Waves of the Population of the Metropolis of Lyon (France) in a Climate Change Context. *International Journal of Environmental Research and Public Health*, *17*(3), 1004. https://doi.org/10.3390/ijerph17031004

Apreda, C., D'Ambrosio, V., & Di Martino, F. (2019). A climate vulnerability and impact assessment model for complex urban systems. *Environmental Science & Policy*, *93*, 11-26. https://doi.org/https://doi.org/10.1016/j.envsci.2018.12.016

Archila Bustos, M. F., Hall, O., Niedomysl, T., & Ernstson, U. (2020). A pixel level evaluation of five multitemporal global gridded population datasets: a case study in Sweden, 1990–2015. *Population and Environment*, *42*(2), 255-277. https://doi.org/10.1007/s11111-020-00360-8

Azhar, G., Saha, S., Ganguly, P., Mavalankar, D., & Madrigano, J. (2017). Heat Wave Vulnerability Mapping for India. *International Journal of Environmental Research and Public Health*, *14*(4), 357. https://doi.org/10.3390/ijerph14040357

Bao, J. Z., Li, X. D., & Yu, C. H. (2015). The Construction and Validation of the Heat Vulnerability Index, a Review. *International Journal of Environmental Research and Public Health*, *12*(7), 7220-7234. https://doi.org/10.3390/ijerph120707220

Barrette, N., Vandersmissen, M.-H., Roy, F., Mercier, G., Brousseau, Y., Berthold, E., Guilbert, E., Lalonde, B., Beaudoin, Y., Genois, A., Bustinza, R., Thibault, M., Bleau, N., Tanguay, L.-P., Dionne, M., Aubin, L., Chartrand, M., Déry, J.-S., Dovonou, P., …Turcotte, S. (2018). *Atlas web de la vulnérabilité de la population Québécoise aux aléas climatiques : Rapport de recherche*. Université Laval – Département de géographie. https://atlas-vulnerabilite.ulaval.ca/wp-content/uploads/2022/03/RapportBarrette2018.pdf

Basu, R., & Samet, J. M. (2002). Relation between elevated ambient temperature and mortality: a review of the epidemiologic evidence. *Epidemiologic reviews*, *24*(2), 190-202. https://doi.org/10.1093/epirev/mxf007

Bélanger, D., Berry, P., Bouchet, V., Charron, D., Clarke, K.-L., Doyon, B., Fleury, M., Furgal, C., Gosselin, P., Lamy, S., Lindsay, L. R., McBean, G., Ogden, N., Séguin, J., Schuster, C. J., & Soskolne, C. L. (2008). *Human health in a changing climate: a Canadian assessment of vulnerabilities and adaptive capacity*. Santé Canada. https://publications.gc.ca/collections/collection_2008/hc-sc/H128-1-08-528E.pdf

Bernard, J., Musy, M., Calmet, I., Bocher, E., & Kéravec, P. (2017). Urban heat island temporal and spatial variations: Empirical modeling from geographical and meteorological data. *Building and Environment*, *125*, 423-438. https://doi.org/10.1016/j.buildenv.2017.08.009

Berry, P., Blagden, P., Campagna, C., Egyed, M., Enright, P., Gosselin, P., Harper, S., Hayes, K., Atkinson, D., Stout, R., Halseth, R., Greenwood, M., Ogden, N., Schnitter, R., & Takaro, T. T. (2022). *La santé des Canadiens et des Canadiennes dans un climat en changement : faire progresser nos connaissances pour agir*. Santé Canada. https://doi.org/10.4095/329546

Bhaduri, B., Bright, E., Coleman, P., & Urban, M. L. (2007). LandScan USA: a high-resolution geospatial and temporal modeling approach for population distribution and dynamics. *GeoJournal*, *69*(1-2), 103-117. https://doi.org/10.1007/s10708-007-9105-9

Bourque, J., Poulin, N. & Cleaver, A. F. (2006). Évaluation de l'utilisation et de la présentation des résultats d'analyses factorielles et d'analyses en composantes principales en éducation. *Revue des sciences de l'éducation*, *32*(2), 325–344. https://doi.org/10.7202/014411ar

Breiman, L. (2001). Random Forests. *Machine learning*, *45*, 5-32. https://doi.org/10.1023/A:1010933404324

British Columbia Coroners Service. (2022). *Extreme Heat and Human Mortality: A Review of Heat-Related Deaths in B.C. in Summer 2021*. Ministry of Public Safety and Solicitor General. https://www2.gov.bc.ca/assets/gov/birth-adoption-death-marriage-and-divorce/deaths/coroners-service/death-review-panel/extreme_heat_death_review_panel_report.pdf

Bush, E., & Lemmen, D.S. (2019). *Rapport sur le climat changeant du Canada*. Gouvernement du Canada. https://doi.org/10.4095/314614

Centre intégré de santé et de services sociaux de Laval. (2019). *Vagues de chaleur de l'été 2018 : Rapport d'enquête épidémiologique*. https://www.lavalensante.com/fileadmin/internet/cisss_laval/Documentation/Sante_publique/Rappo Rap_et_memoires/2019/Rapport_vague_de_chaleur_2018_Laval_final_2019-05-29__2_.pdf

Chen, Q., Ding, M. J., Yang, X. C., Hu, K. J., & Qi, J. G. (2018). Spatially explicit assessment of heat health risk by using multi-sensor remote sensing images and socioeconomic data in Yangtze River Delta, China. *International Journal of Health Geographics*, *17*, 15. https://doi.org/10.1186/s12942-018-0135-y

Chen, S., Yang, Y., Deng, F., Zhang, Y., Liu, D., Liu, C., & Gao, Z. (2022). A high-resolution monitoring approach of canopy urban heat island using a random forest model and multi-platform observations. *Atmospheric Measurement Techniques*, *15*(3), 735-756. https://doi.org/10.5194/amt-15-735-2022

Cheng, W., Li, D., Liu, Z., & Brown, R. D. (2021). Approaches for identifying heat-vulnerable populations and locations: A systematic review. *Science of The Total Environment*, *799*, 149417. https://doi.org/https://doi.org/10.1016/j.scitotenv.2021.149417

Christenson, M., Geiger, S. F., Phillips, J., Anderson, B., Giovanna, L., & Anderson, H. A. (2017). Heat Vulnerability Index Mapping for Milwaukee and Wisconsin. *Journal of Public Health Management and Practice*, *23*(4), 396-403. https://doi.org/10.1097/phh.0000000000000352

Climate Atlas of Canada. (2019). *Very Hot Days (+30°C)*. https://climateatlas.ca/map/canada/plus30_2030_85#z=3&lat=64.24&lng=-83.06

Conlon, K. C., Mallen, E., Gronlund, C. J., Berrocal, V. J., Larsen, L., & O'Neill, M. S. (2020). Mapping Human Vulnerability to Extreme Heat: A Critical Assessment of Heat Vulnerability Indices Created Using Principal Components Analysis. *Environmental Health Perspectives*, *128*(9). https://doi.org/10.1289/ehp4030

Crichton, D. (1999). The Risk Triangle. Dans J. Ingleton (dir.), *Natural Disaster Management* (p. 102-103). Tudor Rose.

Cutter, S. L., Boruff, B. J., & Shirley, W. L. (2003). Social Vulnerability to Environmental Hazards. *Social Science Quarterly*, *84*(2), 242-261. https://doi.org/10.1111/1540-6237.8402002

Dong, J. Q., Peng, J., He, X. R., Corcoran, J., Qiu, S. J., & Wang, X. Y. (2020). Heatwave-induced human health risk assessment in megacities based on heat stress-social vulnerability-human exposure framework. *Landscape and Urban Planning*, *203*, Article 103907. https://doi.org/10.1016/j.landurbplan.2020.103907

Durand C. (2003). *L'analyse factorielle et l'analyse de fidélité*. Université de Montréal – Département de sociologie. http://www.mapageweb.umontreal.ca/durandc/enseignement/methodesquantitatives/facteur9.pdf

Ellena, M., Breil, M., & Soriani, S. (2020). The heat-health nexus in the urban context: A systematic literature review exploring the socio-economic vulnerabilities and built environment characteristics. *Urban Climate*, *34*, 100676. https://doi.org/10.1016/j.uclim.2020.100676

Estoque, R. C., Ooba, M., Seposo, X. T., Togawa, T., Hijioka, Y., Takahashi, K., & Nakamura, S. (2020). Heat health risk assessment in Philippine cities using remotely sensed data and social-ecological indicators. *Nature Communications*, *11*(1), 1581. https://doi.org/10.1038/s41467-020-15218-8

Fernandez, P., Mourato, S., Moreira M., & Pereira, L. (2016). A new approach for computing a flood vulnerability index using cluster analysis. *Physics and Chemistry of the Earth*, *94*, 47-55. https://doi.org/10.1016/j.pce.2016.04.003

Field, C. B., Barros, V. R., Dokken, D. J., Mach, K. J., Mastrandrea, M. D., Bilir, T. E., Chatterjee, M., Ebi, K. L., Estrada, Y. O., Genova, R. C., Girma, B., Kissel, E. S., Levy, A. N., MacCracken, S., Mastrandrea, P. R., & White, L. L. (dir.). (2014). *Changements climatiques 2014 : Incidences, adaptation et vulnérabilité. Résumés, foire aux questions et encarts thématiques.* Groupe d'experts intergouvernemental sur l'évolution du climat (GIEC). https://www.ipcc.ch/site/assets/uploads/2018/03/WGIIAR5-IntegrationBrochure_fr-1.pdf

Florczyk, A. J., Melchiorri, M., Zeidler, J., Corbane, C., Schiavina, M., Freire, S., Sabo, F., Politis, P., Esch, T., & Pesaresi, M. (2020). The Generalised Settlement Area: mapping the Earth surface in the vicinity of built-up areas. *International Journal of Digital Earth*, *13*(1), 45-60. https://doi.org/10.1080/17538947.2018.1550121

Fraser, A. M., Chester, M. V., & Eisenman, D. (2018). Strategic locating of refuges for extreme heat events (or heat waves). *Urban Climate*, *25*, 109–119. https://doi.org/10.1016/j.uclim.2018.04.009

Fraser, A. M., Chester, M. V., Eisenman, D., Hondula, D. M., Pincetl, S. S., English, P., & Bondank, E. (2017). Household accessibility to heat refuges: Residential air conditioning, public cooled space, and walkability. *Environment and Planning B: Urban Analytics and City Science*, *44*(6), 1036-1055. https://doi.org/10.1177/0265813516657342

Gage, E. A., & Cooper, D. J. (2017). Relationships between landscape pattern metrics, vertical structure and surface urban Heat Island formation in a Colorado suburb. *Urban Ecosystems*, *20*, 1229-1238. https://doi.org/10.1007/s11252-017-0675-0

García-Santos, V., Cuxart, J., Martínez-Villagrasa, D., Jiménez, M. A., & Simó, G. (2018). Comparison of Three Methods for Estimating Land Surface Temperature from Landsat 8-TIRS Sensor Data. *Remote Sensing*, *10*(9), 1450. https://doi.org/10.3390/rs10091450

Gareth, J., Witten, D., Hastie, T., & Tibshirani, R. (2013). *An Introduction to Statistical Learning: with Applications in R*. Spinger.

Gasparrini, A., Guo, Y., Hashizume, M., Lavigne, E., Zanobetti, A., Schwartz, J., Tobias, A., Tong, S., Rocklöv, J., Forsberg, B., Leone, M., De Sarios, M., Bell, M. L., Guo, Y.-L. L., Wu, C.-F., Kan, H., Yi, S.-M., Coelho, M. S. Z. S., Saldiva, P. H. N., …Armstrong, B. (2015). Mortality risk attributable to high and low ambient temperature: a multicountry observational study. *The Lancet*, *386*(9991), 369-375. https://doi.org/10.1016/S0140-6736(14)62114-0

Gough, W., Anderson, V., & Herod, K. (2016). *Étude de modélisation de l'Ontario sur le changement climatique et la santé*. Ministère de la Santé et des Soins de longue durée de l'Ontario. https://www.health.gov.on.ca/fr/common/ministry/publications/reports/climate_change_toolkit/climate_change_health_modelling_study.pdf

Grigorescu, I., Mocanu, I., Mitrica, B., Dumitrascu, M., Dumitrica, C., & Dragota, C. S. (2021). Socio-economic and environmental vulnerability to heat-related phenomena in Bucharest metropolitan area. *Environmental Research*, *192*, 110268. https://doi.org/10.1016/j.envres.2020.110268

Guo, X., Huang, G. L., Jia, P., & Wu, J. G. (2019). Estimating Fine-Scale Heat Vulnerability in Beijing Through Two Approaches: Spatial Patterns, Similarities, and Divergence. *Remote Sensing*, *11*(20), 2358. https://doi.org/10.3390/rs11202358

Hair, J. F., Black, W. C., Babin, B. J., & Anderson, R. E. (2014). *Multivariate data analysis* (7e éd.). Pearson Education.

Hajat, S., O'Connor, M., & Kosatsky, T. (2010). Health effects of hot weather: from awareness of risk factors to effective health protection. *The Lancet*, *375*(9717), 856-863. https://doi.org/10.1016/s0140-6736(09)61711-6

Harlan S. L., Brazel, A. J., Prashad, L., Stefanov, W. L., & Larsen, L. (2006). Neighborhood microclimates and vulnerability to heat stress. *Social Science & Medicine*, *63*(11), 2847-2863. https://doi.org/10.1016/j.socscimed.2006.07.030

He, C., Ma, L., Zhou, L., Kan, H. D., Zhang, Y., Ma, W. C., & Chen, B. (2019). Exploring the mechanisms of heat wave vulnerability at the urban scale based on the application of big data and artificial societies. *Environment International*, *127*, 573-583. https://doi.org/10.1016/j.envint.2019.01.057

Ho, H. C., Knudby, A., & Huang, W. (2015). A Spatial Framework to Map Heat Health Risks at Multiple Scales. *International Journal of Environmental Research and Public Health*, *12*(12), 16110-16123. https://doi.org/10.3390/ijerph121215046

Ho, H. C., Knudby, A., Chi, G. Q., Aminipouri, M., & Lai, D. Y. F. (2018). Spatiotemporal analysis of regional socio-economic vulnerability change associated with heat risks in Canada. *Applied Geography*, *95*, 61-70. https://doi.org/10.1016/j.apgeog.2018.04.015

Ho, H. C., Knudby, A., Walker, B. B., & Henderson, S. B. (2017). Delineation of Spatial Variability in the Temperature-Mortality Relationship on Extremely Hot Days in Greater Vancouver, Canada. *Environmental Health Perspectives*, *125*(1), 66-75. https://doi.org/10.1289/ehp224

Houghton, A., & Castillo-Salgado, C. (2020). Analysis of correlations between neighborhood -level vulnerability to climate change and protective green building design strategies: A spatial and ecological analysis. *Building and Environment*, *168*, 106523. https://doi.org/10.1016/j.buildenv.2019.106523

Hulley, G., Shivers, S., Wetherley, E., & Cudd, R. (2019). New ECOSTRESS and MODIS Land Surface Temperature Data Reveal Fine-Scale Heat Vulnerability in Cities: A Case Study for Los Angeles County, California. *Remote Sensing*, *11*(18), 2136. https://doi.org/10.3390/rs11182136

Jagarnath, M., Thambiran, T., & Gebreslasie, M. (2020). Heat stress risk and vulnerability under climate change in Durban metropolitan, South Africa-identifying urban planning priorities for adaptation. *Climatic Change*, *163*(2), 807-829. https://doi.org/10.1007/s10584-020-02908-x

Janicke, B., Holtmann, A., Kim, K. R., Kang, M., Fehrenbach, U., & Scherer, D. (2019). Quantification and evaluation of intra-urban heat-stress variability in Seoul, Korea. *International Journal of Biometeorology*, *63*(1), 1-12. https://doi.org/10.1007/s00484-018-1631-2

Josse, J., & Husson, F. (2016). missMDA: A Package for Handling Missing Values in Multivariate Data Analysis. *Journal of Statistical Software*, *70*(1), 1–31. https://doi.org/10.18637/jss.v070.i01

Kaplan, G. (2019). Evaluating the roles of green and built-up areas in reducing a surface urban heat island using remote sensing data. *Urbani Izziv*, *30*(2), 105-112. https://doi.org/10.5379/urbani-izziv-en-2019-30-02-004

Ketterer, C., & Matzarakis, A. (2015). Comparison of different methods for the assessment of the urban heat island in Stuttgart, Germany. *International Journal of Biometeorology*, *59*, 1299-1309. https://doi.org/10.1007/s00484-014-0940-3

Khatami, R., Mountrakis, G., & Stehman, S. V. (2016). A meta-analysis of remote sensing research on supervised pixel-based land-cover image classification processes: General guidelines for practitioners and future research. *Remote Sensing of Environment*, *177*, 89-100. https://doi.org/10.1016/j.rse.2016.02.028

Kim, D. W., Deo, R. C., Lee, J. S., & Yeom, J. M. (2017). Mapping heatwave vulnerability in Korea. *Natural Hazards*, *89*(1), 35-55. https://doi.org/10.1007/s11069-017-2951-y

Klotz, M., Kemper, T., Geic, C., Esch, T., & Taubenbock, H. (2016). How good is the map? A multi-scale cross-comparison framework for global settlement layers: Evidence from Central Europe. *Remote Sensing of Environment*, *178*, 191-212. https://doi.org/10.1016/j.rse.2016.03.001

Koman, P. D., Romo, F., Swinton, P., Mentz, G. B., de Majo, R. F., Sampson, N. R., Battaglia, M. J., Hill-Knott, K., Williams, G. O., O'Neill, M. S., & Schulz, A. J. (2019). MI-Environment: Geospatial patterns and inequality of relative heat stress vulnerability in Michigan. *Health & Place*, *60*, 102228. https://doi.org/10.1016/j.healthplace.2019.102228

Krstic, N., Yuchi, W., Ho, H. C., Walker, B. B., Knudby, A. J., & Henderson, S. B. (2017). The Heat Exposure Integrated Deprivation Index (HEIDI): A data-driven approach to quantifying neighborhood risk during extreme hot weather. *Environment International*, *109*, 42-52. https://doi.org/10.1016/j.envint.2017.09.011

Lê, S., Josse, J., & Husson, F. (2008). FactoMineR: An R Package for Multivariate Analysis. *Journal of Statistical Software*, *25*(1), 1-18. https://doi.org/10.18637/jss.v025.i01

Li, F., Yigitcanlar, T., Nepal, M., Thanh, K. N., & Dur, F. (2022). Understanding Urban Heat Vulnerability Assessment Methods: A PRISMA Review. *Energies*, *15*, 6998. https://doi.org/10.3390/en15196998

Li, H., Zhou, Y., Li, X., Meng, L., Wang, X., Wu, S., & Sodoudi, S. (2018). A new method to quantify surface urban heat island intensity. *Science of the Total Environment*, *624*, 262-272. https://doi.org/10.1016/j.scitotenv.2017.11.360

Li, W., El-Askary, H., Lakshmi, V., Piechota, T., & Struppa, D. (2020). Earth Observation and Cloud Computing in Support of Two Sustainable Development Goals for the River Nile Watershed Countries. *Remote Sensing*, *12*(9), 1391. https://doi.org/10.3390/rs12091391

Linard, C., Gilbert, M., & Tatem, A. J. (2011). Assessing the use of global land cover data for guiding large area population distribution modelling. *GeoJournal*, *76*(5), 525-538. https://doi.org/10.1007/s10708-010-9364-8

Liu, X., Yue, W. Z., Yang, X. C., Hu, K. J., Zhang, W., & Huang, M. Y. (2020). Mapping Urban Heat Vulnerability of Extreme Heat in Hangzhou via Comparing Two Approaches. *Complexity*, *2020*, 9717658. https://doi.org/10.1155/2020/9717658

Mallen, E., Stone, B., & Lanza, K. (2019). A methodological assessment of extreme heat mortality modeling and heat vulnerability mapping in Dallas, Texas. *Urban Climate*, *30*, 100528. https://doi.org/10.1016/j.uclim.2019.100528

Maragno, D., Dalla Fontana, M., & Musco, F. (2020). Mapping Heat Stress Vulnerability and Risk Assessment at the Neighborhood Scale to Drive Urban Adaptation Planning. *Sustainability*, *12*(3), 1056. https://doi.org/10.3390/su12031056

Marchal, J., Bour, B., Budei, B. C., Nininahazwe, F., Armellin, C., & Varin, M. (2022). *Cartographie des îlots de chaleur et de fraîcheur dans le Québec urbain à l'aide d'imagerie satellitaire Landsat-8 (2013-2014)* (Rapport 2022-29). Centre d'enseignement et de recherche en foresterie de Sainte-Foy inc. (CERFO). https://www.donneesquebec.ca/recherche/dataset/0512ae16-1273-46e2-ae09-a87a80437079/resource/a33969ba-143a-4524-88c3-8ec7485676b1/download/rapport-metho-ilots-chaleur-fraicheur-2013-2014-inspq-cerfo_2023-03-10-0924.pdf

Martin, S. L., Cakmak, S., Hebbern, C. A., Avramescu, M. L., & Tremblay, N. (2012). Climate change and future temperature-related mortality in 15 Canadian cities. *International Journal of Biometeorology*, *56*(4), 605-619. https://doi.org/10.1007/s00484-011-0449-y

Masson-Delmotte, V., Zhai, P., Pirani, A., Connors, S. L., Péan, C., Berger, S., Caud, N., Chen, Y., Goldfarb, L., Gomis, M. I., Huang, M., Leitzell, K., Lonnoy, E., Matthews, J. B. R., Maycock, T. K., Waterfield, T., Yelekçi, O., Yu, R., & Zhou, B. (dir.). (2021). *Climate Change 2021: The Physical Science Basis. Contribution of Working Group I to the Sixth Assessment Report of the Intergovernmental Panel on Climate Change*. Cambridge University Press.

Masson-Delmotte, V., Zhai, P., Pörtner, H.-O., Roberts, D., Skea, J., Shukla, P. R., Pirani, A., Moufouma-Okia, W., Péan, C., Pidcock, R., Connors, S., Matthews, J. B. R., Chen, Y., Zhou, X., Gomis, M. I., Lonnoy, E., Maycock, T., Tignor, M., & Waterfield, T. (dir.). (2018). *Réchauffement planétaire de 1,5 °C : Rapport spécial du GIEC sur les conséquences d'un réchauffement planétaire de 1,5 °C par rapport aux niveaux préindustriels et les trajectoires associées d'émissions mondiales de gaz à effet de serre, dans le contexte du renforcement de la parade mondiale au changement climatique, du développement durable et de la lutte contre la pauvreté*. Groupe d'experts intergouvernemental sur l'évolution du climat (GIEC). https://www.ipcc.ch/site/assets/uploads/sites/2/2019/09/SR15_Summary_Volume_french.pdf

Matthies, F., Bickler, G., Hales, S., & Marín, N. C. (2008). *Heat-health action plans: guidance*. World Health Organization. https://www.who.int/publications/i/item/9789289071918

Mendez-Lazaro, P., Muller-Karger, F. E., Otis, D., McCarthy, M. J., & Rodriguez, E. (2018). A heat vulnerability index to improve urban public health management in San Juan, Puerto Rico. *International Journal of Biometeorology*, *62*(5), 709-722. https://doi.org/10.1007/s00484-017-1319-z

Nayak, S G., Lin, S., Sheridan, S. C., Lu, Y., Graber, N., Primeau, M., Jones Rafferty, C., & Hwang, S.-A. (2017). Surveying Local Health Departments and County Emergency Management Offices on Cooling Centers as a Heat Adaptation Resource in New York State. *Journal of Community Health*, *42*(1), 43-50. https://doi.org/10.1007/s10900-016-0224-4

Nayak, S. G., Shrestha, S., Kinney, P. L., Ross, Z., Sheridan, S. C., Pantea, C. I., Hsu, W. H., Muscatiello, N., & Hwang, S. A. (2018). Development of a heat vulnerability index for New York State. *Public Health*, *161*, 127-137. https://doi.org/10.1016/j.puhe.2017.09.006

Niu, Y. L., Li, Z. C., Gao, Y., Liu, X. B., Xu, L., Vardoulakis, S., Yue, Y. J., Wang, J., & Liu, Q. Y. (2021). A Systematic Review of the Development and Validation of the Heat Vulnerability Index: Major Factors, Methods, and Spatial Units. *Current Climate Change Reports*, *7*(3), 87-97. https://doi.org/10.1007/s40641-021-00173-3

Oke, T. R. (1987) *Boundary Layer Climates* (2e éd.). Routledge.

Oke, T. R., Mills, G., Christen, A., & Voogt, J. A. (2017). *Urban Climates*. Cambridge University Press.

Olofsson, P., Foody, G. M., Herold, M., Stehman, S. V., Woodcock, C. E., & Wulder, M. A. (2014). Good practices for estimating area and assessing accuracy of land change. *Remote Sensing of Environment*, *148*, 42-57. https://doi.org/10.1016/j.rse.2014.02.015

Osborne, J. W., & Costello, A. B. (2004). Sample size and subject to item ratio in principal components analysis. *Practical Assessment, Research, and Evaluation*, *9*(11). https://doi.org/10.7275/ktzq-jq66

Oukawa, G. Y., Krecl, P., & Targino, A. C. (2022). Fine-scale modeling of the urban heat island: A comparison of multiple linear regression and random forest approaches. *Science of the Total Environment*, *815*, 152836. https://doi.org/10.1016/j.scitotenv.2021.152836

Parry, M., Canziani, O., Palutikof, J., van der Linden, P., & Hanson, C. (2007). *Bilan 2007 des changements climatiques : Conséquences, adaptation et vulnérabilité*. Groupe d'experts intergouvernemental sur l'évolution du climat (GIEC). https://www.ipcc.ch/site/assets/uploads/2020/02/ar4-wg2-sum-vol-fr.pdf

Pett, M. A., Lackey, N. R., & Sullivan, J. J. (2003). *Making Sense of Factor Analysis: The Use of Factor Analysis for Instrument Development in Health Care Research*. SAGE Publications, Inc.

Räsänen, A., Heikkinen, K., Piila, N., & Juhola, S. (2019). Zoning and weighting in urban heat island vulnerability and risk mapping in Helsinki, Finland. *Regional Environmental Change*, *19*, 1481-1493. https://doi.org/10.1007/s10113-019-01491-x

Sagris, V., & Sepp, M. (2017). Landsat-8 TIRS Data for Assessing Urban Heat Island Effect and Its Impact on Human Health. *IEEE Geoscience and Remote Sensing Letters*, *14*(12), 2385-2389. https://doi.org/10.1109/LGRS.2017.2765703

Santamouris, M. (2020). Recent progress on urban overheating and heat island research. Integrated assessment of the energy, environmental, vulnerability and health impact. Synergies with the global climate change. *Energy and Buildings*, *207*, 109482. https://doi.org/https://doi.org/10.1016/j.enbuild.2019.109482

Schiavina, M., Melchiorri, M., Pesaresi, M., Politis, P., Freire, S., Maffenini, L., Florio, P., Ehrlich, D., Goch, K., Tommasi, P. & Kemper, T. (2022). *GHSL Data Package 2022*. Publications Office of the European Union. https://doi.org/10.2760/19817

Song, J., Huang, B., Kim, J. S., Wen, J., & Li, R. (2020). Fine-scale mapping of an evidence-based heat health risk index for high-density cities: Hong Kong as a case study. *Science of The Total Environment*, *718*, 137226. https://doi.org/10.1016/j.scitotenv.2020.137226

Stafford, J., & Bodson, P. (2006). *L'analyse multivariée avec SPSS*. Presses de l'Université du Québec.

Statistics Canada. (2017). *Illustrated Glossary – Dissemination block (DB)*. https://www150.statcan.gc.ca/n1/pub/92-195-x/2016001/geo/db-id/db-id-eng.htm

Statistics Canada (2022a). *Canada's large urban centres continue to grow and spread.* https://www150.statcan.gc.ca/n1/daily-quotidien/220209/dq220209b-eng.htm

Statistics Canada. (2022b). *Dictionary, Census of Population, 2021*. https://www12.statcan.gc.ca/census-recensement/2021/ref/dict/index-eng.cfm

Statistics Canada (2022c). *Illustrated Glossary – Census metropolitan area (CMA) and census agglomeration (CA)*. https://www150.statcan.gc.ca/n1/pub/92-195-x/2021001/geo/cma-rmr/cma-rmr-fra.htm

Statistics Canada (2022d). *Illustrated Glossary – Dissemination area (DA)* https://www150.statcan.gc.ca/n1/pub/92-195-x/2021001/geo/da-ad/da-ad-fra.htm

Statistics Canada (2022e). *Population estimates on July 1st, by age and sex*. https://www150.statcan.gc.ca/t1/tbl1/en/tv.action?pid=1710000501&request_locale=en

Statistics Canada (2022f). *The Linkakable Open Data Environment.* https://www.statcan.gc.ca/fr/ecdo

Stehman, S. V. (2009). Sampling designs for accuracy assessment of land cover. *International Journal of Remote Sensing*, *30*(20), 5243-5272. https://doi.org/10.1080/01431160903131000

Strahler, A. H., Boschetti, L., Foody, G. M., Friedl, M. A., Hansen, M. C., Herold, M., Mayaux, P., Morisette, J. T., Stehman, S. V. & Woodcock, C. E. (2006). *Global Land Cover Validation: Recommendations for Evaluation and Accuracy Assessment of Global Land Cover Maps*. Publications Office of the European Union. https://op.europa.eu/s/yCm1

Straub, A., Berger, K., Breitner, S., Cyrys, J., Geruschkat, U., Jacobeit, J., Kühlbach, B., Kusch, T., Philipp, A., Schneider, A., Umminger, R., Wolf, K., & Beck, C. (2019). Statistical modelling of spatial patterns of the urban heat island intensity in the urban environment of Augsburg, Germany. *Urban Climate*, *29*, 100491. https://doi.org/10.1016/j.uclim.2019.100491

Tran, D. N., Doan, V. Q., Nguyen, V. T., Khan, A., Thai, P. K., Huang, C. R., Chu, C., Schak, E., & Phung, D. (2020). Spatial patterns of health vulnerability to heatwaves in Vietnam. *International Journal of Biometeorology*, *64*(5), 863-872. https://doi.org/10.1007/s00484-020-01876-2

Turek-Hankins, L. L., Hino, M., & Mach, K. J. (2020). Risk screening methods for extreme heat: Implications for equity-oriented adaptation. *Plos One*, *15*(11), 0240841. https://doi.org/10.1371/journal.pone.0240841

Voelkel, J., Hellman, D., Sakuma, R., & Shandas, V. (2018). Assessing vulnerability to urban heat: A study of disproportionate heat exposure and access to refuge by socio-demographic status in Portland, Oregon. *International Journal of Environmental Research and Public Health*, *15*(4). https://doi.org/10.3390/ijerph15040640

von Bergmann, J., Shkolnik, D., & Jacobs, A. (2021*). cancensus: R package to access, retrieve, and work with Canadian Census data and geography* (version 0.4.2). [package R]. https://mountainmath.github.io/cancensus/

Wang, M., Zhang, Z., Hu, T., Wang, G., He, G., Zhang, Z., ... & Liu, X. (2020). An efficient framework for producing Landsat-based land surface temperature data using Google Earth engine. *IEEE Journal of Selected Topics in Applied Earth Observations and Remote Sensing*, 13, 4689-4701. https://doi:10.1109/jstars.2020.3014586

Widerynski, S., Schramm, P., Conlon, K., Noe, R., Grossman, E., Hawkins, M., Nayak, S., Roach, M. & Hilts, A. (2017). *The Use of Cooling Centers to Prevent Heat-Related Illness: Summary of Evidence and Strategies for Implementation*. National Center for Environmental Health (US). https://stacks.cdc.gov/view/cdc/47657

Wolf, T., Chuang, W.-C., & McGregor, G. (2015). On the Science-Policy Bridge: Do Spatial Heat Vulnerability Assessment Studies Influence Policy? *International Journal of Environmental Research and Public Health*, *12*(10), 13321-13349. https://doi.org/10.3390/ijerph121013321

Yu, J. S., Castellani, K., Forysinski, K., Gustafson, P., Lu, J. M., Peterson, E., Tran, M., Yao, A., Zhao, J. X., & Brauer, M. (2021). Geospatial indicators of exposure, sensitivity, and adaptive capacity to assess neighbourhood variation in vulnerability to climate change-related health hazards. *Environmental Health*, *20*(1), Article 31. https://doi.org/10.1186/s12940-021-00708-z

Zemtsov, S., Shartova, N., Varentsov, M., Konstantinov, P., Kidyaeva, V., Shchur, A., Timonin, S., & Grischchenko, M. (2020). Intraurban social risk and mortality patterns during extreme heat events: A case study of Moscow, 2010-2017. *Health & Place*, *66*, Article 102429. https://doi.org/10.1016/j.healthplace.2020.102429

Zhang, W., McManus, P., & Duncan, E. (2018). A Raster-Based Subdividing Indicator to Map Urban Heat Vulnerability: A Case Study in Sydney, Australia. *International Journal of Environmental Research and Public Health*, *15*(11), 2516. https://doi.org/10.3390/ijerph15112516

Zhang, W., Zhao, Q., & Pei, M. (2021). How much uncertainty does the choice of data transforming method brings to heat risk mapping? Evidence from China. *Natural Hazards*, *106*, 349-373. https://doi.org/10.1007/s11069-020-04466-y

Zhang, X., Flato, G., Kirchmeier-Young, M., Vincent, L., Wan, H., Wang, X., Rong, R., Fyfe, J., Li, G., & Kharin, V. V. (2019). Les changements de température et de précipitations pour le Canada. Dans E. Bush et D. S. Lemmen (dir), *Rapport sur le climat changeant du Canada* (p. 113-193). Gouvernement du Canada. https://doi.org/10.4095/314614

Zheng, M. X., Zhang, J. H., Shi, L. M., Zhang, D., Sharma, T. P. P., & Prodhan, F. A. (2020). Mapping Heat-Related Risks in Northern Jiangxi Province of China Based on Two Spatial Assessment Frameworks Approaches. *International Journal of Environmental Research and Public Health*, *17*(18), 6584. https://doi.org/10.3390/ijerph17186584

Zuhra, S. S., Tabinda, A. B., & Yasar, A. (2019). Appraisal of the heat vulnerability index in Punjab: a case study of spatial pattern for exposure, sensitivity, and adaptive capacity in megacity Lahore, Pakistan. *International Journal of Biometeorology*, *63*(12), 1669-1682. https://doi.org/10.1007/s00484-019-01784-0

7 APPENDICES

7.1 Appendix 1: List of 156 Mapped CMAs and CAs

Table 44: Complete Table of the CMAs/CAs per Province

Urbans regions (CMA/CA)	Types of urban area	Provinces	Population in 2021
Abbotsford - Mission	CMA	British Columbia	195 726
Alma	CA	Quebec	30 331
Amos	CA	Quebec	18 873
Baie-Comeau	CA	Quebec	26 643
Barrie	CMA	Ontario	212 856
Bathurst	CA	New Brunswick	31 387
Belleville - Quinte West	CMA	Ontario	111 184
Brandon	CA	Manitoba	54 268
Brantford	CMA	Ontario	144 162
Brockville	CA	Ontario	31 661
Brooks	CA	Alberta	14 924
Calgary	CMA	Alberta	1 481 806
Campbell River	CA	British Columbia	40 704
Campbellton (New Brunswick part)	CA	New Brunswick	11 986
Campbellton (Quebec part)	CA	Quebec	1344
Camrose	CA	Alberta	18 772
Canmore	CA	Alberta	15 990
Cape Breton	CA	Nova Scotia	98 318
Centre Wellington	CA	Ontario	31 093
Charlottetown	CA	Prince Edward Island	78 858
Chatham-Kent	CA	Ontario	104 316
Chilliwack	CMA	British Columbia	113 767
Cobourg	CA	Ontario	20 519
Collingwood	CA	Ontario	24 811
Corner Brook	CA	Newfoundland and Labrador	29 762
Cornwall	CA	Ontario	61 415
Courtenay	CA	British Columbia	63 282
Cowansville	CA	Quebec	15 234
Cranbrook	CA	British Columbia	27 040
Dawson Creek	CA	British Columbia	17 878
Dolbeau-Mistassini	CA	Quebec	15 306
Drummondville	CMA	Quebec	101 610
Duncan	CA	British Columbia	47 582
Edmonton	CMA	Alberta	1 418 118
Edmundston	CA	New Brunswick	22 144

Elliot Lake	CA	Ontario	11 372
Essa	CA	Ontario	22 970
Estevan	CA	Saskatchewan	12 798
Fort St. John	CA	British Columbia	28 729
Fredericton	CMA	New Brunswick	108 610
Gander	CA	Newfoundland and Labrador	13 414
Granby	CA	Quebec	90 833
Grand Falls-Windsor	CA	Newfoundland and Labrador	13 853
Grande Prairie	CA	Alberta	64 141
Greater Sudbury	CMA	Ontario	170 605
Guelph	CMA	Ontario	165 588
Halifax	CMA	Nova Scotia	465 703
Hamilton	CMA	Ontario	785 184
Hawkesbury (Ontario part)	CA	Ontario	10 194
Hawkesbury (Quebec part)	CA	Quebec	1816
High River	CA	Alberta	14 324
Ingersoll	CA	Ontario	13 693
Joliette	CA	Quebec	52 706
Kamloops	CMA	British Columbia	114 142
Kawartha Lakes	CA	Ontario	79 247
Kelowna	CMA	British Columbia	222 162
Kenora	CA	Ontario	14 967
Kentville	CA	Nova Scotia	26 929
Kingston	CMA	Ontario	172 546
Kitchener - Cambridge - Waterloo	CMA	Ontario	575 847
Lachute	CA	Quebec	14 100
Lacombe	CA	Alberta	13 396
Ladysmith	CA	British Columbia	15 501
Lethbridge	CMA	Alberta	123 847
Lloydminster (Alberta part)	CA	Alberta	19 739
Lloydminster (Saskatchewan part)	CA	Saskatchewan	16 769
London	CMA	Ontario	543 551
Matane	CA	Quebec	18 474
Medicine Hat	CA	Alberta	76 376
Midland	CA	Ontario	27 894
Miramichi	CA	New Brunswick	27 593
Moncton	CMA	New Brunswick	157 717
Montréal	CMA	Quebec	4 291 732
Moose Jaw	CA	Saskatchewan	34 872
Nanaimo	CMA	British Columbia	115 459
Nelson	CA	British Columbia	19 119
New Glasgow	CA	Nova Scotia	34 397
Norfolk	CA	Ontario	67 490

North Battleford	CA	Saskatchewan	19 374
North Bay	CA	Ontario	71 736
Okotoks	CA	Alberta	30 405
Orillia	CA	Ontario	33 411
Oshawa	CMA	Ontario	415 311
Ottawa - Gatineau (Ontario part)	CMA	Ontario	1 135 014
Ottawa - Gatineau (Quebec part)	CMA	Quebec	353 293
Owen Sound	CA	Ontario	32 712
Parksville	CA	British Columbia	31 054
Pembroke	CA	Ontario	23 814
Penticton	CA	British Columbia	47 380
Petawawa	CA	Ontario	18 160
Peterborough	CMA	Ontario	128 624
Port Alberni	CA	British Columbia	25 786
Port Hope	CA	Ontario	17 294
Portage la Prairie	CA	Manitoba	13 270
Powell River	CA	British Columbia	17 825
Prince Albert	CA	Saskatchewan	45 718
Prince George	CA	British Columbia	89 490
Prince Rupert	CA	British Columbia	13 442
Québec	CMA	Quebec	839 311
Quesnel	CA	British Columbia	23 113
Red Deer	CMA	Alberta	100 844
Regina	CMA	Saskatchewan	249 217
Rimouski	CA	Quebec	53 944
Rivière-du-Loup	CA	Quebec	30 025
Rouyn-Noranda	CA	Quebec	42 313
Saguenay	CMA	Quebec	161 567
Saint John	CMA	New Brunswick	130 613
Sainte-Agathe-des-Monts	CA	Quebec	19 892
Sainte-Marie	CA	Quebec	13 134
Saint-Georges	CA	Quebec	34 833
Saint-Hyacinthe	CA	Quebec	59 980
Salaberry-de-Valleyfield	CA	Quebec	42 787
Salmon Arm	CA	British Columbia	19 705
Sarnia	CA	Ontario	97 592
Saskatoon	CMA	Saskatchewan	317 480
Sault Ste. Marie	CA	Ontario	76 731
Sept-Îles	CA	Quebec	27 729
Shawinigan	CA	Quebec	49 620
Sherbrooke	CMA	Quebec	227 398
Sorel-Tracy	CA	Quebec	41 934
Squamish	CA	British Columbia	24 232

St. Catharines - Niagara	CMA	Ontario	433 604
St. John's	CMA	Newfoundland and Labrador	212 579
Steinbach	CA	Manitoba	17 806
Stratford	CA	Ontario	33 232
Strathmore	CA	Alberta	14 339
Summerside	CA	Prince Edward Island	18 157
Swift Current	CA	Saskatchewan	18 745
Sylvan Lake	CA	Alberta	16 514
Terrace	CA	British Columbia	19 606
Thetford Mines	CA	Quebec	28 287
Thompson	CA	Manitoba	13 035
Thunder Bay	CMA	Ontario	123 258
Tillsonburg	CA	Ontario	18 615
Timmins	CA	Ontario	41 145
Toronto	CMA	Ontario	6 202 225
Trail	CA	British Columbia	14 268
Trois-Rivières	CMA	Quebec	161 489
Truro	CA	Nova Scotia	46 157
Val-d'Or	CA	Quebec	34 037
Vancouver	CMA	British Columbia	2 642 825
Vernon	CA	British Columbia	67 086
Victoria	CMA	British Columbia	397 237
Victoriaville	CA	Quebec	52 936
Wasaga Beach	CA	Ontario	24 862
Wetaskiwin	CA	Alberta	12 594
Weyburn	CA	Saskatchewan	12 247
Whitehorse	CA	Yukon	31 913
Williams Lake	CA	British Columbia	23 608
Windsor	CMA	Ontario	422 630
Winkler	CA	Manitoba	32 655
Winnipeg	CMA	Manitoba	834 678
Wood Buffalo	CA	Alberta	73 837
Woodstock	CA	Ontario	46 705
Yellowknife	CA	Northwest Territories	20 340
Yorkton	CA	Saskatchewan	19 859

7.2 APPENDIX 2: USE OF THE MAPPING TOOL PROTOTYPE BY THE CITY OF VICTORIA IN SUMMER 2022

The online prototype of mapping the vulnerability and exposure to extreme heat waves of populations of the census metropolitan of Victoria was viewed 257 times between the beginning of May and the end of September (Figure 33). There was a spike in page views in June, around June 13th, the meeting date. The tool was available from the beginning of June for stakeholders, which explains the number of consultations. There was also a small spike in September during the survey period.

We can see that the online tool's traffic is not very important during the summer. This partly due to the limited group of people who had access to it and the absence of a major heat waves in British Columbia that summer, unlike the summer of 2021, when the province experienced a historic heat wave and a new Canadian temperature record had been set in the village of Lytton with a temperature of 49.6 degrees Celsius. More than 1000 new local daily temperature records had been recorded between the end of June and the beginning of July (British Columbia Coroners Service, 2022). Moreover, the online tool had not yet been the subject of the communication plan. With this step scheduled for spring 2023.

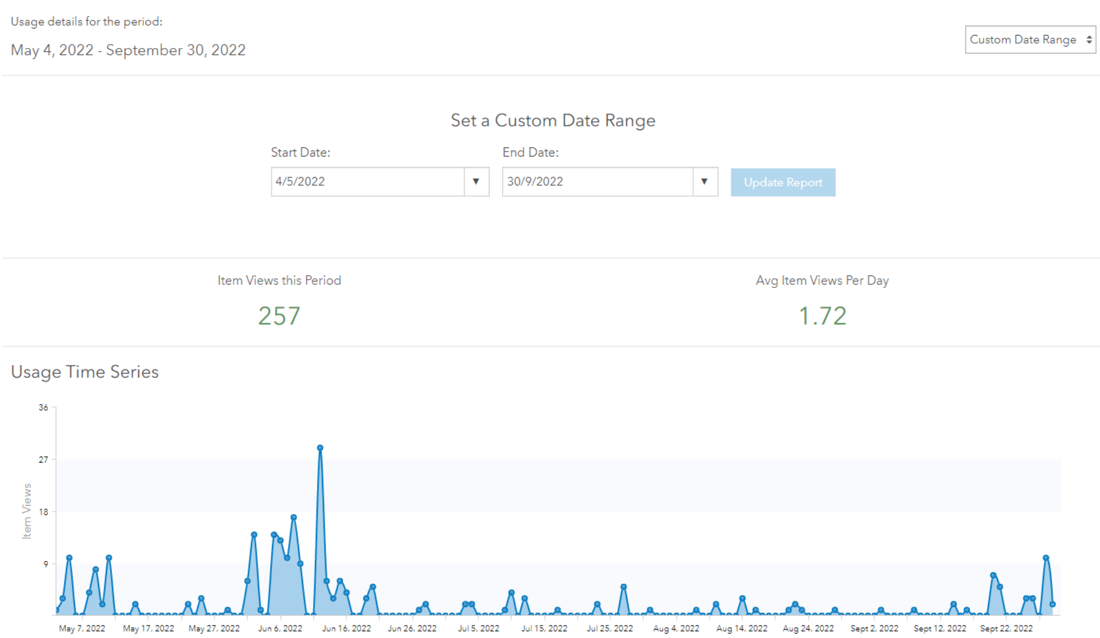

Figure 33: Online mapping tool consultation history

7.3 Appendix 3: Navigation Help (Computer Version)

INTRODUCTION TO NAVIGATION

To move around on the map, hold down the left mouse button and a small hand will appear, allowing you to drag and reposition your view by moving the mouse. If you are using the touchpad on your computer, hold down the left button and move another finger across the touchpad to achieve the same result.

The 156 urban areas covered by the project "Mapping the vulnerability and exposure to extreme heat waves" are those that appear in light grey with a white border on the map of Canada. By zooming in on the region of your choice, the light grey layer will disappear to make way for the heat wave exposure layer.

You will find in the application a total of six themes:

- Exposure to heat waves
- Sensitivity to heat waves
- Coping capacity to heat waves
- Vulnerability to heat waves
- Vulnerability and exposure to heat waves
- Urban heat islands

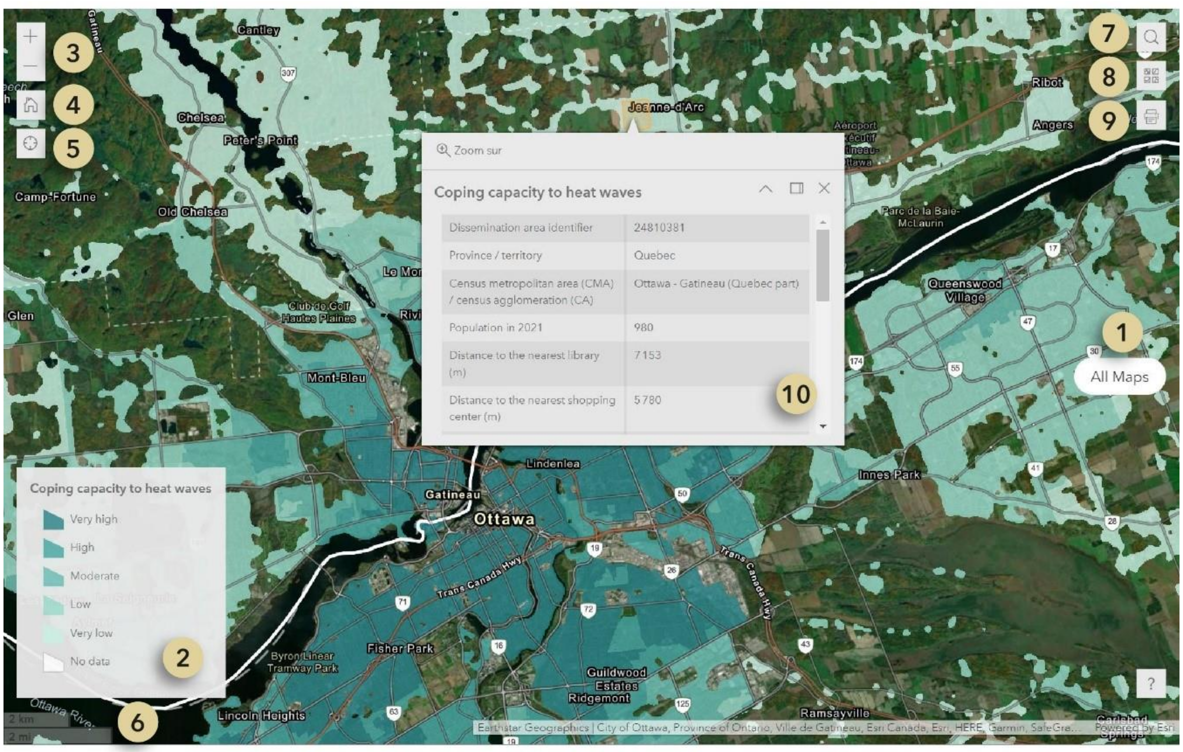

ALL MAPS (Nº 1)

To view the different geographic information layers and change the layer displayed, click on the "All maps" button and select the one you are interested in. There are two modes: "1 map" and "2 maps". If you click on the "1 map" icon, you will be able to select the one you want to view from the 6 maps.

By clicking on the "2 maps" mode, you will be able to view and move around 2 maps simultaneously (vulnerability/exposure and urban heat islands).

LEGEND (Nº 2)

The legend of the selected layer appears automatically with the "1 map" mode and the name of the layer is at the top of the legend.

In the "2 maps" only the name of the theme appears in order to give more space to the data on the maps. However, the legend can be consulted by clicking on the "Layers" button of the respective maps, represented by the icon with three horizontal squares superimposed. Once the window is open, click on the word "Legend" to see it appear.

ZOOM (Nº 3)

You can use the plus and minus symbols to zoom in and out. You can also use the scroll wheel on your mouse to do this. If you're using your computer's touchpad, spread two fingers apart to zoom in on a location and bring two fingers together to zoom out.

Each map has an independent zoom in the "1 map" mode, so you have to zoom back to the region of your choice if you change the map displayed.

DEFAULT MAP VIEW (Nº 4)

Clicking on the house icon will return you to the default map view of Canada.

FIND MY LOCATION (Nº 5)

Find my location (target icon) allows the software to detect where you are and then zoom into your area. This tool may not work depending on your computer's privacy settings with respect to geolocation.

SCALE (Nº 6)

To give you an idea of the relationship between the distance measured on the map and the actual distance on the ground, you can check the graphical scale at the bottom left of the map. It is displayed in kilometers and miles.

SEARCH (Nº 7)

You can search for a specific location or address using the search tool. By entering one or more words in the text box, a drop-down menu will appear with choices. By selecting one of the options and pressing the magnifying glass symbol, the tool will zoom in on your search result.

BASEMAPS (Nº 8)

The basemaps library presents different options that you can select as a background map. By clicking on the icon, a drop-down menu with all the choices will appear. The default basemap for our application is "Imagery Hybrid".

PRINT (Nº 9)

The "Print" tool allows you to create a map representing the selected map area and select a layout that can be saved to your computer or printed later.

By clicking on the printer icon, a drop-down menu with different formats will appear. You must select one and then click on the print button. The procedure may take a few seconds. When you see a circle to the left of the map name, the operation is in progress. When the little circle turns into a page icon, you can click on it and a new tab will appear with your map. To save the map to your computer, right-click on it with your mouse or touchpad and a menu will appear with the option "Save Image As". You can then decide on the name and location of your file. If you have an Apple computer, click with two fingers at the same time to bring up the menu.

If you want to produce a map of a different layer or region, click the "Reset" button to start the process again.

When you click on the "Preview Print Extents" option, the blue area that appears is the area that will be on your map.

*We are aware that the maps produced do not have a legend, this is a problem out of our control that comes from the software that will be adjusted eventually.

POP-UP WINDOW (Nº 10)

You can click on a dissemination area on the map and a pop-up window will appear. This window contains information about the variables and indices. The "Zoom to" tool at the bottom or top of the window allows you to zoom in on the selected polygon.

*There is no pop-up window for the urban heat island map.

7.4 APPENDIS 4: NAVIGATION HELP (TABLET VERSION)

BEFORE YOU BEGIN

For the best experience with the online mapping tool, it is recommended that you use a computer rather than a cell phone or tablet. The larger computer screen provides a better view of the map, and more functionality is available in this format.

INTRODUCTION TO NAVIGATION

To begin, you can zoom in by spreading two fingers apart to enlarge the map or by bringing them together to shrink it. Then, locate the area you want to explore and place a finger on the screen and drag it up, down, left or right to move the map in the desired direction.

Each map zooms out independently in the "1 map" mode, so you must zoom back in on the area of your choice if you change the map displayed.

The 156 urban areas covered by the project "Mapping the vulnerability and exposure to extreme heat waves" are those that appear in light grey with a white border on the map of Canada. By zooming in on the region of your choice, the light grey layer will disappear to make way for the heat wave exposure layer.

You will find in the application a total of six themes:

- Exposure to heat waves
- Sensitivity to heat waves
- Coping capacity to heat waves
- Vulnerability to heat waves
- Vulnerability and exposure to heat waves
- Urban heat islands

ALL MAPS

To view the different geographic information layers and change the layer displayed, press on the "All maps" button and select the one you are interested in. There are two modes: "1 map" and "2 maps". If you click on the "1 map" icon, you will be able to select the one you want to view from the 6 maps.

By pressing on the "2 maps" mode, you will be able to view and move around 2 maps simultaneously (vulnerability/exposure and urban heat islands).

DEFAULT MAP VIEW

Pressing on the house icon will return you to the default map view of Canada.

FIND MY LOCATION

Find my location (target icon) allows the software to detect where you are and then zoom into your area. This tool may not work depending on your tablet's privacy settings with respect to geolocation.

SCALE

To give you an idea of the relationship between the distance measured on the map and the actual distance on the ground, you can check the graphical scale at the bottom left of the map. It is displayed in kilometers and miles.

LEGEND

To access the legend, press on the "Layers" tab, which is represented by three horizontal squares on top of each other. A window will open with two menus ("Layer" and "Legend"). Press on the word "Legend" to make it appear.

BASEMAPS

The basemaps library presents different options that you can select as a background map. By pressing on the icon, a drop-down menu with all the choices will appear. The default basemap for our application is "Imagery Hybrid".

PRINT

The "Print" tool allows you to create a map representing the selected map area and select a layout that can be saved to your tablet or printed later.

By pressing on the printer icon, a drop-down menu with different formats will appear. You must select one and then press on the print button. The procedure may take a few seconds. When you see a circle to the left of the map name, the operation is in progress. When the little circle turns into a page icon, you can press on it and a new tab will appear with your map.

If you want to produce a map of a different layer or region, press the “Reset” button to start the process again.

When you press on the “Preview Print Extents” option, the blue area that appears is the area that will be on your map.

**We are aware that the maps produced do not have a legend, this is a problem out of our control that comes from the software that will be adjusted eventually.*

POP-UP WINDOW

You can press on a dissemination area on the map and a pop-up window will appear. This window contains information about the variables and indices. The "Zoom to" tool at the bottom or top of the window allows you to zoom in on the selected polygon.

*There is no pop-up window for the urban heat island map.

7.5 Appendix 5: Navigation Help (Phone Version)

BEFORE YOU BEGIN

For the best experience with the online mapping tool, it is recommended that you use a computer rather than a cell phone or tablet. The larger computer screen provides a better view of the map, and more functionality is available in this format.

INTRODUCTION TO NAVIGATION

To begin, you can zoom in by spreading two fingers apart to enlarge the map or by bringing them together to shrink it. Then, locate the area you want to explore and place a finger on the screen and drag it up, down, left or right to move the map in the desired direction.

Each map zooms out independently, so you must zoom back in on the area of your choice if you change the map displayed.
The 156 urban areas covered by the project "Mapping the vulnerability and exposure to extreme heat waves" are those that appear in light grey with a white border on the map of Canada. By zooming in on the region of your choice, the light grey layer will disappear to make way for the heat wave exposure layer.
You will find in the application a total of six themes:

- Exposure to heat waves
- Sensitivity to heat waves
- Coping capacity to heat waves
- Vulnerability to heat waves
- Vulnerability and exposure to heat waves
- Urban heat islands

ALL MAPS

To view the different geographic information layers and change the displayed layer, press on the "All maps" button and select the one you want to view from the choice of 6.

LEGEND

To access the legend, press on the "Layers" tab, which is represented by three horizontal squares on top of each other. A window will open with two menus ("Layer" and "Legend"). Press on the word "Legend" to make it appear.

BASEMAPS

The basemaps library presents different options that you can select as a background map. By pressing on the icon, a drop-down menu with all the choices will appear. The default basemap for our application is "Imagery Hybrid".

DEFAULT MAP VIEW

Pressing on the house icon will return you to the default map view of Canada.

FIND MY LOCATION

Find my location (target icon) allows the software to detect where you are and then zoom into your area. This tool may not work depending on your telephone's privacy settings with respect to geolocation.

POP-UP WINDOW

You can press on a dissemination area on the map and a pop-up window will appear. This window contains information about the variables and indices. The "Zoom to" tool at the bottom or top of the window allows you to zoom in on the selected polygon.

*There is no pop-up window for the urban heat island map.